THE
LONDON EDINBURGH AND DUBLIN
PHILOSOPHICAL MAGAZINE
AND
JOURNAL OF SCIENCE.

[SEVENTH SERIES.]

SEPTEMBER 1930.

XXXV. *On Ozone and Atomic Oxygen in the Upper Atmosphere.* *By* S. CHAPMAN, *F.R.S.**

1. IN a recent paper† I have given a tentative theory of the equilibrium and annual changes of the ozone which exists in the upper atmosphere ; the ozone was, for simplicity, treated as if all of it was situated in a uniform layer of the atmosphere, 10 km. thick, between 40 and 50 km. height. The object of the present paper is to consider how, at greater heights, the concentration of ozone, and also of atomic oxygen, is likely to vary.

Any quantitative discussion of these matters is bound to involve speculative assumptions and estimates, but some interesting qualitative considerations, which are scarcely open to doubt, may be developed.

In the first place, the *production* of ozone almost certainly requires the dissociation of molecular oxygen (O_2) into atomic oxygen (O), and the subsequent attachment of the oxygen atoms to oxygen molecules, according to the equations

$$(a) \quad O_2 = 2O,$$

$$(b) \quad O_2 + O = O_3.$$

Some of the O atoms may, however, revert to O_2 molecules, according to the reaction

$$(c) \quad 2O = O_2,$$

* Communicated by the Author.

† Memoirs Roy. Meteor. Soc. iii. No. 26, pp. 103–125 (1930).

while others may combine with ozone and thus again cause reversion to molecular oxygen, *i. e.*,

$$(d) \quad O + O_3 = 2O_2.$$

The reactions (*b*), (*c*), in which two particles combine to form a single molecule, will in general occur only in three-body collisions, the participation of a third particle being necessary in order that the conditions of conserved momentum and energy may be fulfilled; the third particle may be an atom or molecule of any kind.

As the density of the atmosphere diminishes, the chance of a third body taking part in a collision of any given kind diminishes in the same ratio, so that the interval between the genesis of an O atom and its combination with an O_2 molecule or another O atom in an effective three-body collision must be correspondingly lengthened. Thus the free life of the O atoms increases with height, and the ratio of O atoms to O_3 molecules must likewise increase, except in so far as convective mixing restores uniformity. At very great heights recombination must be so slow that the proportion of O atoms to O_2 molecules will become large, and whereas at lower levels the reaction (*b*) must be far more frequent than (*c*), because of the large excess of O_2 molecules there present as compared with O atoms, at high levels the reactions (*c*) will be the more frequent—that is, most of the oxygen atoms revert directly to molecular oxygen, and few of them form ozone.

The green line in the spectrum of the aurora, both polar and non-polar, affords direct evidence of the permanent existence of atomic oxygen (in the neutral state) in some stratum of the upper atmosphere.

The *disappearance* of ozone may occur by the reaction (*d*), in conjunction with atomic oxygen, or by the reaction

$$(e) \quad 2O_3 = 3O_2,$$

which is supposed to be the mode of purely thermal decomposition of ozone, or by dissociation in the manner inverse to (*b*), viz.,

$$(f) \quad O_3 = O_2 + O,$$

thus giving rise to atomic oxygen. The last reaction requires the communication of energy to the ozone molecule; this may be effected either by unusually violent collisions with other molecules of any kind, or by the action of sunlight. Radiation in the band λ 2300–2900 is absorbed by ozone, and is believed to bring about this dissociation;

it is by this and other ozone absorption-bands in the solar spectrum that the existence, amount, and height of the ozone in the earth's atmosphere are detected and measured.

The *production* of atomic oxygen by the process (*f*) may at particular levels be greater than by the process (*a*), but the latter is the more fundamental; if it ceased, and O atoms were formed only from ozone, the amount of ozone would slowly diminish.

The reciprocal reactions (*f*) and (*b*) form a cyclic process, and if every O atom formed by (*f*) reverted to O_3 by (*b*), the combined number of O atoms and O_3 molecules would remain constant; but actually the number must diminish by the reactions (*c*), (*d*), and (*e*), so that unless there were replenishment by the formation of new O atoms direct from O_2, not from O_3, the number of O atoms and O_3 molecules would steadily diminish to zero.

The formation of O atoms from O_2 may occur either by absorption of ultra-violet sunlight, in the band λ 1300–1800, or by bombardment of the atmosphere (as during auroræ) by corpuscles from without; probably both actions occur, though at the equator sunlight is likely to be the chief agent. In this case, and elsewhere so far as dissociation by sunlight is concerned, the formation of O atoms either from O_2 or O_3 will proceed by day but not by night, and a daily variation in the numbers of O atoms and O_3 molecules per c. c. will arise. During the night the atomic oxygen can only decrease, while the ozone may either decrease or increase. The daily variation of the atomic oxygen will necessarily decrease with height, owing to the increasing free life of each atom.

These general considerations, while indicating certain definite conclusions, cannot give numerical results for the O and O_3 concentrations at actual heights, on the basis merely of present observed data. The ozone observations indicate the total amount of ozone in each square cm. column of atmosphere, and also the mean height of the ozone; but they cannot without further assumptions indicate the detailed distribution of the ozone, especially at high levels, where the absolute density, whatever the relative concentration, must be very low. Hence the numerical development of the discussion, in the former paper and also here, is necessarily of a speculative character.

2. Let n_1, n_2, n_3, n respectively denote the number per c. c. of O atoms, O_2 and O_3 molecules, and of air molecules, at height h. Also let the number of reactions per c. c. per sec.

at this height of the types (*b*), (*c*), (*d*), (*e*) be denoted respectively by

$$K_{12}n_1n_2, \quad K_{11}n_1^2, \quad k_{13}n_1n_3, \quad k_{33}n_3^2,$$

where the large K's refer to the three-body collisions mentioned in § 1, and are proportional to the density of the air, *i. e.*, to n; thus $K_{12} \equiv k_{12}n$, $K_{11} \equiv k_{11}n$. The small k's are independent of the density, but may depend on the temperature; this dependence is likely to be small over the range of temperatures involved, and will not be considered here.

3. Let the intensity of the radiations in the bands λ 1300–1800 and λ 2300–2900, at height h, be respectively denoted by I_2, I_3, and let the absorption per cm. of air traversed be denoted by $\sigma_2 n_2 I_2$, $\sigma_3 n_3 I_3$ in the two cases, being proportional to the numbers of the absorbing molecules and to the intensity of the radiation. Then I_2 and I_3 satisfy the differential equations

$$a_2 \equiv \frac{dI_2}{dh} = \sigma_2 n_2 I_2, \quad . \quad . \quad . \quad . \quad . \quad (1)$$

$$a_3 \equiv \frac{dI_3}{dh} = \sigma_3 n_3 I_3. \quad . \quad . \quad . \quad . \quad . \quad (2)$$

The numbers a_2 and a_3 are proportional to the number of O_2 or O_3 molecules dissociated per c. c. per second, and by suitable choice of the units in which I_2 and I_3 are measured they will actually equal the number of molecules dissociated; it will be supposed that the units are so chosen. For example, if each quantum dissociates one molecule, then the intensities of the two bands must be measured, not in ordinary energy units, but in numbers of quanta of their respective wavelengths; if, however, only one quantum in ν_2 or ν_3 is effective for dissociation, then I_2 and I_3 must be measured in units equal to ν_2 or ν_3 quanta respectively.

The density of the atmosphere, and therefore also K_{11}, K_{12}, varies as $\exp(-h/H)$, where H depends on the temperature and mean molecular weight of the constituents; so long as the composition is nearly uniform n_2 will vary in like manner. It cannot be assumed, however, that n_1 or n_3 vary in this way, nor do they sensibly affect the mean molecular weight, or H, so long as O and O_3 are rare constituents of the air. This is true as regards O_3 even in the layer of maximum ozone density.

So long as n_2 varies as $\exp(-h/H)$, and H is constant, (1) can be integrated, giving

$$I_2 = (I_2)_\infty \exp\{-\mu H \exp(-h/H)\}, \quad . \quad . \quad (3)$$

where $\mu \equiv \sigma_2 n_2 \exp(h/\mathrm{H})$ and is therefore constant; $(\mathrm{I}_2)_\infty$ is the value of I_2 outside the earth's atmosphere. Also

$$a_2 = \sigma_2 n_2 \mathrm{I}_2 = \mu \mathrm{I}_2 \exp(-h/\mathrm{H})$$
$$= \mu(\mathrm{I}_2)_\infty \exp\{-(h/\mathrm{H}) - \mu \mathrm{H} \exp(-h/\mathrm{H})\}. \quad . \quad (4)$$

At great heights this increases downwards approximately as $\exp(-h/\mathrm{H})$, or proportionally to n_2; this is in the region of small absorption, where I_2 has nearly its maximum value $(\mathrm{I}_2)_\infty$. As we descend, the second term in the index of the exponential becomes important, and a_2 rises to a maximum, after which it tends rapidly to zero.

Though n_3, unlike n_2, cannot be assumed to vary as $\exp(-h/\mathrm{H})$, it is clear that at great heights I_3 must be nearly constant, and a_3 proportional to n_3; since most of the radiation in the Hartley band (λ 2300–2900) is ultimately absorbed, I_3 must tend to zero within or at the base of the ozone layer, and therefore in the lower part of this layer a_3 decreases downwards more rapidly than in proportion to n_3.

4. It will provisionally be supposed that the amounts of O and O_3 in each element of air are determined solely by the processes of dissociation and reaction occurring in the element, and are unaffected by convection and diffusion. Then the equations of change of n_1, n_2, n_3 by day are as follows :—

$$\frac{dn_1}{dt} = 2\mathrm{N}_2 + \mathrm{N}_3 - n_1(2\mathrm{K}_{11}n_1 + \mathrm{K}_{12}n_2 + k_{13}n_3), \quad . \quad . \quad . \quad (5)$$

$$\frac{dn_2}{dt} = \mathrm{N}_3 - \mathrm{N}_2 - \mathrm{K}_{12}n_1n_2 + \mathrm{K}_{11}n_1^2 + 3k_{33}n_3^2 + 2k_{13}n_1n_3, \quad (6)$$

$$\frac{dn_3}{dt} = -\mathrm{N}_3 + \mathrm{K}_{12}n_1n_2 - 2k_{33}n_3^2 - k_{13}n_1n_3, \quad . \quad . \quad . \quad . \quad (7)$$

where

$$\mathrm{N}_2 \equiv a_2 \cos(\pi t/t_0), \qquad \mathrm{N}_3 \equiv a_3 \cos(\pi t/t_0); \quad . \quad . \quad (8)$$

here a_2 and a_3 are taken to denote the numbers of O_2 or O_3 molecules dissociated per c. c. per sec. at noon, while N_2 and N_3 are the corresponding numbers at time t reckoned forward or backward from noon; t_0 denotes the duration of sunlight. The daily variation represented by (8) represents the facts only roughly, but sufficiently well for the present purpose.

The equations of change of n_1, n_2, n_3 at night are obtainable from (5)–(7) by omitting the N's.

For simplicity we will in the first instance consider the conditions above the equator at the equinoxes, so that t_0 represents half a day or, in seconds,

$$t_0 = 4{\cdot}32 \,.\, 10^4. \quad . \quad . \quad . \quad . \quad . \quad . \quad (9)$$

Since n_1 and n_3 do not increase or decrease indefinitely, but maintain nearly constant values (especially near the equator), the average values of (dn_1/dt) and (dn_3/dt) must be zero; hence also the daily average values of the right-hand sides of (5) and (7) must be zero. The average daily values of N_2 and N_3 may be expressed as λn_2, μn_3, where λ and μ tend to constant limiting values with increasing height; *e. g.*, λ and μ are approximately $\sigma_2 I_2/\pi$ and $\sigma_3 I_3/\pi$. Consequently, the n's referring to daily mean values, we have

$$2\lambda n_2 + \mu n_3 = n_1(2K_{11}n_1 + K_{12}n_2 + k_{13}n_3), \quad . \quad . \quad (10)$$

$$K_{12}n_1n_2 = \mu n_3 + 2k_{33}n_3^2 + k_{13}n_1n_3. \quad . \quad . \quad . \quad (11)$$

Now the n's of every kind must ultimately decrease with increasing height; hence on the right of (11) the last two terms, which contain n_3 multiplied by other n's, must ultimately become small compared with the term μn_3, and at sufficiently great heights we must have approximately

$$n_3 = (k_{12}/\mu)n_1n_2n. \quad . \quad . \quad . \quad . \quad . \quad (12)$$

Thus n_3/n must decrease upwards proportionately to n_1n_2, *i. e.*, the proportion of ozone to the other molecules must decrease rapidly; presumably in this region there will be a corresponding decrease of temperature, if ozone be the main cause of the high temperature in the upper atmosphere.

On the left-hand side of (10) the term $2\lambda n_2$ must ultimately outweigh the term μn_3, because at sufficiently great heights the ratio of the latter to the former is $K_{12}n_1n_2/2\lambda n_2$ or $k_{12}n_1n/2\lambda$. Likewise the term $K_{12}n_1n_2$ on the left, which is of the same order as μn_3, may be omitted. Hence $2\lambda n_2$ must ultimately tend to equality with $2K_{11}n_1^2 + k_{13}n_1n_3$, and the latter term is negligible at sufficiently great heights. Thus (10) approximates to

$$2\lambda n_2 = 2K_{11}n_1^2 = 2k_{11}n_1^2n, \quad . \quad . \quad . \quad . \quad (13)$$

or

$$n_1 = \surd\{(\lambda/k_{11})(n_2/n)\}. \quad . \quad . \quad . \quad . \quad (14)$$

Since n_1 must itself decrease upwards, the proportion n_2/n of molecular oxygen in the air must necessarily diminish. But n_1/n_2, the proportion of atomic to molecular oxygen, must increase upwards, because

$$n_1/n_2 = \surd\{\lambda/(k_{11}nn_2)\}, \quad . \quad . \quad . \quad . \quad (15)$$

which tends to infinity with increasing height—that is, the oxygen at great heights must tend to be completely dissociated.

The heights at which the limiting equations (12) and (14) become approximately true are unfortunately very uncertain, because the values of the k's and of λ, μ are unknown. An attempt will be made, however, to gain some idea as to their order of magnitude, on the basis of the theory given in the former paper already cited.

5. It was provisionally supposed that at the level h_m of maximum ozone density the most important reaction is (*b*), and that

$$K_{12}n_2 > 6 \cdot 10^{-3}.$$

The conception there tentatively arrived at regarding the processes in the layer where the O_3 concentration is greatest is as follows :—during the day O atoms are formed, mainly by dissociation of O_3 (since a_3 much exceeds a_2), but their increase is limited by their rapid combination with O_2 to re-form O_3 ; thus the approximate value of n_1 by day is

$$\frac{a_3}{K_{12}n_2}\cos\pi\frac{t}{t_0} \quad . \quad . \quad . \quad . \quad . \quad . \quad . \quad (16)$$

At sunset the O atoms that are left ((16) not being quite accurate in representing them as zero) recombine rapidly, so that n_1 varies as $\exp(-K_{12}n_2t)$; in less than 7 minutes they are reduced to one-tenth their sunset value, and therefore during most of the night there is practically no atomic oxygen. Thus the daily dissociation of O_3 and O_2 is only temporary, and soon after sunset its effects have almost disappeared. The maximum loss of ozone, near noon, is $a_3/K_{12}n_2$, and since the daily variation of n_3 is shown by observation to be small, probably less than $\frac{1}{10}n_3$, a lower limit (as above stated) for $K_{12}n_2$ can be deduced.

The daily dissociation of O_2 and O_3 does not directly determine the mean value of n_3, but does so in an indirect way, because the O atoms formed by the sunlight do not all form ozone on recombination ; a few of them participate in the reactions (*c*) and (*d*), and it is through these reactions that the equilibrium of n_3, and its slow annual variation, (north or south of the equator) are mainly determined. Nevertheless, the values of N_3 and $K_{12}n_2$, which are the chief factors determining the amount n_1 of atomic oxygen existing during each day, thereby govern the number of the reactions (*c*) and (*d*). The reaction (*e*) also affects the ozone equilibrium, but reasons are given (*l. c.*) for believing its influence to be very slight.

From a consideration of the annual variation of n_3 very tentative estimates of $k_{13}(=8.10^{-20})$ and $K_{11}(=8.10^{-18})$ at the level h_m were deduced. Moreover, n_2 being approximately 10^{16} at this level, it follows that $K_{12}>6.10^{-19}$. These numbers are quoted as possibly indicating the order of magnitude of the recombination coefficients, though they are admittedly uncertain. The value of k_{33} is estimated (from chemical data) as about 2.10^{-25} at 300° K, or 10^{-20} at 400° K.

6. Let

$$\sigma_2 I_2 \equiv \alpha_2, \quad \sigma_3 I_3 \equiv \alpha_3, \quad . \quad . \quad . \quad . \quad (17)$$

so that

$$a_2 = \alpha_2 n_2, \quad a_3 = \alpha_3 n_3 ; \quad . \quad . \quad . \quad (18)$$

α_2 and α_3 increase upwards, but only to finite limiting values $\sigma_2(I_2)_\infty$, $\sigma_3(I_3)_\infty$. Taking

$$a_2 = 2.10^6, \qquad a_3 = 5.10^9$$

at level h_m, where

$$n_2 = 10^{16}, \qquad n_3 = 8.10^{12} \text{ about},$$

we have

$$\alpha_2 = 2.10^{-10}, \quad \alpha_3 = 6.10^{-4}$$

at h_m.

7. The equation of daily variation of O_3 is (7), which, by use of (8) and (18), may be written in the form

$$\frac{d \log n_3}{dt} = -\alpha_3 \cos \frac{\pi t}{t_0} + \frac{K_{12} n_1 n_2}{n_3} - 2k_{33} n_3 - k_{13} n_1. \quad (19)$$

At the level h_m the last two terms are negligible compared with the others on the right, and this must persist for some distance above h_m, so that the equation will be used in the approximate form

$$\frac{d \log n_3}{dt} = -\alpha_3 \cos \frac{\pi t}{t_0} + \frac{K_{12} n_1 n_2}{n_3} . \quad . \quad . \quad . \quad (20)$$

This holds during the day ($t=-\frac{1}{2}t_0$ to $t=\frac{1}{2}t_0$) ; during the night the term containing α_3 is absent. Since n_3 and $\log n_3$ do not indefinitely increase with time, but (at the equator, where there is no annual variation) merely undergo a daily cycle, the integral of $d \log n_3/dt$ over a whole day must be zero. Hence

$$\frac{2t_0}{\pi} \alpha_3 = \int \frac{K_{12} n_1 n_2}{n_3} dt, \quad . \quad . \quad . \quad . \quad (21)$$

where the integral on the right is extended over the whole 24 hours ($2t_0$) ; or, what is equivalent,

$$\alpha_3 = \pi \left[\frac{K_{12} n_1 n_2}{n_3} \right], \quad \ldots \ldots \quad (22)$$

where the square brackets denote that the daily mean value of the enclosed expression is intended. Thus, the daily mean value of $K_{12}n_1n_2/n_3$, being equal to α_3, must with increasing height tend to the finite limit $\sigma_3(I_3)$.

Ozone is formed only by the reaction (*b*), and the term $K_{12}n_1n_2/n_3$ on the right of (14) may be termed the (ozone-) "production" term ; the term $-\alpha_3 \cos(\pi t/t_0)$ may be called the (ozone-) dissociation term. The dissociation curve, representing the variations of this term throughout the day, is here taken to be of the same form at all heights (though this is not strictly true), and its amplitude increases with height to a finite limit. The "production" curve, representing the daily variation of $K_{12}n_1n_2/n_3$, must enclose an area equal to that of the dissociation curve, since n_3 and $\log n_3$ are periodic in a day (at least at the equator, where there is no annual variation). At the level h_m the two curves are as shown in fig. 1, the production (shown by a dotted line) almost balancing the dissociation (shown by a full line) at all times.

The factor $K_{12}n_2$ in the production term decreases upwards as $\exp(-2h/H)$ so long as the O_2 concentration in the air remains fairly constant ; since H is about 8·5 km., this exponential decreases approximately in the ratio 10 to 1 for each 10 km. change of level. Thus, taking h_m to be 45 km., at 55 km. $\exp\{(h_m-h)/H\}$ is 0·1, at 65 km. it is 0·01, and at 80 km. it is about 0·0003. The corresponding change in $K_{12}n_2$ greatly affects the form of the production curve. At night ozone is formed at the expense of O at the rate $K_{12}n_1n_2$, so that the O disappears at least as rapidly as $\exp(-K_{12}n_2t_0)$. At the level h_m nine-tenths of the O remaining at sunset has disappeared in less than 7 minutes ; 10 km. higher the same decrease will take 10 times longer—that is, in 70 minutes or less. At 80 km. only a small fraction of O will have disappeared, *by formation of ozone*, even by the following dawn ; this fraction is $1-\exp(-K_{12}n_2t_0)$, or $K_{12}n_2t_0$ itself when this is small. Taking $K_{12}n_2 = 6.10^{-3}$ at h_m, at 80 km. only about 80 per cent. of the O left at sunset has become transformed into O_3 by dawn.

During the night n_1 decreases (owing to this and also to other reactions), while n_3 increases ; hence $K_{12}n_1n_2/n_3$ decreases for both reasons. The night-time increase in n_3

must be balanced by an equal day-time decrease, and *vice versâ* for the O. Thus $K_{12}n_1n_2/n_3$ increases by day, though not necessarily throughout the whole daylight period; indeed, the night-time increase of n_3 or $\log n_3$ must continue for a

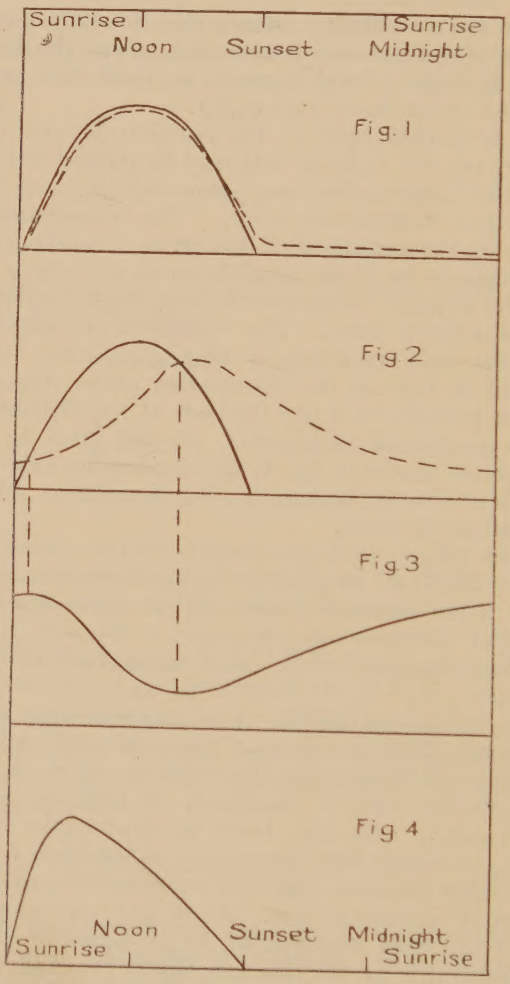

short time after dawn, before the dissociation has increased sufficiently to balance the new production.

At the level h_m we have estimated α_3 as 6.10^{-4} at 80 km., and above h_m it will be somewhat greater. At dawn at these levels n_3 is greater than at sunset by not less than

$K_{12}(n_1)_{\text{dawn}} n_2 t_0$, since n_1 has its least value at dawn; hence $(n_3)_{\text{dawn}} \geq K_{12}(n_1)_{\text{dawn}} n_2 t_0$, and $(K_{12} n_1 n_2/n_3)_{\text{dawn}} \leq 1/t_0$, *i. e.*, $1/(4{\cdot}32.10^4)$, or $0{\cdot}23.10^{-4}$; this is much less than α_3. From this value it sinks slightly further to a minimum shortly after sunrise; very soon, however, as O_3 (and O_2) become dissociated, increasing n_1 and decreasing n_2, $K_{12} n_1 n_2/n_3$ begins to rise to a maximum which must be attained somewhat before sunset, when again the production of O_3 gains on the dissociation. From these considerations, and the equality of area of the two graphs, it follows * that the production graph at these high levels must be somewhat like the dotted curve in fig. 2. The maximum of $K_{12} n_1 n_2/n_3$ must be not much less than α_3.

The curve giving n_3 itself is determined, apart from an arbitrary constant, by the curves of fig. 2, and is as shown in fig. 3. The form of $\alpha_3 n_3 \cos(\pi t/t_0)$ during the day is given in fig. 4. The curves of figs. 2–4 probably tend towards a limiting form with increasing height.

The area of fig. 4 represents the total daily dissociation of ozone according to the equation

$$\frac{dn_3}{dt} = -\alpha_3 n_3 \cos\frac{\pi t}{t_0} + K_{12} n_1 n_2, \quad . \quad . \quad . \quad (23)$$

omitting the smaller terms on the right (*cf.* 20). This area may be expressed as $2t_0 A \alpha_3 [n_3]$, where $[n_3]$ denotes the mean value of n_3 throughout the whole 24 hours, and A is a constant which would be $1/\pi$ if n_3 were constant, and which is probably not much different from this—say between $\frac{1}{4}$ and $\frac{1}{2}$—when n_3 has the form shown (apart from an undetermined additive constant) by fig. 3. Since the integral of $K_{12} n_1 n_2$ throughout the day, that is $2t_0 K_{12} [n_1] n_2$, must equal the area of fig. 4, we have

$$\frac{[n_3]}{[n_1]} = \frac{K_{12} n_2}{A \alpha_3}, \quad . \quad . \quad . \quad . \quad . \quad . \quad (24)$$

a result already suggested, though not proved, by (22).

In (24) α_3 increases with height to a finite limit, while $K_{12} n_2$ decreases proportionately to $\exp(-2h/H)$ so long as the oxygen-nitrogen ratio does not depart much from its normal value. Thus, $[n_3]/[n_1]$ must decrease at least as rapidly as $\exp(-2h/H)$. At the level h_m, $[n_3]$ is about 8.10^{12}, while $[n_1]$ is approximately $(1/\pi)(n_1)_{\text{noon}}$; probably

* The complete variation of n_2 and n_3 can be worked out by quadratures, but in view of the uncertainty as to the numerical values of certain of the factors involved this is at present scarcely worth while.

$(n_1)_{\text{noon}}$ is not more than ${}_{10}^{1}n_3$; taking it to be *equal* to ${}_{10}^{1}n$, or 8.10^{11}, $[n_3]/[n_1]$ will be about 10π at this level; but the real value can be determined only when the daily variation of the ozone content of the atmosphere can be measured. If $[n_3]/[n_1]$ is 10π at 45 km., then at 80 km. it will be less than 0·01.

Owing to the rapid upward decrease of $[n_3]$ $[n_1]$ the neglected terms in (19) are still less important than at the latter level, so that the above argument needs no revision on their account.

8. By adding (5) and (7) we obtain the equation governing the variation of n_1+n_3, namely,

$$\frac{d(n_1+n_3)}{dt} = 2(\mathrm{N}_2-\mathrm{K}_{11}n_1^2-k_{13}n_1n_3-k_{33}n_3^2)\ ; \quad (25)$$

this is independent of the processes (*b*) and (*f*)—that is, of the dissociation and formation of ozone. This equation holds during daylight; at night the term N_2 must be omitted. The ratio of the term $k_{33}n_3^2$ to the term $\mathrm{K}_{11}n_1^2$, at the level h_m, appears (*l. c.*) to be negligible; at greater heights it varies approximately as $(k_{33}/\mathrm{K}_{11})\{[n_3]/[n_1]\}^2$—that is, proportionately to $\exp(-3h/\mathrm{H})$; thus $k_{33}n_3^2$ can be neglected at all heights above h_m. The ratio of the term $k_{13}n_1n_3$ to $\mathrm{K}_{11}n_1^2$ will vary approximately as $\exp(-h/\mathrm{H})$ above h_m: at h_m, according to the very tentative estimates mentioned at the end of § 5, the daily mean value of the ratio is about $\frac{1}{3}$ (taking $[n_3]/[n_1]$ as 10π, and k_{13}/K_{11} as ${}_{100}^{1}$), so that at 80 km. it will be about ${}_{200}^{1}$; at and above 80 km., therefore, $k_{13}n_1n_3$ can be neglected, so that (25) reduces to

$$\begin{aligned}\frac{d(n_1+n_3)}{dt} &= 2(\mathrm{N}_2-\mathrm{K}_{11}n_1^2) \qquad (h>80\text{ km.})\\ &= 2\left\{\alpha_2 n_2 \cos\frac{\pi t}{t_0}-\mathrm{K}_{11}n_1^2\right\} . \quad . \quad . \quad (26)\end{aligned}$$

Hence, as in § 7, since the daily variation of n_1+n_2 is cyclic,

$$[n_1^2] = \frac{1}{\pi}\frac{\alpha_2 n_2}{\mathrm{K}_{11}} = \frac{1}{\pi}\frac{\alpha_2 n_2}{k_{11}n}, \quad . \quad . \quad . \quad . \quad (27)$$

writing $\mathrm{K}_{11}=k_{11}n$, where k_{11} is independent of the air density. The right-hand side of (27) varies with height owing both to α_2, which increases upwards to a finite limit, and to n_2/n, though the latter is nearly constant so long as only a small fraction of the oxygen is dissociated, and so long as the oxygen-nitrogen ratio is maintained uniform by

convective mixing; the latter may be effective up to 100 km. or more. Thus, at and somewhat above 80 km., $[n_1^2]$ probably varies only slightly with height; its magnitude can scarcely be estimated at present, but if the values of $\alpha_2 n_2$ (2.10^6) and K_{11} (8.10^{-15}) tentatively estimated for the level h_m are adopted, we get $[n_1]^2 = 8.10^{23}$ approximately, or, at levels where n_1 does not vary much throughout the 24 hours (as is the case above 80 km.), $[n_1] = 3.10^{11}$, the same as the estimated mean value of n_1 at level h_m.

So long as $[n_1]$ is varying slowly with height it follows from § 7 that $[n_3]$ varies as $\exp(-2h/\mathrm{H})$; at 80 km., taking $[n_3]/[n_1]$ as 0·01, as estimated, we have $[n_3] = 3.10^9$. At this level n_2 will be of order 10^{14}, so that there only a small fraction of the oxygen exists in the atomic form or as ozone. At 120 km., however, where n_2 is of order 10^{12}, the value 3.10^{11} for $[n_1]$ represents a considerable proportion of dissociated oxygen (at this level the ozone concentration has become very small, n_3 being less than 10^5).

9. The estimates of n_2 which have been quoted in § 8 are based on the assumption that the oxygen-nitrogen ratio is maintained nearly constant by convective mixing; this need not be very rapid in order to counteract the rate of diffusive separation, which is slow until great heights are attained. The mixing will also affect the distribution of atomic oxygen and ozone, tending to make it more uniform; thus, it will tend to make the ozone decrease upwards less rapidly than has been estimated in § 7. If interchange between different levels, by mixing or diffusion, were absent, the atomic oxygen would remain nearly constant in absolute density (n_1) over a wide range of height, its relative concentration therefore increasing upwards; convective mixing must tend to make the concentration more nearly uniform, thus increasing n_1 in the lower levels at the expense of the upper ones. The extent to which this tendency is effective will depend on the relation between the rate of interchange of air between different levels by mixing, the rate at which the light atomic oxygen rises by diffusion, and the rate at which the atomic-oxygen density at any level tends, by dissociation or recombination, to the equilibrium value determined by (21); the first of these rates is entirely unknown, the second increases with height, while the third decreases with height. To prove the last of these statements it is only necessary to consider the total number of oxygen atoms formed in a day at level h by dissociation; this is $2\int N_2\,dt$, or (taking $\alpha_2 n_2 = 2.10^6$ at level h_m) $(2t_0/\pi).2.10^6 \exp\{(h_m - h)/\mathrm{H}\}$,

that is, $5.10^{10} \exp\{(h_m - h)/\mathrm{H}\}$, or $\frac{1}{6}[n_1] \exp\{(h_m - h)/\mathrm{H}\}$, according to the above estimate of $[n_1]$. Thus, at 80 km., for example, where the exponential factor is about $\frac{1}{25}$, it would take 330 days to attain the equilibrium value of $[n_1]$ if originally there were no atomic oxygen and if, during these 330 days, there were no reactions removing the oxygen atoms. Thus it is clear that a departure from the equilibrium state, by convective mixing or diffusion, would be restored only very slowly, at and above 80 km., by dissociation and recombination.

Owing to our ignorance of the degree of convective mixing it is impossible to form any definite conclusion as to the precise value of $[n_1]$ at any level above 80 km., but, as we ascend, diffusion must become relatively more important, and this will tend to make atomic oxygen predominate over molecular nitrogen and oxygen. If, above some high level such as 120 km., convective mixing ceases, the state at higher levels will be intermediate between the distributions corresponding to purely diffusive and purely reactive equilibrium: according to the former, n_1 would vary with height approximately in proportion to $\exp(-h/2\mathrm{H})$, corresponding to the fact that the atomic weight of oxygen is roughly half the mean molecular weight of air, while n_2 would vary nearly as $\exp(-h/\mathrm{H})$—that is, as n_1^2. The equilibrium between dissociation and recombination, given by (21) as $n_2 \propto n_1^2 n$, implies a more rapid rate of decrease of n_2/n_1 with height than would correspond to diffusive equilibrium. The actual state at very high levels, assuming hydrogen, helium, and atomic nitrogen to be absent, will be one in which the fractional concentration of molecular oxygen diminishes upwards somewhat more rapidly than would correspond with an undissociated mixture of molecular nitrogen and oxygen in diffusive equilibrium. There is, however, no apparent reason why atomic nitrogen should not be present as well as atomic oxygen, and according to Slipher and Sommer there is definite evidence for this in the auroral spectrum *.

10. While the foregoing discussion is unavoidably speculative in so far as it involves numerical estimates, two main conclusions stand out as highly probable. The existence of ozone implies a mechanism which will form atomic oxygen by dissociating oxygen molecules: this mechanism is almost certainly, at least in part, ultra-violet radiation, which will be absorbed gradually as it passes through the highest

* V. M. Slipher and M. A. Sommer, *Naturwiss.* xvii. p. 802 (1929).

atmospheric strata, there dissociating oxygen. At sufficiently great heights recombination will be slow, so that little ozone will be formed, and atomic oxygen will accumulate; and it will rise by diffusion until (in the absence of hydrogen and helium), together with atomic nitrogen, it becomes the chief atmospheric constituent. On the other hand, as we descend the oxygen atoms will more and more readily attach themselves to oxygen molecules, to form ozone. These, in brief, are the reasons which render it likely that (1) the ozone concentration diminishes rapidly with height above the level of maximum concentration, and especially above the level at which convective mixing is important, and (2) the atomic oxygen concentration increases upwards until it exceeds that of molecular oxygen.

XXXVI. *The Effect of the Surrounding Medium on the Life of Floating Drops.* *By* L. D. Mahajan, *M.Sc., Professor of Physics, Mohindra College, Patiala* *.

IN a previous paper † the author gave some general accounts of the "Liquid Drops on the same Liquid Surface." The author has now tried to find out if there is any effect of the surrounding medium on the life of the liquid drops floating on the same liquid surface. Several gases and liquids have been tried, and their densities, viscosities, and surface-tensions found at various temperatures. It is found that the nature of the surrounding medium affects the life of the floating drops. Calmness of the weather and viscosity of the surrounding medium have an effect on the life of the drops.

Method.

A very fine nozzle was attached to the jet-end of the burette. The liquid was dropped from the burette through the nozzle on the surface of the same liquid, kept in a shallow dish. The nature of the surrounding medium was varied by simply changing the surrounding medium, air, into some other gases, or some light liquids (lighter than the liquid used to form the drops) at room-temperature or at high

* Communicated by the Author.

† J. B. Seth, C. Anand, and L. D. Mahajan, "Liquid Drops on the same Liquid Surface," Phil. Mag. vii. pp. 247–253 (Feb. 1929).

temperature. Fig. 1 represents the method when the surrounding medium is some gas instead of air, and fig. 2

Fig. 1.

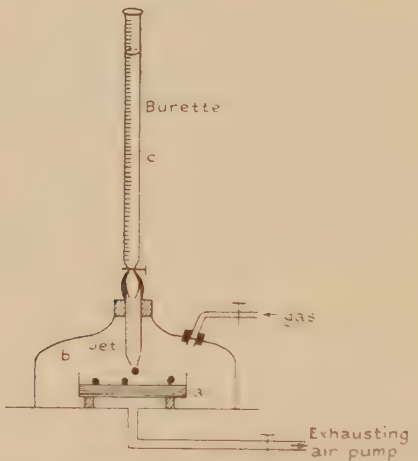

a, shallow dish containing water; *b*, vessel containing CO_2; *c*, burette containing water.

Fig. 2.

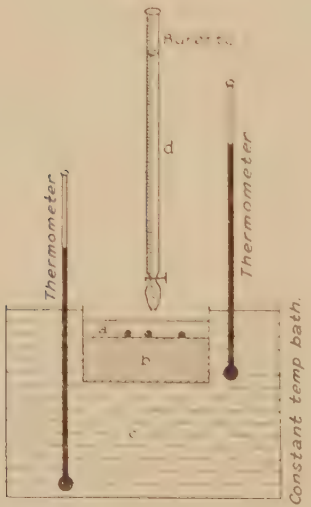

a, olive oil; *b*, water; *c*, constant temp. bath; *d*, burette containing water.

represents the method when the surrounding medium is some light liquid instead of air.

The observations in the following Table were taken :—

No.	Liq. of Drops.	Surrounding Medium.	Mean Life of a Drop.	Viscosity of the Surr. Med.
			sec.	
1.	Water	Air	·5	$1{\cdot}84\times10^{-4}$
2.	„	Carbon dioxide...	·5	$1{\cdot}9\times10^{-4}$
3.	„	Petrol	4·0	·02
4.	„	Olive-oil at 80° C.	13·5	·083
5.	„	„ „ „ 60° C.	45·0	·19
6.	„	„ „ „ 50° C.	76·0	·43
7.	„	„ „ „ 20° C.	180·0	·95
1.	Boys' Soap Solution	Air	4·5	$1{\cdot}84\times10^{-4}$
2.	„ „ „	CO_2	4·5	$1{\cdot}9\times10^{-4}$
3.	„ „ „	Petrol	12·5	·02
1.	Aniline	Air	3·0	$1{\cdot}84\times10^{-4}$
2.	„	CO_2	3·0	$1{\cdot}9\times10^{-4}$
3.	„	Water	8·0	·01

A curve, for the case of water-drops, is drawn (fig. 3) showing the relation between the mean life of the drop and the viscosity of the surrounding medium. The form of the curve shows that, as the viscosity of the surrounding medium increases, the life of the drop also increases in the same manner.

Discussion.

Under ordinary circumstances, at the room-temperature neither water nor olive-oil is able to form good drops; but when the medium surrounding the drops is changed to some more viscous substance the life of the drop is greatly increased. Then the drop becomes very stable. The stability increases as the viscosity of the surrounding medium increases. This fact is quite evident from the experimental results tabulated above and the curve shown in fig. 3. Hence the more viscous the surrounding medium the stabler the drops are and the longer the life they have. The density and the surface-tension of the surrounding medium have no effect on the life of the floating drops.

This shows that the effect of the surrounding medium is caused by the cushions of the surrounding medium formed in between the drop and the free liquid surface. The more viscous the surrounding medium, the stronger the layer which tends to prevent the drop from combining or mixing with the free liquid surface.

The above theory is supported by another important fact, namely, that it is very difficult to get water-drops floating on the water surface if the surrounding air (surrounding medium) is disturbed, for this tends to remove the cushion away from beneath the water-drop floating on the water surface. Moreover, it is also observed in this case that the

Fig. 3.

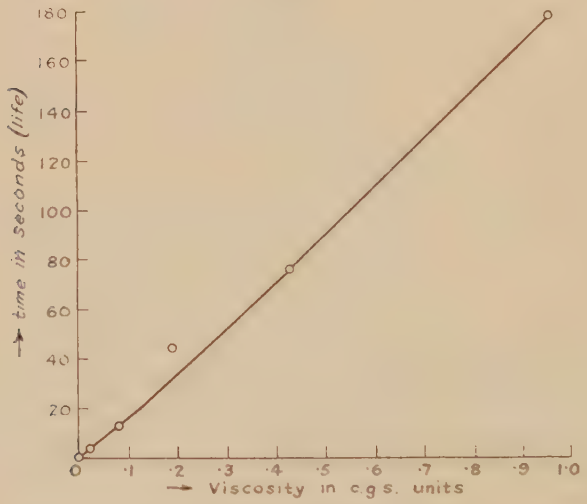

surrounding air (surrounding medium) should be free from dust particles. The second condition is fulfilled if the water be splashed continuously for about twenty minutes before the actual experiment is performed.

Conclusion.

Further experiments are being performed to find out the actual mathematical relation between the life of a floating drop and its properties, which the author hopes to give in a future paper.

Physics Laboratory,
Mohindra College, Patiala.
March 31, 1930.

XXXVII. *The Space Distribution of X-Ray Photoelectrons from a Solid Film.* *By* Lewis Simons, *D.Sc., Reader in Physics, Birkbeck College (University of London)* *.

IN a recent work Auger and Perrin † have investigated the hypothesis that the probability of photoelectric ejection at an angle ξ to the electric vector of a plane polarized wave is proportional to $\cos^2\xi$. Wentzel ‡ has deduced this result from the view point of wave mechanics. It has been verified in the case of the emission of photoelectrons from gases by Auger §. At the outset it must be stated, however, that the phenomenon is complicated by the asymmetry produced in what would otherwise be a longitudinally symmetrical distribution by considerations such as the transfer of momentum from the incident quantum to the photoelectron and the interaction of the magnetic force in the wave-front upon it ‖. These effects will be small in comparison with the major one, and their influence on the lateral asymmetry required by the "cosine squared" law for a plane polarized wave will be correspondingly small.

The angular distribution of photoelectrons from solids has been investigated by Watson ¶. In this case magnetic spectra were obtained of the photoelectrons ejected at various angles to the wave-front of homogeneous X-rays incident upon metal foils. The photographic records show that the maximum velocity of ejection of the photoelectrons is the same in all directions. This is an important conclusion from the point of view of the validity of Einstein's photoelectric equation, also as in the case of gases the emitted particles preponderate in a direction a little forward of that given by the probability law. Watson makes this direction about 80° to the forward direction of the beam. In a more recent paper Watson and Van der Akker ** have gone farther in demonstrating photographically the way in which the numbers of K, L, M, etc. photoelectrons fall off with respect to one another with increasing obliquity of the unpolarized beam upon the radiator. The general nature

* Communicated by the Author.

† P. Auger and F. Perrin, *C. R.* clxxx. p. 1742 (1925); *Jour. de Physique*, viii. 2, p. 93 (1927).

‡ G. Wentzel, *Zeit. f. Physik*, xl. p. 574 (1926). *Cf.* Beck, *loc. cit.* xli. p. 443 (1927).

§ Auger, *Jour. de Physique*, ix. 7, p. 225 (1928).

‖ Carrelli, 'Nature,' June 1st, 1929, p. 836.

¶ E. C. Watson, Phys. Rev. xxx. p. 479 (1927).

** Proc. Roy. Soc. A, cxxvi. p. 138 (1929).

of their results will be referred to later. The probability law, however, could hardly be investigated by Watson's method. In passing it should be noticed that this probability law, together with Einstein's photoelectric law, would require, not only that the maximum velocity of ejection should be independent of direction, but also that all unscattered photoelectrons of minor velocities should have the same spatial distribution as the most rapid ones. In the work described below the method of the retarding electric field has been used. The angle of incidence of X-rays upon

Fig. 1.

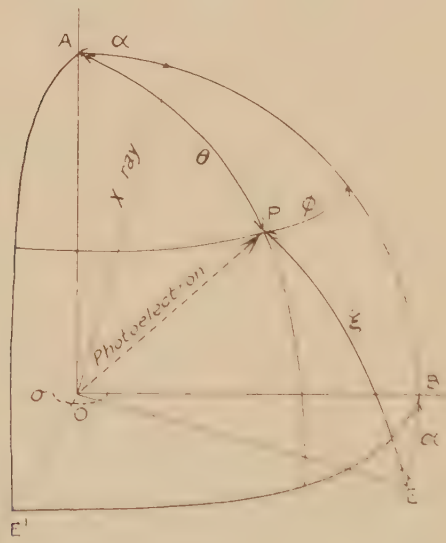

a thin gold film has been varied and the photoelectric currents measured in the ordinary manner. The author believes that he has succeeded in verifying the probability law, and other interesting results have been obtained.

In fig. 1 let us suppose that the fixed surface σ at O emits electrons in all directions under the influence of a plane polarized ray making an angle α to OA, the normal to σ, and lying in the plane AOB. Let OE represent the direction of the electric vector in the wave-front. The direction of ejection of the electron OP makes an angle ξ with the direction of the electric vector in the light producing it. The angles θ and ϕ define the direction of OP.

Regard the problem as of the same type as for gas molecules flying through a surface element σ. The electrons moving in the direction OP with a velocity v would fill a cylinder of base σ and height $v\cos\theta$ in 1 sec. Similarly, all the electrons of any velocity moving in the direction OP would in 1 sec. fill a similar cylinder of height $\cos\theta\,\Sigma v$. Confining our attention, however, to electrons of one velocity, we may say that the number passing per sec. through a small aperture $d\omega$ of which OP is axis is proportional to $\cos\theta\,d\omega$ or to

$$\sin\theta\cos\theta\,d\theta\,d\phi. \quad . \quad . \quad . \quad . \quad . \quad \text{(i.)}$$

Supposing, now, there is an added probability which is independent of other factors and of the velocity, viz. the probability of ejection in the direction OP is proportional to $\cos^2\xi$, then the number of electrons passing through the aperture will now be proportional to $\sin\theta\cos\theta\cos^2\xi\,d\theta\,d\phi$. Now, in the spherical triangle APE,

$$\cos\xi = -\sin\alpha\cos\theta + \cos\alpha\sin\theta\cos\phi; \quad . \quad . \quad \text{(ii.)}$$

hence P, the number of electrons passing per second through a given conical aperture with OA as axis and of semi-vertical angle $\bar{\theta}$, which we may call the gathering angle, will be given by

$$P_{\bar{\theta}} \propto \int_0^{\bar{\theta}} \int_0^{2\pi} \sin\theta\cos\theta(-\sin\alpha\cos\theta + \cos\alpha\sin\theta\cos\phi)^2 \, d\theta\,d\phi. \quad . \quad . \quad \text{(iii.)}$$

If $\alpha = 0$, then $P_{d\theta}$, the probability of photoelectron emission between angles θ and $\theta + d\theta$ to the ray, will be given by the usual expression

$$P_{d\theta} \propto \sin\theta\cos\theta\,d\theta. \quad . \quad . \quad . \quad . \quad . \quad \text{(iv.)}$$

whilst generally

$$P_{\bar{\theta}} \propto \sin^4\bar{\theta}(1+\sin^2\alpha) + 4\sin^2\alpha\sin^2\bar{\theta}\cos^2\bar{\theta}$$

when we are dealing with emission within a cone of semi-vertical angle $\bar{\theta}$, the ray making an angle α to the axis of the cone.

The following cases are important to this work, viz.:

if $\bar{\theta} = 0$, then $P_{\bar{\theta}} = 0$,

„ $\bar{\theta} = \frac{\pi}{2}$, „ $P_{\pi/2} \propto (1 + \sin^2\alpha)$.

In this latter case we are dealing with the emission of electrons from the element σ, lying in the diametral plane

of a hemisphere, to the hemispherical space around it, the ray being inclined at an angle α to the axis of symmetry of the hemisphere. Twice as many particles would emerge when the ray is glancing along the surface $\left(\alpha=\frac{\pi}{2}\right)$ as when the ray is normal to σ ($\alpha=0$). There has not been introduced any question as to the absorption of the particles in the material from which they emerge, nor of any momentum and energy interchange between the effective quantum and the electron.

Conditions of the experimental work must now be considered briefly in order to show that the above limiting values of θ are valid, as otherwise it would be necessary to consider a much fuller analysis of a difficult mathematical problem which would involve an exact knowledge of the distribution amongst velocities of the particles and the relation between the retarding potential and the effective semivertical angle θ *.

It has already been shown by the writer that the surface of a thin metallic film irradiated by X-rays is the source of two distinct groups of electrons †. The more rapid group consists of the primary photoelectrons, whilst the well-marked slower and more copious stream is probably produced by some secondary action. A Maxwell distribution in speeds exists amongst members of the slower group, for which the most probable speed was determined to be of the order 3 electron volts. The character of the curve was independent of the wave-length of the incident X-rays and of the metal emitting. When a retarding potential below -15 volts or an accelerating potential above $+15$ volts was applied to the film little, if any, changes in current could be observed. A typical curve representing current leaving the film against applied potential is shown in fig. 2. The fast group was named β and the slower group δ-rays. In interpreting the curve it was assumed that the maximum ordinate gave a measure of the number of electrons of both types leaving the film per sec. and the smallest ordinate the number of the β type. Rudberg has recently extended these observations in the soft X-ray region and justified the writer's conclusions ‡, his soft X-rays being about 100 times the wave-length of those employed in the above research. The fact that

* *Cf.* O. W. Richardson's thermionic problem; for a summary see Lorentz, 'Lectures on Theoretical Physics, I.' p. 171 (1927).

† Phil. Mag. xlvi. p. 473 (1924).

‡ E. Rudberg, Proc. Roy. Soc. A, cxx. p. 385 (1928).

Rudberg was able to bake out a fair part of the δ current in some cases, and also that Farnsworth * has stated that the whole of the δ current is due to surface gas films, does not invalidate any conclusions concerning the directional relationships between the incident X-rays and the photoelectrons, whatever be the source of the latter.

In the light of the above, consider now the experimental arrangements adopted in this work. Let the small circular element of the film σ emitting electrons be mounted at the

Fig. 2.

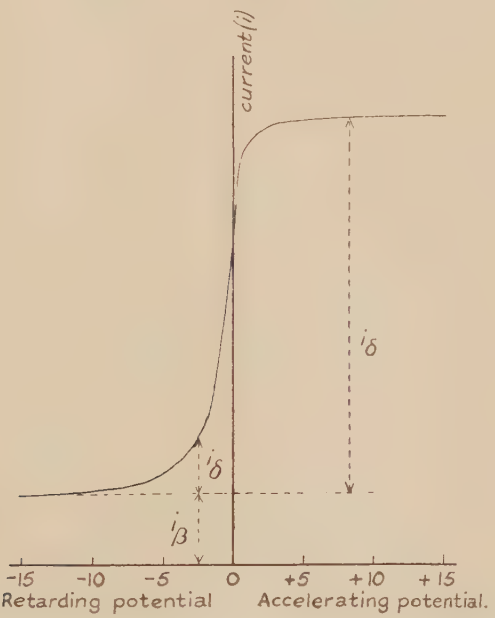

centre of an extended conducting plane near to, and parallel to which is another conducting plane. An accelerating or retarding potential can be applied between the two. Assuming that a retarding potential of -15 volts has an insignificant influence upon the β-rays, but completely returns all the δ-rays to the plane from which they emerge, then the effective angle $\bar{\theta}_\beta$ of the conical aperture from which the β-rays pass from σ to the opposite extended plane remains practically $\pi/2$, whilst $\bar{\theta}_\delta$, the corresponding angle for the δ-rays, is zero, as none get across. As the angle of incidence

* Phys. Rev. xxxi. p. 413 (1928).

α of the X-rays on the surface σ is now varied, we have :— Retarding potential of 15 volts: all δ-rays stopped, no influence on β rays :

$$\theta_\delta = 0 ; \qquad I_\delta = 0 ;$$
$$\theta_\beta = \pi/2 ; \quad I_\beta \propto (1 + \sin^2 \alpha).$$

Again, if the potential difference between the plates is zero, both the β- and the δ-particles will be unaffected. Assuming tentatively that the δ particles have the same fundamental distribution as the β-particles, then for this case we have :— No potential difference between the plates: no influence on either δ or β rays :

$$\theta_\delta = \pi/2 ; \quad I_\delta \propto (1 + \sin^2 \alpha) ;$$
$$\theta_\beta = \pi/2 ; \quad I_\beta \propto (1 + \sin^2 \alpha) ;$$

providing such curves are drawn for various settings of α. This would show that for a given setting of α it is legitimate to subtract the *total* ionization current when the potential difference between the plates is zero from that when it is 15 volts retarding (say). The result is a measure of the δ-current. The constant of proportionality is the same throughout. Or otherwise the difference between maximum and minimum ordinates of curves drawn in fig. 2 gives the δ-current, whilst the minimum ordinate gives the β-current. As a matter of fact, the potential difference between the plates was not zero as above, but an accelerating potential of +15 volts was applied for the maximum ordinate. Probably the effect of this is to create artificially the conditions of an infinite plane for the δ-particles, most of which have so small a proper velocity of emission.

The Polarization of the X-ray Beam.

The above considerations are for a plane polarized beam. In experimental work the complete polarization of an X-ray beam cannot be accomplished. An ordinary X-ray beam cannot be employed in consequence of its partial polarization. Arguing from the principle of the incoherence of independent monochromatic light trains, Auger and Perrin * have assumed that completely unpolarized monochromatic light may be regarded as two phase independent beams of equal intensity polarized at an angle of $\pi/2$ to each other. Indeed, it is only by making such an assumption, together with the $\cos^2 \xi$ law already quoted, that the obvious lateral symmetry of the ejected electrons about an unpolarized ray may be deduced.

* *Journ. de Phys.* viii. p. 93 (Feb. 1927).

The scheme adopted therefore in these experiments was to take every instrumental reading for each of four settings of the X-ray tube corresponding to four directions of the cathode ray stream separated by angles of $\pi/2$ to each other. The mean of the four readings was taken to be the effect of a perfectly unpolarized beam.

Fig. 4 shows the schematic arrangement of apparatus. The axis of the X-ray tube could be moved in a vertical plane about the anticathode as centre. The plane of the disk emitting electrons was vertical. This could be rotated about a fixed vertical diameter, thus varying α (fig. 1).

Let us now choose two arbitrary directions at right angles to each other, both lying in the plane of the wave-front. These directions, according to the above, will correspond to the directions of the equal electric vectors in the unpolarized

Fig 3.

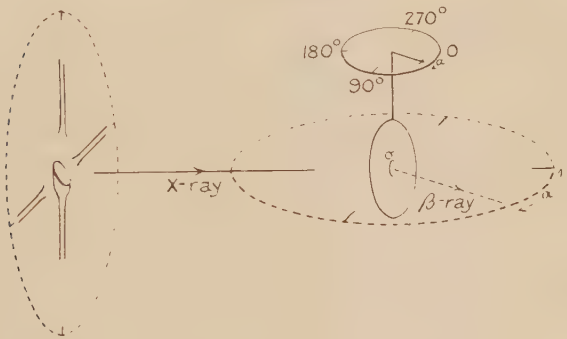

X-ray beam, the one (OE, fig. 1) lying in the plane of the paper, and the other, OE′, perpendicular to it. As the ray moves through a given angle α to the normal OA, the direction OE also moves through an angle α, but OE′ remains unaffected. When $\alpha=0$, *i. e.*, when the ray is normal to the disk, one-half of the observed effects will be due to either polarity. The half due to OE′ will remain unaffected for any variation of α, whilst that due to OE should alter with α, according to the expression given above.

Description of Apparatus.

Geometrical accuracy and the elimination of spurious X-ray effects were the chief factors governing the design of the apparatus. Fig. 4 shows a section to scale. The disk σ was made by sputtering gold in air on to celluloid 0·003 inch in thickness. From the large uniform piece a

small circular piece 1·2 cm. in diameter was cut by needle-point spring compasses. The colour of the film was pale blue by transmitted white light, and estimating from the mass of an ordinary gold leaf, the gold of the film was probably not more than 10^{-6} cm. in thickness. A piece of silk gauze was stretched taut on the brass ring A, the mesh of the gauze being closed with a thin mixture of pure graphite and sugar solution, and when dry the disk was laid exactly on the middle of this, gold film uppermost, and a little of the conducting solution was carried just over the edge of the disk, making contact with the gold and thereby

Fig 4.

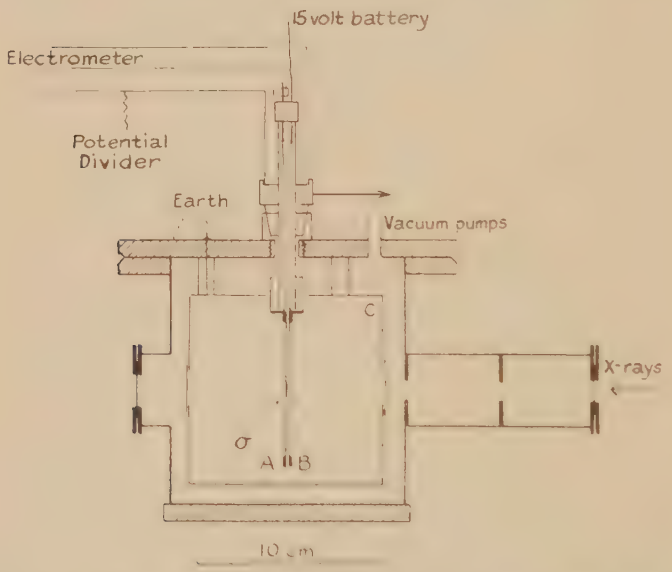

giving a continuous conducting plane surface. At B we have an exactly similar brass ring with a piece of silk gauze stretched over it. In this case the mesh was left open, but the fibres were rendered conducting by being carefully smoked with a paraffin lamp. This gauze has a mesh of 37 per cm. and weighs 0·033 gm. cm.$^{-2}$. The two planes A and B were mounted accurately parallel to each other, their distance apart being about 0·15 cm. The mounting was such that when they were turned by the conical head shown, the centre point of σ remained stationary. Leads were carried up through a brass tube; that from A went to the Wilson electrometer, and from B to a 15-volt battery. By

means of the little lug shown at the top, any cross connexion could be made. The contact point of the electrometer was accurately central on this lug, ensuring that there would be no change in the electrostatic capacity of the system when it was rotated. A thin aluminium accurately made vessel C, smoked within and provided with conducting gauze windows, surrounded the planes A and B. This was earthed, and served the purpose of limiting the space around the working system. The X-ray beam was limited by suitable lead stops, so that the disk was only just immersed in it. Details of the X-ray tube, the null method of recording, etc., will be found in the author's paper quoted above.

Heterogeneous X-ray Beam used.

The photoelectrons were liberated from the gold by the heterogeneous beam from an ordinary Coolidge radiator pattern X-ray tube. The experiments were embarked upon primarily for the purpose of studying the mode of production of the δ-rays. It has already been stated that the distribution curves for these were practically independent of the wave-lengths used, and as a compromise had to be made amongst many factors for securing a workable speed for taking readings, it was felt that the added complexity in using any method at this stage for securing homogeneity was unjustified. The disk σ had to be small, in order that the plates A and B may be regarded as infinite ; B must be near to A to secure a uniform field ; this increases the capacity, and as the potential difference between them was kept constant by hand during observation of the leaf system, it will be seen that long runs were impossible.

Experimental Results.

The currents below (Table I.), which are in arbitrary units and without any corrections, were taken for settings of α in all four quadrants. An angle of 45°, for example, between the X-rays and the normal to the film was taken as physically equivalent to one of 315°, providing every mean reading is the result of four settings of the X-ray tube to eliminate polarization as has already been described. The β-currents were obtained with a retarding potential of -15 volts between A and B; the δ-currents, by subtracting the corresponding β-currents from those obtained with an accelerating potential of $+15$ volts between A and B. Angles between 65° and 115° for the X-rays on the film could not be employed, as within this range the X-rays would have fallen upon the supporting brass rings.

It is not proposed, at this stage, to attempt to apply any experimental corrections to the above results, such as, for example, the increasing area of carbon immersed in the beam for increasing obliquity of the X-rays on the film giving a corresponding increase in the photoelectric current from the carbon. More serious corrections, by far, are involved by the varying absorption of the fast and slow photoelectrons in the film itself, varying degrees of scattering of these rays, and the recoiling effects. The plan has been rather to make a best fit of the results on to the three curves: (i.) $I = A$, corresponding to the theoretical emission due to the electric vector OE′ (fig. 1), as the current due to this remains constant for variations of α; (ii.) $I = A(1 + \sin^2 \alpha)$.

TABLE I.

Currents due to completely unpolarized X-rays.

Angle between normal to film and X-rays.	Mean value of β-current.	Mean value of δ-current.	
0°	181	517	Electrons from face of emergence of X-rays.
22°·5 (337°·5)	194	544	
45° (315°)	217	579	
65° (295°)	237	615	
115° (245°)	243	671	Electrons from face of incidence of X-rays.
135° (225°)	216	625	
157°·5 (202°·5)	186	572	
180°	180	536	

corresponding to currents due to the electric vector OE, which, if Auger and Perrin's results be true, should vary in this manner, as shown above; and (iii.) any residues there may be over.

The curves drawn in the manner described are seen in fig. 5. The two upper quadrants are for the δ or slow rays (column 3, Table I.). The lower two quadrants the β or fast rays (column 2 of the table). The two right-hand quadrants represent the figures for the two types of rays from the emergence side of the X-rays on the film, the two left-hand quadrants the corresponding rays from the incidence side. The angle indicated is α, that between the X-rays and the

normal to the film corresponding to the direction of the retarding or accelerating electrostatic field.

By altering the scale of the pair of interdependent curves i. and ii. in any one quadrant (interdependent through the value of A), both the magnitude and the shape of the corresponding residual curve iii. in that quadrant will be simultaneously altered. It is to be remembered that curve iii. contains all the errors due to experimental inaccuracy,

Fig. 5.

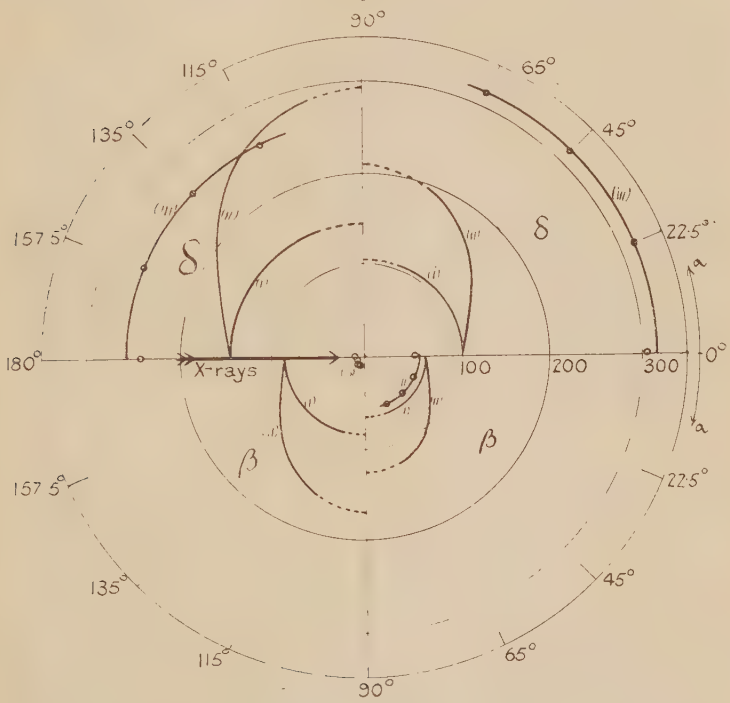

Photoelectric emission produced by a fixed, completely unpolarized, heterogeneous X-ray beam from a small movable constant area of sputtered gold film. a is the angle between the beam and the normal to the film. The radius vector I is proportional to the number of δ (below 15 volts) and β (above 15 volts—normal velocity) particles. The δ-electrons are accompanied by the β-electrons, but these have been put into the lower two quadrants for clearness. The experimental results are the sums of curves (i.), (ii.), and (iii.). Curve (i.) is $I=A$ (constant) due to the electric vector normal to the paper. Curve (ii.) is $I=A(1+\sin^2 a)$ due to the equal electric vector lying in the plane of the paper. Curve (iii.) is the experimental residue due to both vectors, containing electrons diffused, scattered, and distributed by unknown causes.

together with other factors already mentioned that have not been taken into consideration.

If we accept the view that the predominant factor is simple diffusion of the electrons on emergence from the film, then the directive influence of the electric vector in the incident X-rays will have disappeared, *i. e.*, ξ will have disappeared in the expression (iii.) for P_θ : and thus for particles represented by the residual curves (iii.) there will be a uniform radial distribution, providing we can say that the effective gathering angle θ is independent of α. This appears to be the case.

There are, of course, a number of ways in which a uniform distribution of electrons independent of the angle α might arise, but the following is of special interest in this connexion. Instead of the surface σ emitting electrons, imagine a small volume quite transparent to the electronic radiation arising from within it. The number of particles passing through a small conical aperture per second of which OP is axis (fig. 1) is now proportional to $\sin\theta d\theta d\phi$. This omission of the cosine term from (i.) means that, apart from Auger's hypothesis that the favoured direction of emission should be along the electric vector, the normal to σ is not a favoured direction. Introducing the probability condition proportional to $\cos^2\xi$, we have

$$P \propto \int_0^\theta \int_0^{2\pi} \sin\theta\cos^2\xi\, d\theta\, d\phi.$$

If $\alpha=0$ in expression (ii.) for $\cos\xi$, then

$$P_{d\theta} \propto \sin^3\theta\, d\theta \quad . \quad . \quad . \quad . \quad . \quad . \quad . \quad . \quad . \quad . \quad (v.)$$

and $$P_\theta \propto \tfrac{2}{3}(1-\cos^3\theta) - \cos^2\alpha\sin^2\theta\cos\theta,$$

which is independent of α if $\theta=\frac{\pi}{2}$. In other words, the number of electrons reaching any given hemispherical surface with the small radiator as centre will be independent of the angle between the direction of the exciting polarized X-rays and the axis of symmetry of the hemisphere.

It so happens that the formula recently proposed for the photoelectric phenomenon has the form *

$$P_{d\theta} \propto (A+B\cos\theta)\sin^3\theta\, d\theta,$$

which, if divided into its two terms, would give the two *independent* sets of particles required by expressions (iv.)

* Sommerfeld, 'Atombau und Spektrallinien Wellenmechanischer Erganzungsband,' 1929, p. 218.

and (v.). This might easily be interpreted either as a volume and area effect respectively, or, in other words, ξ favoured and (ξ and normal) favoured respectively.

In the paper referred to above by Watson and Van der Akker the interesting conclusion is arrived at that the probability distribution laws differ for photoelectrons from various levels, and a theoretical suggestion due to Oppenheimer is mentioned that the space distribution of the K- and L_I-electrons follows the $\cos^2\xi$ law, whilst that of the L_{II}- and L_{III}-electrons follows the law $a_{(v)} + b_{(v)}\cos^2\xi$, a and b being constants depending on the frequency. Now, if this latter be substituted in expression (iii.), it will be seen that two independent sets of particles would arise, the first following the distribution law already quoted, viz.,

$$\propto (1 + \sin^2\alpha);$$

the second, constant and independent of α for a constant value of θ. In practice this would amount to an emission from a plane and from a transparent volume respectively, as already shown, and diffusion need not be introduced for interpreting the curves. One conjectures, therefore, that the plane and the volume are in some way identifiable with the atomic configurations from which the photoelectrons originate.

Deductions from Curves. (Fig. 5.)

If the method described above for drawing the curves of fig. 5 is valid, then from these and the data from which they are drawn, we deduce the following :—

The total number of β-electrons is approximately the same from both sides of the film.

There is greater diffusion amongst those going forward with the X-rays than amongst those travelling opposite to the X-rays producing them

All the β-rays coming from the "incidence" side of the film obey the theoretical considerations given above, suggested by Auger and Perrin.

It is suggested that that factor in the X-rays responsible for the production of the β-rays is very strongly absorbed. The majority of the β-rays are produced at the surface of the film upon which the X-rays are incident. This would account for the greater diffusion of those β-rays that emerge from that surface of the film remote from the X-ray tube. Absorption of this nature has recently been suggested by O. W. Richardson * in dealing with the soft X-ray region.

* Proc. Roy. Soc. A, cxix. p. 531 (1928).

An alternative suggestion to the above is that the admixture of the Compton recoiling electrons in the stream of β-rays moving forward in the same direction as the X-rays producing them somewhat masks the distribution given by the $\cos^2\xi$ law. No preponderance in number emerging from this side of the film is apparent; but even, according to the Compton theory, the number of electrons taking part in the modified scattering would be very small for a substance of such high atomic weight as gold. The same general principles seem to govern the emission of the slow δ-particles.

A larger fraction of those moving forward with the X-rays than of those moving in the reverse direction have a uniform radial distribution.

On the other hand, we should expect a greater general diffusion of these slow particles; this is apparent even for those moving in the reverse direction to the X-rays.

If the δ-particles are produced in a secondary manner, as many experiments suggest, the fact that such large fractions of both β- and δ-rays obey the $\cos^2\xi$ law points to the conclusion that the electric vector operates on the electron after its expulsion from the parent atom, for otherwise it is very difficult to see why the distribution of δ-particles should be of any other type than a uniformly radial one.

The total number of δ-particles moving backwards exceeds the number moving forwards for all angles of incidence, *e. g.*, for normal incidence of X-rays there are 4 per cent. more moving backwards than forwards with the X-rays, which increases to 9 per cent. for the largest angle of incidence used. This observation is not without precedent, for it agrees with certain experiments of W. Seitz *, whilst Stenberger's work on back diffusion of primary electrons † of high speed falling on metals indicates the complexity of this subject. He, too, picks out a special slow group of particles always present and independent of the speed of the primary particles producing them, and limits the group to 36 volts. In the present work this group is taken to be marked by a maximum of about 45 volts *resultant* velocity.

Arguing, then, that any secondary effects, such as diffusion, multiple ionization, etc., disturbing the ideal distribution of particles from an infinitely thin layer would, in a thicker layer, most probably tend ultimately to produce a uniform spherical distribution, these experiments have then analysed

* *Phys. Zeit.* xxv. p. 546 (1924).
† *Ann. d. Phys.* lxxxvi. 6, p. 825 (1928).

the particle stream from a very thin film due to a polarized beam into the two portions—those that, after production, have suffered a further disturbance and those that have not. The former portion have a uniform radial distribution ; the latter portion are distributed as to their number according to the law which is both classical and modern. Einstein's law and most theories of atomic structure require that the photo-electric velocities shall not be influenced by direction of emission.

We conclude, then, that the number of particles moving in a given direction times their average energy measures the square of the resolved part in that direction of the amplitude of the electric vector of the ray, or, as stated by Auger and Perrin, the probability of ejection of a particle in a given direction is proportional to the square of the cosine of the angle between this direction and that of the electric vector in the light producing it.

XXXVIII. *On the Capture of Electrons by Swift α-particles.* By J. C. Jacobsen *.

IT was found by Henderson † that α-particles, when passing through different substances, changed their charge by capture and loss of electrons. The matter was examined in more detail by Rutherford ‡. A beam of α-particles was sent through a screen of mica into an evacuated chamber, and the charge of the α-particles measured by deflexion in a magnetic field. On a zinc-sulphide screen, which was placed at the other end of the chamber, two beams were observed—the main beam, which is due to α-particles which have left the mica-leaf with a double charge, and the midway beam, due to α-particles which have captured an electron. At low velocities neutral α-particles were also observed. It was further found that an α-particle in passing through a substance changes its charge so rapidly that, for a given velocity of the α-particle, a state of equilibrium is established between the number of double-charged and single-charged α-particles. When this is the case, a mean free path λ_2 and λ_1 may be introduced for double-charged and single-charged α-particles respectively. When N_2 and

* Communicated by Prof. N. Bohr, Ph.D.
† Proc. Roy. Soc. cii. p. 496 (1923).
‡ Phil. Mag. xlvii. p. 277 (1924).

N_1 are the number of double-charged and single-charged α-particles, it can be easily shown that

$$\frac{N_1}{\lambda_1} = \frac{N_2}{\lambda_2}.$$

A determination of λ_1 in a gas can be carried out by measuring the decrease in N_1 when the deflexion-chamber is filled with the gas to a suitable pressure. If λ_1 is the mean free path referred to atmospheric pressure, the number N_p of single-charged α-particles is given by

$$N_p = N_1 e^{-\frac{pl}{76\lambda_1}} \qquad (p \text{ in cm.}), \quad . \quad . \quad . \quad (1)$$

where l may be called the effective length of the deflexion-chamber. On account of the finite width of the beam this is somewhat smaller than the geometrical length. For α-particles with a velocity $0{\cdot}94\ v_0$ the result was $\lambda_1 = 0{\cdot}011$ mm. in air. It was further found that for a given velocity of the α-particles the ratio $N_2 : N_1$ was nearly the same for the substances celluloid, mica, and silver. This could be shown by interposing a thin sheet of the substance to be examined on the inner side of the mica-leaf: when the sheet is sufficiently thin the velocity of the α-particles is not changed, while, on the other hand, the thickness is sufficient to set up a new equilibrium state between single- and double-charged α-particles. These results showed a remarkable similarity between the ratio of the probabilities for capture and loss in elements of widely differing atomic numbers. From general considerations, however, we are led to expect that for elements of very small atomic number this ratio is decidedly smaller than in heavier substances*. Indeed, from simple mechanical considerations it follows that for small nuclear charges the chance of collisions leading to capture—which claim the interaction of at least three particles—is exceedingly small compared with the chances for capture in atoms, where the presence of the nucleus has a considerable influence on the result of a collision between the α-particle and the electron. The problem has been treated in detail by Thomas†, from whose calculations it follows that for swift α-particles the probability of capture in hydrogen would be about 10^4 times smaller than in air.

The main object of the present investigation was to examine the capture of electrons in hydrogen. Experiments were made with air also, because the interpretation of

* *Cf.* Bohr, *Zs. f. Phys.* xxxiv. p. 142 (1925).
† Thomas, Proc. Roy. Soc. cxiv. p. 561 (1927).

the results with hydrogen must be carried out by comparison with a gas. The apparatus was similar to that employed by Rutherford. The α-particles entered the deflexion-chamber through a mica window. The slit which defined the beam of α-particles had a width of 0·41 mm. The scintillations were counted with a Watson "holoscopic" objective together with a low-power eyepiece ; a rectangular aperture in the eyepiece limited the field of view to a width of 2·2 mm. Close to the aperture in the eyepiece rotating sector disks could be placed, which cut down the number of scintillations in the ratio 1 : 2, 1 : 4, and 1 : 8. The pole-pieces of the magnet were circular, with a diameter of 146 mm., the deflexion of the main beam of α-particles was 18 mm. In a few experiments photographic counting of the α-particles was employed. The velocity of the α-particles in the experiments here referred to was 0·89 of the initial velocity of the α-particles from RaC. The active sources were platinum wires with radium active deposit. The technique used in photographic counting is given in a subsequent paper*.

It can be demonstrated quite simply that the probability of capture in hydrogen is several times smaller than that in air. Suppose that with vacuum in the apparatus singly charged and doubly charged α-particles are present in numbers N_1 and N_2. When gas is admitted at a suitable pressure N_1, and when capture takes place also N_2, will decrease. At the same time a continuous distribution of scintillations appears between the main beam and the midway beam, because when an α-particle changes its charge on its way through the apparatus the deflexion for an α-particle originally single charged becomes larger, and that for one originally doubly charged becomes smaller. Roughly speaking the processes $He^{++} \rightarrow He^{+}$ and $He^{+} \rightarrow He^{++}$ contribute by the same amount to the continuous distribution when the relation $N_1 : N_2 = \lambda_1 : \lambda_2$ is fulfilled, so that the number of scintillations in the continuous distribution must be smaller in hydrogen than in air, if capture does not take place in hydrogen. If the pressure of hydrogen and of air is so adjusted that N_1 has decreased in the same ratio in the two gases, the number to be expected in hydrogen will be about half of that in air.

This was found to be the case. The result of an experiment is shown in fig. 1, where the position and strength of the midway beam are indicated by dotted lines on the left side, while the dotted lines on the right indicate the position of the main beam. With vacuum in the apparatus

* See p. 413.

$N_1 : N_2$ was about 1 : 150. The pressure of air and hydrogen was chosen such that N_1 had decreased in the same ratio (about 1 : 10). The necessary pressure was determined previously. It is seen that with air the number of scintillations in the continuous distribution is from 2 to 3 times higher than with hydrogen. This means that the contribution to the continuous background from capture is much smaller in hydrogen than in air, since the contribution due to loss is the same in the two gases. A preliminary account of this result has been given previously *.

Fig. 1.

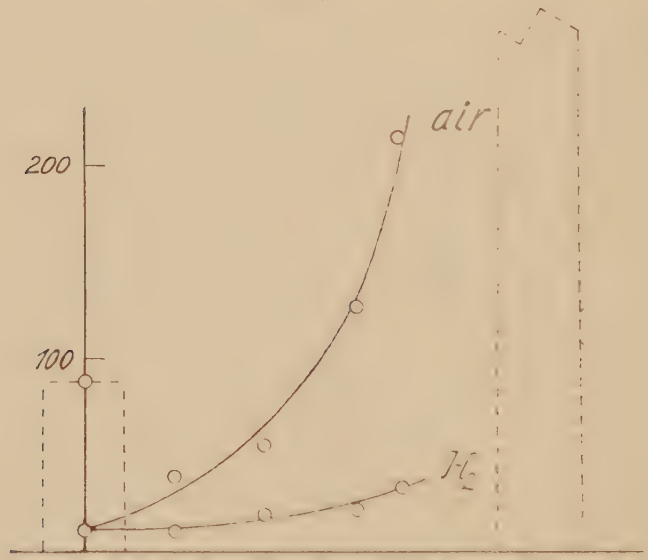

This experiment shows, in a qualitative way, that the probability of capture is several times smaller in hydrogen than in air. After this had been found, an attempt was made to obtain quantitative information by a calculation of the number of α-particles in the continuous distribution as a function of the pressure : it was hoped to get in this way an upper limit for the probability of capture in hydrogen. It was soon found that agreement between calculation and experiment could only be expected when the countings were carried out on the midway beam or close to it. This is due to the fact that with vacuum in the apparatus a "background" is already present between the main and the

* 'Nature,' June 19 (1926).

midway beam. The origin of this is not clear; it disappears when the magnetic field is cut off, so it must be due to an inhomogeneity in the velocity of the α-particles, originating in some way from the source itself or from the passage through the mica-leaf. With a field of view of width 2·2 mm., which was employed throughout, the number of scintillations in the background was generally about 10 per cent. of N_1. When a gas is admitted into the apparatus the background will change in a manner which is difficult to estimate, especially close to the main beam; only in the close vicinity of the midway beam can a correction be carried out with some accuracy.

The method which was finally adopted consisted in determining the change in the number of scintillations with increasing pressure, first with the microscope focussed on the midway beam, then with the microscope moved 2·2 mm.

Fig. 2.

(width of the field of view) towards the main beam. The two positions will be denoted by I. and II. in the following pages.

The apparatus is shown schematically on fig. 2. It is assumed that the path of an α-particle which moves without changing its charge is circular throughout its whole length. When R is the radius of the circle, the deflexion is given by

$$\Delta = \frac{l_2(l_1+l_2)}{\sqrt{4R^2-(l_1+l_2)^2-l_2^2}}.$$

Suppose now that a singly charged α-particle loses its electron at a distance x from the ZnS screen, so that it moves through a distance l_1+l_2-x with a single charge and a distance x with a double charge. The change δ in the deflexion of the α-particle can be calculated as the distance between two circles with radii R and $\frac{1}{2}$R (fig. 3).

Neglecting small quantities, δ is given by

$$(x<l_2) \qquad \delta=\frac{1}{2}\frac{x^2}{R}, \quad . \quad . \quad . \quad . \quad . \quad . \quad . \quad . \quad (2)$$

$$(x>l_2) \qquad \delta=\frac{1}{2}\frac{x^2}{R}-\frac{1}{2}\frac{(x-l_2)^2}{R}\cdot\frac{l_1+l_2}{l_1}. \quad . \quad (2\,a)$$

If, similarly, a doubly charged α-particle captures an electron

Fig. 3.

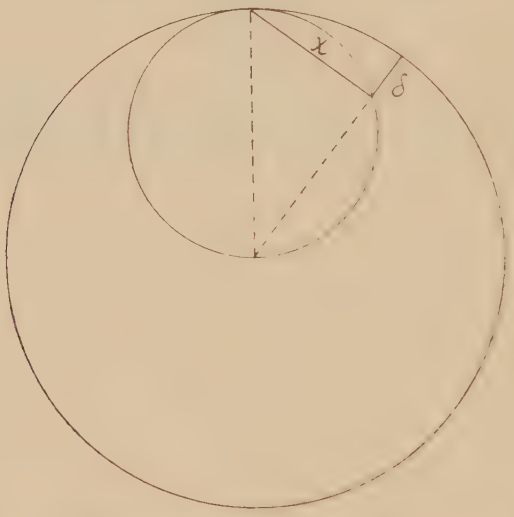

at a distance y from the mica-leaf, it will strike the screen at a distance δ from the midway beam, given by

$$(y<l_1) \qquad \delta=\frac{1}{2}\frac{y^2}{R}\cdot\frac{l_2}{l_1}, \quad . \quad . \quad . \quad . \quad . \quad . \quad . \quad (3)$$

$$(y>l_1) \qquad \delta=\frac{l_2(l_1+l_2)-(l_1+l_2-y)^2}{2R} \quad . \quad . \quad (3\,a)$$

In the following λ_1 and λ_2 denote the actual mean free paths of singly and doubly charged α-particles at a given pressure. With the microscope in position I. the number of α-particles as a function of the pressure is given by

$$n_1=N_1 e^{-\frac{l-x_1}{\lambda_1}}, \quad . \quad . \quad . \quad . \quad . \quad . \quad . \quad (4)$$

where $l=l_1+l_2$ and x_1 is determined from (2) corresponding to $\delta=1{\cdot}1$ mm. (half width of field of view).

If capture takes place there is added a number n_2 of α-particles which have captured an electron at distances from the mica-leaf such that they come inside the field of view. If y_1 is the value of y in (3) which corresponds to $\delta = 1{\cdot}1$ mm., the probability that an α-particle, which has left the mica-leaf with a double charge, comes inside the field of view is the product of (1) the probability $\frac{y_1}{\lambda_2}$ that the α-particle captures an electron between $y=0$ and $y=y_1$; (2) the probability that such an α-particle reaches the ZnS screen without losing its electron; this is given approximately by

$$\tfrac{1}{2}\left(e^{-\frac{l-x_1}{\lambda_1}} + e^{-\frac{l-y_1}{\lambda_1}}\right).$$

For n_2 we thus get

$$n_2 = N_2 \cdot \frac{y_1}{\lambda_2} \cdot \frac{1}{2}\left(e^{-\frac{l-x_1}{\lambda_1}} + e^{-\frac{l-y_1}{\lambda_1}}\right).$$

The number of α-particles which come into the field of view is thus, without capture

$$n_1 = N_1 e^{-\frac{l-x_1}{\lambda_1}}, \quad \ldots\ldots\ldots \quad (4)$$

with capture

$$n_1 + n_2 = N_1 e^{-\frac{l-x_1}{\lambda_1}} \left\{1 + \frac{y_1}{L} \cdot \frac{1}{2}\left(1 + \frac{y_1 - x_1}{\lambda_1}\right)\right\}, \quad (5)$$

where

$$L = \frac{N_1}{N_2}\lambda_2.$$

If, now, we put $\lambda = \bar{\lambda} \cdot \frac{76}{p}$, the number of α-particles is obtained as a function of the pressure. The values for the constants used in the final experiments were $\Delta = 8{\cdot}6$ mm., $l_1 = 9{\cdot}2$ cm., $l_2 = 7{\cdot}0$ cm., $2R = 133$ cm.

In fig. 4 are shown the results of the measurements in hydrogen and air. The abscissa is the pressure in cm. Hg, the ordinate $\log_e$ of the number of scintillations. Different experiments are brought to the same scale by putting $N_1 = 100$. It appears that within the experimental error the number of single-charged α-particles decreases exponentially with increasing pressure.

For hydrogen the value of $\bar{\lambda}_1$ (λ_1 referred to atmospheric pressure) is determined from (4). The result is

$$\bar{\lambda}_1 = 6{\cdot}8 \cdot 10^{-3} \text{ cm. (760 mm., 25° C.)}.$$

For air we use (5). This formula contains two variables, namely, λ_1 and L. If it is assumed—and this will be tested later—that $N_1 : N_2 = \lambda_1 : \lambda_2$, then $L = \lambda_1$ and λ_1 can be found by trial. The formula fits the measurements for

$$\bar{\lambda}_1 = 0{\cdot}60 . 10^{-3} \text{ cm. (760 mm., 25° C.).}$$

The curve given by (5), which is shown as a full line on fig. 3, is slightly concave. The deviation from a straight

Fig. 4.

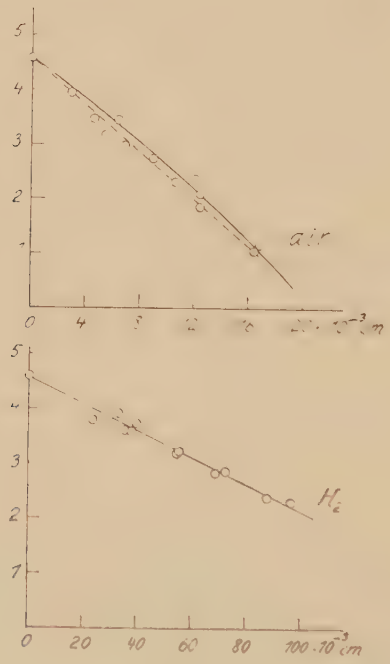

line (dotted curve) is, however, small compared with the experimental errors, so that the experiments are equally well represented by the simple exponential formula (4). If this formula is used, the result is

$$\lambda_1 = 0{\cdot}75 . 10^{-3} \text{ cm.}$$

It appears from the analysis given here that in determinations of the mean free path for loss a correction is required if capture takes place. In the case here considered the correction amounts to 20 per cent.

It is unsatisfactory, however, that this correction cannot be derived from the experiments, but appears only as the result of a calculation; and further, that the assumption $N_1 : N_2 = \lambda_1 : \lambda_2$ which was made for air has not been tested. The deviation from a simple exponential curve, which is indicated by (5), is so small that it cannot be utilized. The experiments were therefore continued with the microscope in position II. As before, the number of scintillations was determined as a function of the pressure in hydrogen and in air.

The results showed a difference between hydrogen and air which was well beyond the experimental error, and which afforded a test of the validity of the assumption $N_1 : N_2 = \lambda_1 : \lambda_2$ for air.

The calculation of the number of α-particles to be expected can be carried out as follows:—As mentioned above, position II. was obtained by moving the microscope 2·2 mm. (width of field of view) from the midway beam towards the main beam. When a singly charged α-particle changes its charge at a distance x from the ZnS-screen, put

$x = x_1$ corresponding to $\delta = 1{\cdot}1$ mm.
$x = x_2$ „ „ $\delta = 2{\cdot}2$ „
$x = x_3$ „ „ $\delta = 3{\cdot}3$ „

When a doubly charged α-particle changes its charge at a distance y from the mica leaf, put

$y = y_1$ corresponding to $\delta = 1{\cdot}1$ mm.
$y = y_2$ „ „ $\delta = 2{\cdot}2$ „
$y = y_3$ „ „ $\delta = 3{\cdot}3$ „

The values of x and y are calculated from (2), (2 a), (3), and (3 a). The contribution from the midway beam is given by

$$n_1 = \frac{N_1}{\lambda_1} e^{-\frac{l-x_2}{\lambda_1}} (x_3 - x_1). \quad . \quad . \quad . \quad . \quad . \quad (6)$$

The contribution from the main beam cannot be given in finite terms, partly because some of the α-particles here considered change their charge twice. The probability that a doubly charged α-particle changes its charge first at a distance from the mica-leaf between y and $y + dy$ and next at a distance from the ZnS screen between $x + dx$ and x, is given by

$$\frac{dy}{\lambda_2} e^{-\frac{l-y-x}{\lambda_1}} \frac{dx}{\lambda_1}; \quad . \quad . \quad . \quad . \quad . \quad . \quad (7)$$

y may here vary from 0 to y_3, x from 0 to x_3: when $y_3 \geq y > y$. the factor $\frac{dx}{\lambda_1}$ has to be omitted. The calculation was carried out by a numerical integration, the path of the α-particle being divided into intervals of about 1 cm.

The results of the measurements are shown in fig. 5 for hydrogen and air. The abscissa is the actual mean free path λ_1 given by $\lambda_1 = \lambda \frac{76}{p}$; the ordinate the number of scintillations. The results from different experiments are brought to the same scale by putting $N_1 = 100$.

The curves drawn are those found by the calculation indicated above. For hydrogen only the contribution

Fig. 5.

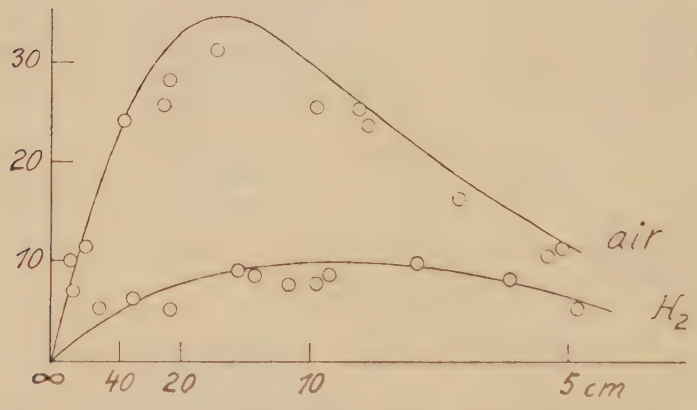

from the midway beam was taken into account. The curve for hydrogen thus represents the number to be expected when no capture takes place. For $\bar{\lambda}_1$ was used the value found previously $\bar{\lambda}_1 = 6{\cdot}8 \,.\, 10^{-3}$ cm. For air was used $\bar{\lambda}_1 = 0{\cdot}60 \,.\, 10^{-3}$ cm., $\bar{\lambda}_2 = \bar{\lambda}_1 \cdot \frac{N_2}{N_1}$.

Considering the approximate character of the calculation, the results obtained from it fit the experiments fairly well. As already mentioned, two general assumptions were used in the calculations, namely: (1) that in hydrogen the probability of capture can be neglected for the purpose of this calculation, (2) that the equilibrium state between single- and double-charged α-particles is the same for mica and for air for the same velocity of the α-particles.

The agreement between calculation and experiment is sufficient to show the validity of these assumptions.

The number of α-particles plotted on fig. 5 are not those actually counted. As mentioned previously, with the microscope in position II. scintillations are seen already with vacuum in the apparatus. A correction for this was carried out under the assumption that with a gas in the apparatus the "vacuum background" would change in the same ratio as the midway beam. The following figures, which are taken from an experiment with hydrogen, give an idea of the magnitude of the correction :—

$p.10^3$. cm.	I.	II.	Correction.	n_1.
0	1·00	14·6	—	—
24	0·576	13·2	−8·4	4·8
48	0·316	12·4	−4·6	7·8
52	0·286	11·7	−4·2	7·5
105	0·080	8·1	−1·2	6·9

p is the pressure. The figures under I. give the fraction of the midway beam which is left at the corresponding pressures calculated from $\bar{\lambda}_1 = 6{\cdot}8 \,.\, 10^{-3}$ cm. Column II. gives the number of scintillations per minute, corresponding to $N_1 = 100$; the actual value of N_1 in the experiment was 700. The correction at $p = 24 \,.\, 10^{-3}$ cm. is taken to be $0{\cdot}576 \times 14{\cdot}6 = 8{\cdot}4$ etc. The correction turns out to be so large that the experimental accuracy is chiefly limited by it, especially at low pressures. The countings in position II. with hydrogen were carried out chiefly to get some idea of an upper limit for the probability of capture in hydrogen. From the results in fig. 5 it can be shown that λ_2 in hydrogen must be at least ten times larger than in air when the pressure is so adjusted that λ_1 is the same in the two gases. This limit is very far from the value for λ_2 given by Thomas's calculation. The experimental accuracy is so small, however, that no quantitative test of the theory seems possible.

The value of $\bar{\lambda}_1$ in hydrogen can be calculated by a simple application of the Thomson ionization theory. The experiments give the mean free path of a helium ion in an atmosphere of hydrogen. Since the probability of capture depends on the relative velocity only, $\bar{\lambda}_1$ may be considered as the average distance between ions produced by a molecule of hydrogen, which moves through an atmosphere of helium ions. For swift α-particles the electrons in the hydrogen molecule are further considered as free.

In the theory it is assumed that a collision between an atom and a swiftly-moving electrified particle results in ionization when the energy given to an electron during the collision is higher than the ionization energy. The number of ions per cm. is given by

$$A_w = \frac{2\pi e^2 E^2 N n}{m V^2}\left(\frac{1}{W} - \frac{1}{Q_0}\right),$$

where

$$Q_0 = \frac{2mM^2V^2}{(m+M)^2};$$

E, M, and V are charge, mass, and velocity for the moving particle, e and m charge and mass for the electron, W the ionization energy for the particular electron.

In the case here considered $W = 54{\cdot}5$ volts, for an electron $Q_0 = \frac{1}{2}mV^2$, for a hydrogen nucleus $Q_0 = 2mV^2$.

By introducing $e = 4{\cdot}774 \,.\, 10^{-10}$, $N = 2{\cdot}76 \,.\, 10^{19}$, $n = 1$, we obtain for an electron

$$A'_w = \frac{1{\cdot}78 \,.\, 10^6}{\eta}\left(\frac{1}{54{\cdot}5} - \frac{1}{\eta}\right),$$

where η is the energy, expressed in volts, of an electron which moves with the velocity of the α-particle. For a proton we obtain

$$A''_w = \frac{1{\cdot}78 \,.\, 10}{\eta}\left(\frac{1}{54{\cdot}5} - \frac{1}{4\eta}\right).$$

The number of ions per cm. produced by two electrons and two protons is thus

$$A_w = \frac{7{\cdot}12 \,.\, 10^6}{\eta}\left(\frac{1}{54{\cdot}5} - \frac{5}{8\eta}\right) = \frac{1}{\lambda_1}.$$

For α-particles with velocity $0{\cdot}89 \,.\, 2{\cdot}19 \,.\, 10^9$ cm., η is 825 volts, which gives

$$\lambda_1 = 6{\cdot}5 \,.\, 10^{-3} \text{ cm.}$$

The experimental value for λ_1 is $6{\cdot}2 \,.\, 10^{-3}$ cm. (76 cm., 0° C.). The well-known difficulty in determinations of the number of ions produced by α- and β-particles, that part of the ionization is of secondary origin, is not present here, where the number of primary ions is determined directly.

My thanks are due to Professor Bohr for continuous interest throughout the work.

XXXIX. *Note on Photographic Counting of α-particles.* By J. C. Jacobsen*.

FOR the direct counting of single α-particles only the scintillation method has proved of value. The various methods which have been developed for counting by electrical means all suffer from the disadvantage that counting cannot be carried out in the presence of γ-radiation. A photographic method would at first sight seem promising, and a large number of investigations have been carried out on this subject. Kinoshita † found that when α-particles were sent perpendicular to a photographic plate the relation between blackening and number of α-particles was represented by a curve which went through the zero point. This is an important result, since it proves that the photographic effect of α-particles is not cumulative. It was further found that proportionality existed between blackening and number of α-particles when the blackening was small.

In spite of these results the photographic method of counting has apparently never been used for quantitative work. The method seems promising at first sight, partly because a much larger number of α-particles can be counted than by the scintillation method, and partly because the result of an experiment is preserved, so that a counting can be repeated.

In the experiments which are reported here the photographic method and the scintillation method were used with the same apparatus and under nearly identical conditions. The α-particles were sent through a mica-leaf into an evacuated chamber which was placed between the pole-pieces of a magnet. To the other end of the chamber either a zinc-sulphide screen or a plate-holder could be attached. The plate-holder could be moved without letting air into the apparatus, so that four exposures could be made on the same plate close to one another. For further details of these experiments the reader is referred to a foregoing paper ‡.

The plates used were Hauff lantern-plates. The developer was Rodinal 1 : 40, time of development 1 minute at a temperature of 15° to 17° C. After fixation the plates were washed in distilled water and dried; a microscope cover-glass was attached with Canada balsam to protect the plate. The determination of the blackening was carried out by direct

* Communicated by Prof. N. Bohr, Ph.D.

† Proc. Roy. Soc. lxxxiii. p. 432 (1910).

‡ See p. 401.

counting of the grains. An image of the plate was thrown on a ground-glass plate with a linear magnification of about 1500 ; the light source was a pointolite lamp. By lead-pencil lines the ground-glass plate was divided into squares with sides of 3 cm. length ; the number of squares, in which the grains were counted, varied from 2 to 40, according to the density of the plate and the accuracy which was aimed at. The fine screw of the microscope had to be moved continuously during the counting to search out the grains in different depths in the gelatine.

On the figure are shown the results of an experiment. The countings were carried out on a beam of double-charged α-particles. The source was a glass tube closed by a mica-

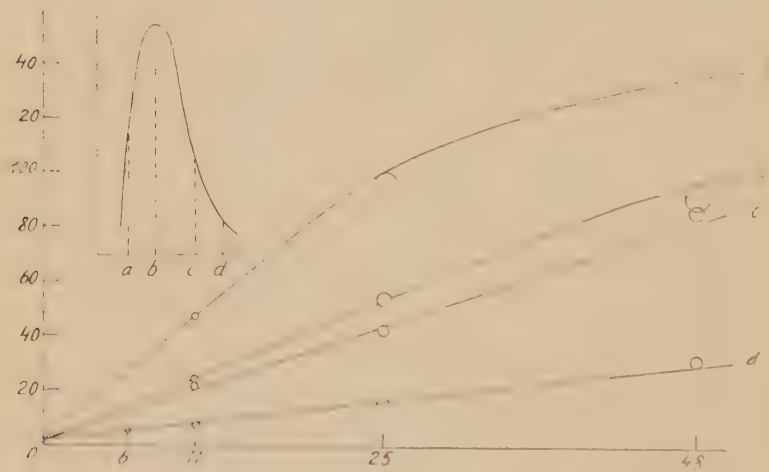

leaf, which contained radium emanation. The geometrical width of the beam was about 2 mm. Four exposures were made on the same plate, with exposure times 6, 11, 25, and 48 minutes, with vacuum in the apparatus. The countings on this plate were carried out chiefly to test the proportionality between number of α-particles and number of grains. On the figure to the left is shown the distribution of blackening inside the beam. Four points, a, b, c, and d, were selected on the beam, where the countings were carried out. Since the activity of the source may be considered as constant, the number of grains in the four exposures for each of the points a, b, c, and d should be in the ratio 6 : 11 : 25 : 48, when the number of grains is proportional to the number of α-particles. On the figure the number of grains in each of the

squares of the ground-glass plate mentioned above is plotted against the time of exposure. The radius of the circle surrounding each point gives the statistical mean error, determined by the number of grains actually counted. It is seen that proportionality exists so long as the number of grains is smaller than about 80 per square; this corresponds to 200,000 grains per square millimetre. The fog on the plate was 2·0 grains per square, or 5000 per square millimetre, shown as the point where the curves meet. The range of the α-particles in this experiment was about 2 cm.; it seems a reasonable assumption that the number of grains produced by one α-particle cannot differ much from unity, but no attempt was made to obtain an estimate of this quantity.

From this and other similar experiments it was concluded that the photographic counting presents no real difficulties, in so far as proportionality exists between number of grains and number of α-particles within certain limits. The chief difficulty is the fogging of the plates, and this in fact gives a very serious limitation to the method. The number of grains per square millimetre of the fog was generally about 5000; this means that the smallest number of α-particles which can be determined with any accuracy is about 10,000 per square millimetre. In most experiments where a small fraction of the total number of α-particles has to be counted this is far beyond what can be obtained with reasonable quantities of radioactive substances. The fog can be partly eliminated by treating the plate with chromic acid, but the smallest number of grains which has ever been obtained was 2000 per square millimetre.

Another serious limitation is given by the fact that the photographic effect ceases when the velocity of the α-particles is below a certain limit. This point was not examined in detail, but an orientating experiment, where the velocity of the α-particles was 0·3 times the velocity of the α-particles from RaC, showed that the sensitivity was so small that no practical use could be made of the method. It is very unfortunate that the photographic action ceases at about the same velocity of the α-particles as that at which the counting of scintillations begins to present serious difficulties.

With the experimental arrangement used any action of β-rays was eliminated, since the rays had to travel a distance of 15 cm. through a magnetic field of about 5000 gauss before reaching the plate. The photographic action of γ-rays seems to be exceedingly small; with a γ-ray activity of 150 millicurie-hours at a distance of 15 cm. no increase of the fog could be detected.

In the experiments here mentioned the α-particles were sent perpendicular to the plate. In another series of experiments grazing incidence was used. In this way tracks are obtained consisting of a number of grains; it was hoped in this way to obtain a distinction between grains produced by α-particles and grains belonging to the fog. It was soon found that such a distinction cannot be carried out with any certainty. The reason for this is that the number of grains in each track varies very much; tracks containing 10 grains were frequently observed, but, judging from the fog of the plate, tracks containing only one grain were present at the same time in a considerable number.

Summary.

The conditions necessary to carry out photographic counting of α-particles have been investigated.

Quantitative work is possible with swift α-particles when the number lies between 10,000 and 200,000 per square millimetre of the plate.

XL. *The Visibility of Radiation and Dark Adaptation.* *By* R. A. Houstoun, *D.Sc., Lecturer on Physical Optics in the University of Glasgow* *.

§ 1. THE relative visibility of the different colours of the spectrum at high intensities has been measured with very great care in America. First of all we had the determination of H. E. Ives,† then the determinations of W. W. Coblentz and W. H. Emerson,‡ of E. P. Hyde, W. E. Forsythe, and F. E. Cady §, and of K. S. Gibson and E. P. Tyndall ||. The results are in good agreement, and when graphed against the wave-length are not unlike the probability curve, though the general opinion has been that they have no connexion with the latter. I should, however, have been surprised if the distribution had been a symmetrical probability curve with respect to λ, for then it would have been skew with reference to ν or $1/\lambda$, and there

* Communicated by the Author.
† Phil. Mag. xxiv. p. 853 (1912).
‡ Bull. Bur. Stds., xiv. p. 167 (1918).
§ Astrophys. Journ. xlviii. p. 65 (1918).
|| Bur. Stds. Sci. Papers, No. 475 (1923).

is no reason why the variation in the properties of the molecules of the photochemical substance dissociated by the light should favour the one system of measurement

Fig. 1.

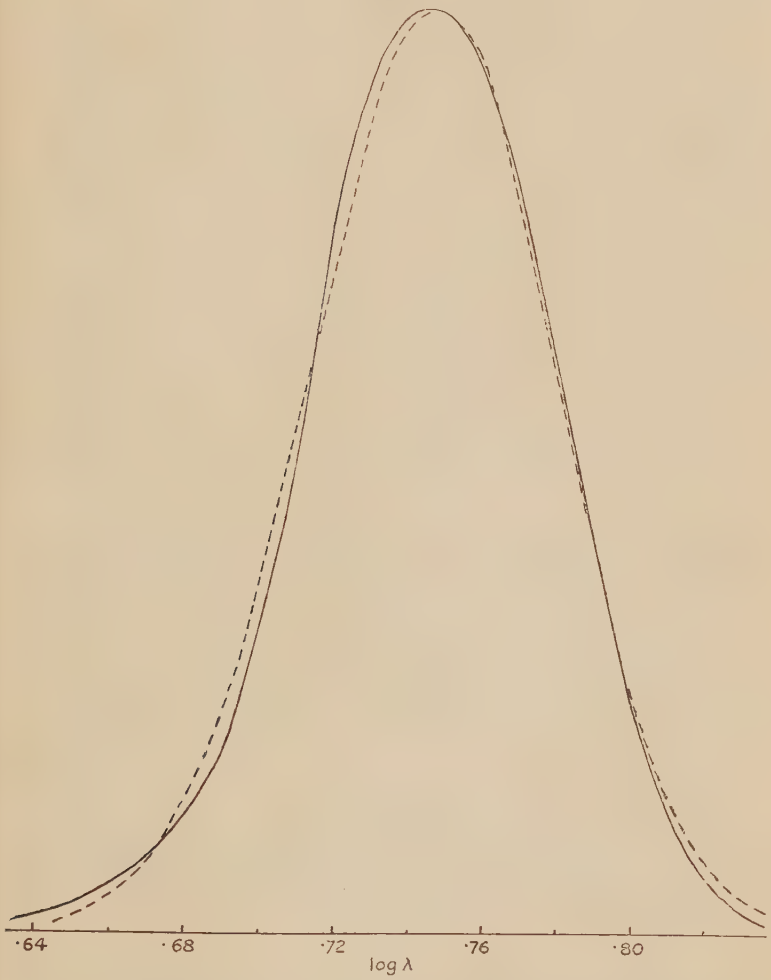

rather than the other. If, however, we graph the results against log λ or log ν, or the logarithm of any power of λ, the shape of the curve is always the same ; it seems, then, to express only a property of the eye itself. In fig. 1 I have

graphed the values of the relative visibility recommended by Gibson and Tyndall as a result of a consideration of their own work and the work of their predecessors, taking log λ as abscissa. The values are shown by the full line and the dotted curve is a probability curve fitted to them by trial and error. The fit is an extremely good one.

Hecht* has determined the relative visibility of the colours of the spectrum for an intensity not much above the threshold of visibility, so little above the threshold that the spectrum appeared monochromatic, and he found that the curve representing the mean result for 48 observers had the same form as that represented in fig. 1, but that it was displaced 48 $\mu\mu$ towards the blue end of the spectrum. His curve is thus also a probability curve when expressed in terms of log λ.

The question arises as to the shape of the curve at intermediate intensities. This has been investigated so far only by A. König †, but on account of his great experience the results are very valuable. They show that, as the intensity is increased, the shape of the curve remains approximately constant, that it moves at first slowly, then more rapidly, and finally slowly again across into the position for high intensities. There are two characteristic conditions of the eye involved, and the change takes place from the one to the other. König matched different parts of the spectrum with a constant intensity in the green, and gives his results in slit-widths. The weak part of the investigation is the measurement of the energy distribution in the spectrum of the gas-flame employed as source. This he was not in a position to do himself. He also omits to make the slit-width correction. Nutting ‡ has, however, done this, and gives the results directly as visibility, making them comparable with the results of the investigators already mentioned in this paper. I have graphed Nutting's results as a function of λ, and determined the positions of the maximum for the different intensities. They are given in the following table :—

	S.	A.	B.	C.	D.	E.	F.	G.	H.
Log intensity	$\bar{4}\cdot4$?	$\bar{3}\cdot4$	$\bar{2}\cdot6$	$\bar{1}\cdot8$	0·4	1·0	1·6	2·2	2·8
Maximum.....	503$\mu\mu$	505	507	508	515	535	540	542	544

* Journ. Gen. Physiol. v. p. 1 (1922).
† 'Collected Works,' p. 144.
‡ Bull. Bur. Stds. vii. p. 238 (1911).

The letter is König's name for the intensity, and the intensity is given in terms of his arbitrary unit. This unit is the "brightness of a surface of magnesium oxide distant 1 metre from a 0·1 cm.² surface of platinum at its melting point as seen through a diaphragm of area equal to 1 sq. mm." This area of platinum should give 2·0 international candles, so the objective brightness of the surface would be 0·2 millilambert. The intensity of illumination of the retina is obtained by multiplying this result by the area of the pupil in sq. mm., and is then said to be expressed in photons, a unit introduced by Troland. König's unit of intensity should thus equal one-fifth photon. We have assumed that magnesium oxide diffuses the incident light perfectly according to the cosine law, but the correction to be applied here does not seem to have ever been determined with accuracy, and, in any case, there is reason to believe that the value given by König for his unit is very far wrong. The intensity F was determined both by König and a colleague, apparently by viewing two fields rapidly one after the other, and the values 36·9 and 54·9 found respectively. In order to have a round number I have adopted the value antilog 1·6.

The positions of the maxima given in the table are rough determinations. The end values 544 $\mu\mu$ and 503 $\mu\mu$ do not agree with the values of Gibson and Tyndall and of Hecht, namely, 555 $\mu\mu$ and 507 $\mu\mu$. An agreement might be obtained by repeating Nutting's calculation in the light of the recent data and a careful study of the whole question, but this is in the meantime deferred. The change takes place principally between C and F. The equation to the dotted curve in fig. 1 is

$$e^{-\frac{(\log \lambda - \log 555)^2}{2\times 0{\cdot}0342^2}}.$$

The equation to Hecht's curve is, consequently,

$$e^{-\frac{(\log \lambda - \log 507)^2}{2\times 0{\cdot}0342^2}}.$$

Within the limits of experimental error König's intermediate curves can be obtained by superposing his end ones and altering the ratio of the maximum ordinates of each. What the exact ratio should be for each intensity is difficult to determine. It may be shown, by trial, that the shift of the maximum is roughly proportional to the

ratio of the maximum ordinates, *i. e.*, if the ratio is 9 to 1, the maximum shifts one-tenth of the distance from one to the other of the characteristic positions. From the preceding results we consequently obtain the following table, in which the two lower rows give the ratio of the components present in the mixture.

	S.	A.	B.	C.	D.	E.	F.	G.	H.
Log intensity	$\bar{4}{\cdot}4$	$\bar{3}{\cdot}4$	$\bar{2}{\cdot}6$	$\bar{1}{\cdot}8$	0·4	1·0	1·6	2·2	2·8
Low	1	·95	·90	·88	·71	·22	·10	·05	0
High	0	·05	·10	·12	·29	·78	·90	·95	1

§ 2. Let us now approach the problem from another standpoint. König and Brodhun determined the least perceptible increase of intensity ΔI for various values of I, and expressed the results in curves giving ΔI/I, *i. e.*, Δ(log I) in terms of log I. In a recent paper * I suggested that, instead of Δ(log I), it was better to graph the reciprocal of this quantity in terms of log I. The ordinates are then great when the sensibility of the eye to increase of intensity is great, and there is the additional advantage that we are able to attach a special meaning to the area of the curve. For let S denote the magnitude of the sensation. Then the rate of increase of sensation with log I is given approximately by

$$\frac{d\mathrm{S}}{d\,(\log \mathrm{I})} = \frac{k}{\Delta\,(\log \mathrm{I})},$$

where k is a constant of proportionality. Hence

$$\mathrm{S} = \int \frac{k d\,(\log \mathrm{I})}{\Delta \log \mathrm{I}},$$

and if the area of the curve is represented in fig. 2. the sensation at P is represented by the area to the left of the ordinate. The result holds, no matter what the shape of the curve is. But the interesting feature is that the curve is a probability curve, *i. e.*, it is of the same nature as the curve we have used to represent the visibility throughout the spectrum. This was shown in the former paper by graphing the mean of König and Brodhun's data for white, for 605 $\mu\mu$, and for 470 $\mu\mu$.

In addition to these wave-lengths, König and Brodhun made observations at 670 $\mu\mu$, 575 $\mu\mu$, 505 $\mu\mu$, and 430 $\mu\mu$, and they state, with reference to their data, that both

* Phil. Mag. viii. p. 520 (1929).

observers were in good agreement, and that the results were the same at all wave-lengths except at low intensities, when there was a divergence between the three more and the three less refrangible wave-lengths. This deviation started at 50 on the intensity scale for König and at 10 on the intensity scale for Brodhun. In view of this statement the best method of summarizing their results seems to be to take the mean of their values for all wave-lengths and graph its reciprocal. This has been done in the case of fig. 3 for König and of fig. 4 for Brodhun. The abscissæ are the logarithms of the intensity ; the latter is measured on the scale already referred to. The ordinates are

Fig. 2.

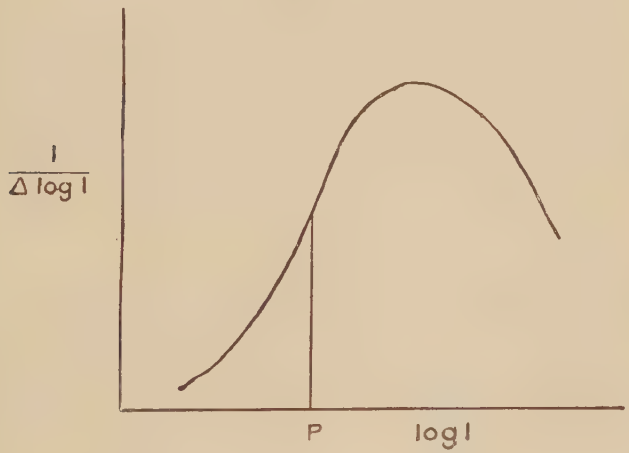

$(I - \Delta I)/\Delta I$ or simply $I/\Delta I$, as the difference between these two expressions can be neglected except for the lowest intensity. When the results fall into two groups, the mean of each is plotted separately ; in this case the greater ordinate refers to the blue end of the spectrum. In each figure a Gaussian curve has been fitted by trial and error to the data.

It was stated in my former paper that König and Brodhun did not correct their data for the variation in the aperture of the pupil. This is erroneous ; the observations were made with a uniform aperture of 1 sq. mm. area, and hence required no correction. This information is not given in their paper on the subject, but in a paper written

by König* ten years later, and has been overlooked by Hecht.

Fig. 3.

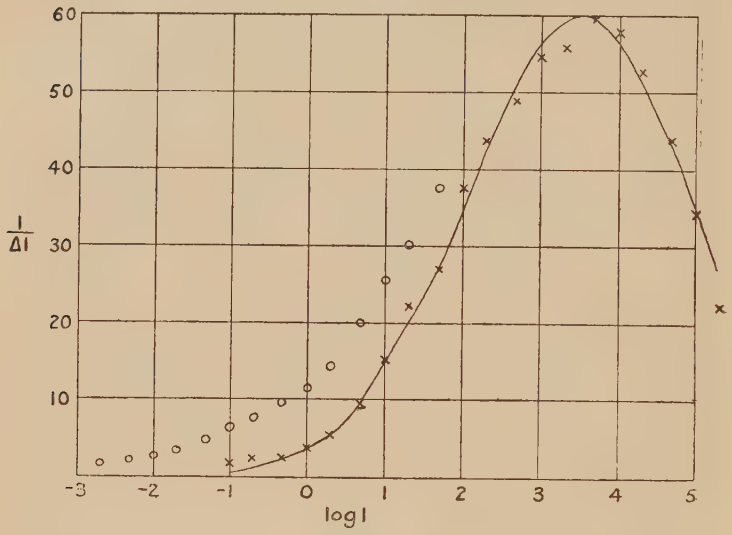

Fig. 4.

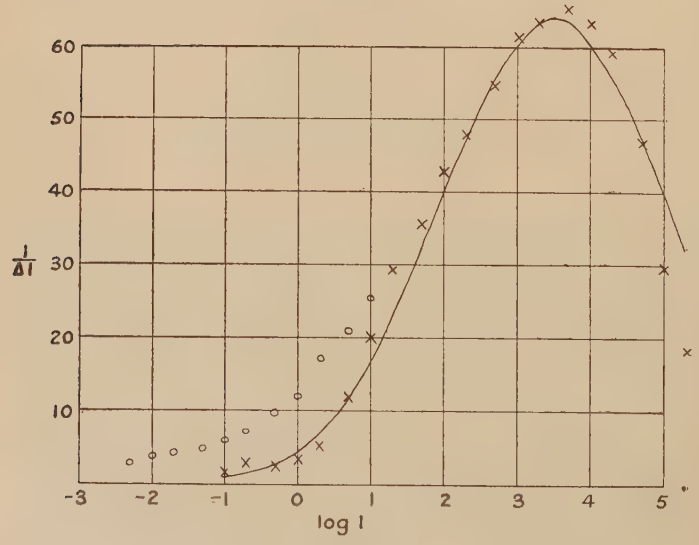

* 'Collected Works,' p. 381.

It is obvious, from figs. 3 and 4, that the Gaussian curve fits the data for the red end of the spectrum well considering the difficulties of the observations; but there is a deviation for the blue end of the spectrum. Let us confine our attention at present to the red end. The Gaussian curve in fig. 3 is represented by

$$e^{-\frac{(\log I-3{\cdot}5)^2}{2\times 1{\cdot}45^2}}.$$

Thus in the red end of the spectrum the sensation of brightness is given by

$$\int_{-\infty}^{\log I} e^{-\frac{(\log I-3{\cdot}5)^2}{2\times 1{\cdot}45^2}}\, d(\log I).$$

It was suggested in the former paper that the percipient elements of the retina had different intensity thresholds, that the sensation of brightness was proportional to the number of elements active, and that the increase in sensation was due to more elements coming over the threshold as the intensity increased. Let us suppose now that each element has its own wave-length, and that the complete distribution is given by

$$e^{-\frac{(\log I-3{\cdot}5)^2}{2\times 1{\cdot}45^2}-\frac{(\log \lambda-\log 555)^2}{2\times 0{\cdot}034^2}}\, d(\log I)\, d(\log \lambda).$$

If monochromatic light of a range $d(\log \lambda)$ is incident upon the photochemical substance, it liberates electrons of a range of velocities given by the quantum relation, and we suppose that certain only of the percipient elements are susceptible to electrons of this velocity. There is no product term in the index of the exponential, and consequently no correlation between variation with log I and with log λ; the one change is quite independent of the other. If we adhere to the former assumption, namely, that the sensation of brightness is proportional to the number of percipient elements, both the variation with intensity in the red and the variation with wave-length at high intensities are fully explained. The question now arises as to the explanation of the Purkinje effect, *i.e.*, the shift of the maximum of the visibility curve towards the blue with decrease in intensity.

The figures on p. 420 represent only the relative values of the two components which we found necessary to represent this shift. As König used the same unit of intensity in his work on the visibility curve and on Weber's law, it is

easy to calculate the absolute value of the high-intensity component. It should simply be proportional to

$$\int_{-\infty}^{\log I} e^{-\frac{(\log I - 3{\cdot}5)^2}{2\times 1{\cdot}45^2}}\, d(\log I).$$

This has been done in the following table:—

	C.	D.	E.	F.	G.	H.
Log I.	$\bar{1}{\cdot}8$	0·4	1·0	1·6	2·2	2·8
High	5	17	42	96	180	311
Low	37	42	12	11	9	0

The row marked "High" gives numbers proportional to the maximum ordinate of the high-intensity component at the different intensities in question, and the row marked "Low" numbers proportional to the maximum ordinate of the low-intensity curve, calculated by means of the former table of ratios. The result is only approximate, and values are not given for the three lowest intensities S, A, and B, as they would be worthless altogether.

Let us return now to the consideration of fig. 3. The circles are the mean of König's results for 505 $\mu\mu$, 470 $\mu\mu$, and 430 $\mu\mu$. Let us say that they represent 470 $\mu\mu$. Now at 470 $\mu\mu$ the high-intensity component has 0·091 of its maximum value and the low-intensity component about 0·67 of its maximum value. The quotient of the second of these quantities by the first is 7·4. If we multiply the low-intensity row in the preceding table by 7·4 and add it to the high-intensity row, we obtain numbers representative of the sensation at 470 $\mu\mu$ for the intensities in question, and if we differentiate the result with respect to log I we ought to obtain the curve represented by the circles in fig. 3. As a matter of fact, the addition of the low-intensity curve brings in the necessary correction in the right direction, of the right order of magnitude, and at the right place. But that is all we can say. The want of agreement is not due, I think, to the cumulative effect of the various approximations I have made, but to the uncertainty of the observations, and to a difference in the degree of dark adaptation in the data under comparison.

In any case the deviation at low intensities in the blue in König and Brodhun's observations on Weber's law is due to the same cause as the Purkinje effect, and it must be

possible to bring it into numerical relation with the latter; and the formulæ employed above seem to be the best way of doing this, whatever may be thought of the theoretical views which have led to the construction of the formulæ.

§ 3. It is customary to suppose that vision at high intensities is due to the cones. These form the photopic mechanism, whereas at low intensities vision is due to the rods which form the scotopic mechanism. This view is referred to as the duplicity hypothesis; it is due to Von Kries, and finds wide, but not universal, support. The Purkinje effect is caused by the shift from the one mechanism to the other.

It seems to me an unnecessary complication to postulate a second mechanism. When we go into the dark, the rods do not begin to function at once, according to the duplicity theory. Time must be allowed for dark adaptation, a process which does not affect the cones to the same degree. The rods therefore exist in two states. Thus, to explain two conditions of the eye we assume two mechanisms, one of which has two states. It is obviously simpler to assume one mechanism with two states.

§ 4. The view has been advanced by Hecht that the photochemical substance in the retina is dissociated by exposure to light, and recombines in the dark according to the equation for a bimolecular reaction. The two states of the scotopic mechanism referred to above are consequently characterized by a difference in the quantity of photochemical substance available. Let a be the concentration of the dissociated substance at the instant $t=0$, when dark adaptation starts, and $a-x$ the concentration at time t. Then

$$\frac{d}{dt}(a-x) = -k(a-x)^2,$$

whence

$$k = \frac{x}{at(a-x)}.$$

Let I denote the intensity at the visual threshold. Then Hecht assumes that in the periphery of the retina $a-x$ is proportional to log I, while in the fovea it is proportional to $I-c$, where c is a constant. A different law is necessary in the second case, because the extent of foveal dark

adaptation is so very much less; here the threshold diminishes only to about one-eighth of its initial value, whereas in the former case it diminishes to a ten-thousandth of its initial value. But there is no physical reason given for the difference in the law in the two cases; the structure of rods and cones is not so different that we would expect them to obey two radically different laws. Moreover the numerical examples which he gives, one for each case, do not appear to support his contention. If we take the figures for peripheral dark adaptation *, and calculate the value of k as shown in the table, we do not get agreement; k rises to a maximum in the middle of the range, and then diminishes to less than half its maximum value, giving a mean of ·00130 as against 0·0143 as stated in the paper, where the details of the calculation are not shown. If we add 0·45 to $a-x$, k becomes more nearly constant, the values being, in order, ·0104, ·0119, ·0112, ·0125, ·0134, ·0108, ·0098, ·0092, ·0057; but we have no theoretical justification for doing this, and there is still the rise in the middle and the descent at the end, which gives rise to the surmise that this is the wrong type of formula altogether.

t, time.	$a-x$, log of threshold intensity.	x.	$k=\frac{x}{at(a-x)}$.
0 min.	4·41	0	—
2	4·00	0·41	1162×10^{-5}
5	3·40	1·01	1347
8·5	2·97	1·44	1293
12	2·47	1·94	1485
20	1·78	2·63	1676
31	1·51	2·90	1405
39·5	1·34	3·07	1315
45	1·27	3·14	1246
72	1·27	3·14	779

If we take the figures for foveal dark adaptation†, and work out the values for k, we obtain the results in the following table, which gives a mean value of k equal to 0·00222:—

* Journ. Gen. Physiol. ii. p. 499 (1920).
† Journ. Gen. Physiol. iv. p. 113 (1921).

t, time.	I, threshold intensity corrected for pupil.	$a-x$.	x.	$k=\frac{x}{at(a-x)}$.
0 sec.	39·8	33·3	0	—
9·3	25·7	19·7	13·6	223×10^{-5}
22·2	15·8	9·8	23·5	324
52·4	11·5	5·5	27·8	283
128·9	9·5	3·5	29·8	198
188·9	7·57	1·57	31·73	321
377·9	7·28	1·28	32·02	199
618·9	6·62	0·62	32·68	256
917·9	6·30	0·30	33·00	360
1209·9	5·50	−0·50	33·8	−168

This time there is no systematic deviation, but the values exhibit a considerable amount of irregularity, one of them being negative. Still the agreement is good, considering the difficulties of the experiment. But, taking the two cases together, it does not appear probable that dark adaptation is due to the recombination of a photochemical substance.

It is doubtful whether the equation for a bimolecular reaction applies to the molecules of the photochemical substance under the conditions in which they exist in the rods and cones. Also we obtain the same measure of agreement with the equation in the case of the opening of the pupil of the eye in the dark. This has been measured very carefully by Reeves *, and the following table gives the mean of his results for seven observers. The first column gives time in seconds and the second the diameter of the pupil in millimetres. The eye was light-adapted; at $t=0$ the illumination was shut off, and the numbers show the rate at which the eye opened in the dark. I have applied the same procedure as in Hecht's treatment of foveal dark adaptation, taken the difference of the diameter and a constant, namely 7·7 mm., put the result equal to $a-x$, and calculated

$$\frac{x}{t(a-x)},$$

which should be proportional to k for each value of d. The results are shown in the third and sixth columns.

* Psych. Rev. xxv. p. 340 (1918).

The agreement is as good as in the other two cases, and it has never been suggested that the recombination of a photochemical substance is the cause of this change. Consequently, there is the less reason for supposing that it is the cause of dark adaptation.

t.	d.	$\frac{x}{t(a-x)}$.	t.	d.	$\frac{x}{t(a-x)}$.
0 sec.	2·8	—	9 ...	6·2	0·252
0·5 ...	3·1	0·130	15 ...	6·5	·205
1·0 ...	3·5	·167	29 ...	6·8	·153
1·5 ...	3·9	·193	60 ...	7·2	·147
3 ...	4·7	·211	180 ...	7·5	·130
5 ...	5·5	·245	300 ...	7·6	·160

§ 5. A totally different explanation is suggested by the experiments of Dreser and Wölfflin*. They injected strychnine under the skin, and found a distinct increase of one-fourth or one-fifth in the amplitude of accommodation. The rate of adaptation appeared also to be increased. Now strychnine favours conduction between the nerve-endings. The impulse has to cross synaptic junctions in the outer and inner reticular layers of the retina on its way to the brain. Dark adaptation may consequently be due to the nerve-endings making better contact in the reticular layers.

A suggestive experiment is recorded by Adrian and Matthews† on the eye of the conger-eel. In the eels they experimented on the optic nerve is about 15 mm. long, and the retina contains both rods and cones, differing little from the mammalian retina. The number of fibres in the optic nerve is, however, considerably less, about 10,000. The eye and optic nerve were removed from the head, and the nerve placed upon two electrodes. These were connected to a capillary electrometer, the deflexions of which were magnified by a three-valve amplifier and recorded on cinematograph film. When the retina was exposed to light, the action-current in the nerve-fibres recorded itself as a series of oscillations on the film. The action-current did not start immediately the image was focussed on the retina; there was an interval, the latent period, between the starting signal and the commencement of the current.

* Graefe's *Arch. für Ophthalm.* lxv. p. 302 (1907).
† Journ. of Physiol. lxv. p. 273 (1928).

When four disks of light, each 0·22 mm. in diameter, set at equal distances on a circle of 1 mm. diameter, were focussed on the retina, they gave a shorter latent period than when one alone was focussed. But there was no shortening when the diameter of the circle was raised to 2–3 mm. Then a strychnine solution was applied to the retina, and the latent period for the four areas when the diameter was 2–3 mm. became much shorter than for any one singly. The interaction of the different areas obviously took place in the retina, since the eye was separated from the brain, and it was greatly increased by the action of strychnine. Thus, since strychnine increases lateral conduction and dark adaptation, it is probable that the latter is due to a better forward conduction.

It is a mistake to regard the retina as a mosaic of receptors leading by independent pathways to the different fibres of the optic nerve. No doubt there is a closer connexion to one particular fibre, but the same fibre is open to the spread of excitation from other parts of the synaptic layers. The system seems to adjust itself automatically to the best way of coping with the image. If the latter is a bright one, with plenty of detail, the receptors work independently; if it is dim, they work in groups.

§ 6. The most interesting example of this automatic adjustment is Ricco's law of foveal vision. This law states that, if the image of a uniformly bright disk is thrown on the retina, and the brightness is diminished until the disk is just visible, the total quantity of light received on the image is constant, provided that the angle subtended by the disk does not exceed one or two degrees.

The table below gives observations verifying the law, as yet unpublished, obtained by Mr. James F. Shearer and myself five years ago. The first column gives the angle subtended at the eye by the radius of the object, expressed in minutes. The next column gives the quantity of light entering the pupil of the eye, in each case expressed in arbitrary units. Each result is the mean of three observations. The eye was very thoroughly dark adapted. If the law holds, this column should be constant, and it will be observed that the constancy holds up to an angle of about 6 degrees. It was found during the experiments, that a point-source was just visible, when it gave as much

light as one-tenth candle at 1 kilometre. The third column gives the degree of illumination of the retina in photons calculated on this basis. For the purpose of the calculation the area of the pupil was assumed to be 45 square millimetres.

Angle subtended by radius of disk, in minutes.	Quantity of light falling on image, in arbitrary units.	Intensity of illumination, in photons.
0·175	2·25	174
·35	3·23	43·4
·70	3·91	10·9
1·40	2·35	2·72
2·80	3·42	0·680
5·59	2·74	0·170
13·76	3·81	0·0280
21·84	3·08	0·0112
43·67	2·47	0·0028
349·4	3·19	0·000044
699	11·3	—
1000	30·8	—

The figures are very striking. They show that, though the area on the retina increased four million times, the quantity of light incident on it necessary to produce excitation remained substantially the same.

In making the measurements a Fullolite lamp was placed outside a small hole in the window of a light-tight room. The rays from this hole divered on to a large ground-glass screen, the distance of which from the hole could be varied. A circular aperture was placed in front of this screen and viewed by the observer, while the screen was moved towards the aperture until the image disappeared. The observer usually sat at about a distance of 2 metres from the aperture, and the hole at the window was capable of a wide range of variation. At the point of extinction form-vision goes; the observer does not see a disk, but is conscious of a luminous something extending over an area.

§ 7. Hecht explains the Purkinje effect by assuming that both rods and cones are excited by the same photochemical substance, but that it is immersed in media of different refractive index in the two cases. The displacement is then to be ascribed to the operation of Kundt's law. Kundt in 1874 dissolved substances that produced absorption bands, using different solvents, and found that the position of the band varied with the

solvent. He came to the conclusion that the greater the refraction and dispersion of the solvent, the further was the band displaced towards the red, and his conclusion has persisted in the literature of the subject until this day under the name of Kundt's law, in spite of the fact that it was not borne out by subsequent investigation. The band moves as often the one way as the other, and generally there is a marked change in intensity and shape, in comparison with which the shift in position can be neglected. This has been shown in a striking manner by Georg. J. Katz*. Hence I am dubious about the validity of the explanation, and it is not relevant unless the rods are percipient elements; but it has the merit of tackling the problem in a physical manner.

I suggest the following alternative explanation:—Let us suppose that the photochemical substance has, under standard conditions, an extremely narrow absorption band. In the eye, owing to variations in density, action of surface forces, etc., no two molecules are in the same condition. These narrow curves are, consequently, distributed about a mean according to the laws of statistics, and their resultant is shaped like a probability curve. Hence the shape of the visibility curve at high intensities.

To get the shape at low intensities, consider the quantum relation

$$h\nu = \tfrac{1}{2}mv^2,$$

and suppose it applicable to the case of high intensities. ν is the frequency of the incident light, and v the velocity with which the electron impinges on the percipient element. Let us suppose that at low intensities the electron has to do a certain amount of work W to reach the same place. Then the final velocity v is caused by a different frequency ν', according to the equation

$$h\nu' = \mathrm{W} + \tfrac{1}{2}mv^2.$$

By subtraction

$$h(\nu' - \nu) = \mathrm{W}h \quad \text{or} \quad \nu' - \nu = \mathrm{W}/h,$$

that is, at the low intensity all frequencies are increased by the same amount W/h.

§ 8. When a surface is illuminated by a beam of, for example, red light, there are three kinds of unit involved in the measurement of the degree of illumination. First

* Inaug.-diss., Erlangen (1898).

of all there is the energy per sq. cm. per sec., as it would be indicated by a thermopile. Then there is the intensity in metre-candles ; this could be obtained by placing a rod in front of the surface and throwing a second shadow by means of a standard candle. The result follows, on balancing the shadows, according to the principle of the shadow photometer, although the somewhat difficult operation of heterochromatic photometry is involved. The intensity of the illumination in metre-candles determines the objective brightness of the surface. Subjective brightness, the sensation of brightness, is another matter. Equality of sensation can be determined by a photometer, but the absolute measurement of sensation cannot be effected in this way. We must fall back on the number of just perceptible increments between the degree of sensation in question and the threshold value.

In their celebrated paper on Weber's law, König and Brodhun raise the question as to whether any numerical value can be given to the sensation of brightness Suppose we have equally bright red and blue surfaces. Then we would expect the sensation of brightness which they excite to be measured by the same number. But according to the measurements of König and Brodhun, a greater number of steps is required to reach zero sensation from the blue surface than from the red surface.

I think there is here a confusion of thought. We ought to expect agreement only if the just perceptible increments are measured by a light-adapted eye. If we consider the point P in fig. 2, the area to the left of the ordinate through P measures the sensation for the value of log I in question. When the eye becomes dark-adapted, this area increases, and at the same time the area on the right decreases, the total area remaining constant, since the number of nerve-fibres is fixed anatomically.

In fig. 2 the quantity I is measured in photometric units. If the light is not monochromatic, and the distribution of the energy over the different wave-lengths is known, I can be calculated from a knowledge of the visibility function, but only for one state of adaptation of the eye. The diagram has a meaning only for one state of adaptation. If the latter alters, the visibility function alters, and points on the axis of abscissæ shift relatively to one another, unless the light is monochromatic or approximately monochromatic.

XLI. *Weber's Law and Visual Acuity.* *By* R. A. Houstoun, *D.Sc.*, *and* James F. Shearer, *M.A.*, *B.Sc.*, *Lecturers in the University of Glasgow* *.

§ 1. If I is the brightness of a surface and ΔI its least perceptible increment Dr. Houstoun showed recently †, from the results of König and Brodhun, that when $I : \Delta I$ was graphed as a function of log I it formed a Gaussian probability curve, and stated that investigations would be set on foot to test the matter further. The present paper describes some of these investigations.

König and Brodhun found that their results were independent of the wave-length of the light employed, except at low intensities, where there was a difference between the two halves of the spectrum. This has been shown in a previous paper to be due to "rod vision" coming into play. We therefore did not resolve the light spectrally, but merely passed it through filters.

As source of light we employed principally a 220-volt Pearl Osram lamp: this was used up to 250 volts. A similar 125-volt lamp was used occasionally up to 250 volts, and the brightness was regulated in each case by altering the current through the lamps. This was found preferable to using neutral filters. The candle-power of these lamps was determined in terms of an 8 C.P. lamp on a long photometer bench for a wide range of currents, using a wedge photometer with red, green, and blue filters. Observations were then made at lower currents with a special photometer, in which the surface of the lamp itself was used as one of the comparison surfaces, being compared directly with a white paper surface which could be illuminated by lamps at various distances. By this means the candle-power of the lamp could be measured through a range of from 1 to 10^7.

After preliminary experiments with a half-shadow polarimeter the following different arrangements were tried:—

(1) A Wollaston prism was mounted on the prism table of a spectrometer the telescope of which was fitted with a rotating nicol eyepiece. The image then consisted of two rectangles plane polarized at right-angles to one another,

* Communicated by the Authors.

† Phil. Mag. viii. p. 520 (1929).

and the slit-width was regulated so that these rectangles touched one another sharply. Their intensities were altered by turning the nicol. This arrangement was abandoned because the magnification and definition of the eyepiece were not satisfactory.

(2) The same apparatus was used with an ordinary eyepiece, and the intensities were altered by rotating a nicol in front of the slit.

(3) An aperture A of diameter 2 mm. was fitted with a magnifying lens (fig. 1), and through it the eye of the

Fig. 1.

observer looked down at the sharp edge E of a glass rhomb R. The beams of light from the two faces of this rhomb came from the surface of the lamp L through neutral wedges W_1 and W_2 after reflexion by a mirror M. The angles of the prism and the distances were calculated so that the beams diverging from E came from the same part of the surface of the lamp. D is a diaphragm with a circular hole in it. Thus the eye saw a half-shadow field the intensities of which could be altered by moving the wedges. The sides of the rhomb were about 3 cm. in length, the circular hole was of 1 cm. radius, and the distance AE about 12 cm.

(4) This is the same arrangment as (2) with a plate polarizer substituted for the slit nicol. This plate polarizer consisted of two glass plates mounted in front of the telescope object-glass, with their surfaces making an angle of 30° with the axis of the telescope. They could be rotated about this axis by a rack-and-pinion motion. The light from the Wollaston prism was in this case only partially polarized. The plate polarizer transmitted more light and gave a better definition than a nicol. It was calibrated by means of the slit nicol.

The power of the eye to discriminate differences in intensity fluctuates considerably from time to time, and the object of using so many different arrangements was to study the conditions necessary for constant results. These are the sharpness of the dividing line, perfectly uniform illumination of the two fields, the size of the fields, and the mechanical arrangement for altering the relative intensity. With the third arrangement it was possible to alter the size of the field. The following table shows the effect of doing this :—

Angle subtended by radius	2·39°	1·55°	0·78°	0·39°	0·19°	·009°
Least perceptible increment....	9·5	6·4	3·6	7·9	13·4	22

The field consisted of two semicircular disks, and the upper row shows the angle subtended by the radius of the field in degrees. The lower row gives $\Delta I/I$ measured in per cent. for each field, the result in each case being the mean of four determinations by J.F.S. for red light at the intensity of maximum sensibility. It decreases to a minimum at 0·78° and increases for smaller fields. The surround was the same in each case, dark but not absolutely black.

The fourth arrangement gave the best results. With this apparatus it was possible to start with the slit slightly too narrow, focus the narrow band between the two fields very sharply, then widen the slit until it just disappeared. At some points there was then a trace of overlapping and at others a slight shadow, but there was always a section where the junction was perfect, and it was here that the observations were made.

In making the observations the apparatus was adjusted until one half of the field was the darker, and the reading taken. It was then adjusted until the other half was darker, and the reading taken again. The least perceptible increment was calculated from half the difference of these readings.

We give some results in the following tables :—

I.

Intensity.	R.A.H. Red.
$\bar{2}$·86	0·59
$\bar{1}$·36	3·42
$\bar{1}$·86	7·77
0·36	15·7
0·86	22·1
1·36	23·3
1·86	25·8
2·36	20·8
2·86	18·8
3·36	16·1
3·68	13·8

II.

Intensity.	R.A.H. Red.
$\bar{1}$·1	1·7
$\bar{1}$·5	3·0
0·0	6·7
0·5	12·0
1·0	13·1
1·5	17·0
2·0	18·8
2·5	20·1
3·0	14·5
3·5	12·5
3·9	9·2

III. IV. V.

Intensity.	J.F.S. Red.	R.A.H. Red.	R.A.H. Blue.
$\bar{2}$·33			·1·54
·67			2·03
$\bar{1}$·00	1·62	1·3	3·01
·33	2·10	2·0	4·44
·67	3·46	3·1	6·02
0·00	6·75	5·0	7·46
·33	12·8	7·7	10·1
·67	21·5	12·3	12·9
1·00	31·2	16·2	17·1
·33	36·2	22·8	21·2
·67	38·0	23·5	29·4
2·00	41·7	25·6	29·9
·33	41·1	26·1	32·5
·67	38·5	26·4	29·4
3·00	30·0	21·3	27·9
·33	27·1	20·4	22·6
·67	21·4	17·2	
4·00		14·9	
·33		13·4	

Of these series I. was taken by arrangement 2, series II. and III. by arrangement 3, and series IV. and V. by arrangement 4. In the case of I., IV., and V. the image consisted of two vertical rectangles each $14^\circ \times 65'$ which touched on a long side, in the case of IV. it was a disk the radius of which subtended 0·78° at the eye, and in the case of II. it was a much larger disk. I. is the mean of nine determinations, II. of eighteen, III. of eighteen, and IV. and V. of ten each. The most presentable of the results, III. and IV., are graphed in fig. 2.

As our object was to determine the variation of the least perceptible increment with intensity, and as the values vary irregularly from day to day, it was our practice to take two readings for every intensity at one sitting, starting from one end of the range and working to the other. In

series I., II., and III. the observer did not read the scales himself, and his eye was highly but not perfectly dark adapted at the low end. On considering the matter it seemed to us that the eye should be in the same state for all readings if they were to be comparable. In series IV. and V., therefore, the observer set the current, read the scale of the polarizer, and entered up the current himself, all by the aid of a two-volt lamp in, of course, a darkened room. We considered that these operations would bring the eye into the same condition before every pair of readings.

Fig. 2.

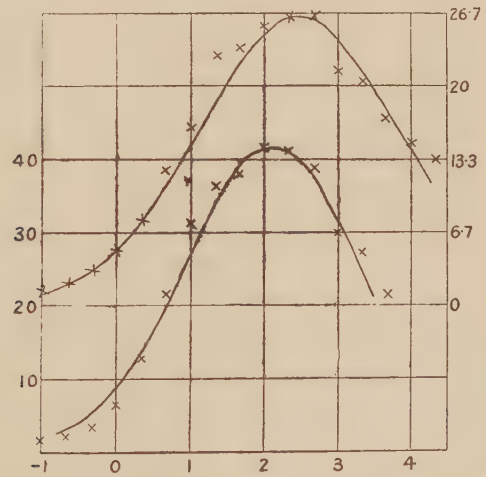

The four principal brightness levels are regarded as 0·001 ml. for exteriors at night, 0·1 ml. for interiors at night, 10 ml. for interiors in daylight, and 1000 ml. for exteriors in daylight. This corresponds to $\bar{3}{\cdot}5$, $\bar{1}{\cdot}5$, 1·5, and 3·5 on the above intensity scale.

It is the logarithm of the intensity in photons that is entered in the tables. The relative value of the candle-power of the lamp at different currents was known from the calibration-curve of the lamp, and to find absolute values it was necessary to standardize one particular current. This was done in the following manner :—An 8 C.P. carbon lamp was measured in terms of a Hefner lamp at its rated voltage. The reflexion coefficient of a certain kind of white paper was determined in terms of the reflexion

coefficient of a fresh magnesium oxide surface for perpendicular incidence, and found to be 78 per cent. of the latter. The paper was then assumed to reflect in this direction 0·75 times as much light as a perfectly diffusing surface. In arrangements 2 and 4 a piece of clear glass was set up in front of the eyepiece with its surface at 45° to the axis of the latter, so that the eye saw both the field by transmission and the white paper illuminated by the 8 C.P. lamp by reflexion side by side. Suppose now that the brightness of both halves of the field is to be 1 millilambert. Viewed through the glass they will be dimmed each to a different extent. The brighter half will then be 0·98 millilambert. The distance of the lamp from the paper was adjusted so that the brightness of the reflected image of the latter had this value, incidence and reflexion being normal, and the current adjusted until paper and field were equally bright. Thus the current is standardized.

There is, however, a pitfall here which shows the necessity for introducing the new unit, the photon. The millilambert is an objective unit of brightness. It is always the same, no matter what the diameter of the pupil is. Now, the subjective brightness varies with the area of the pupil. It is the latter which is measured in photons. The eye-ring of the spectrometer did not fill the aperture of the pupil at any of the intensities used in the experiments, and when the comparison was made the beam from the white paper filled the full aperture of the latter. To obtain the subjective brightness at the current in question we have to multiply by the area of the pupil for this brightness. This was taken from Reeves' data, and assumed to be 23 sq. mm. When the comparison was made the white paper had thus an apparent objective brightness of 0·98 millilambert and a subjective brightness of $0{\cdot}98 \times 23$ photons. It is subjective brightnesses which are balanced. To find the objective brightness of the half of the field in question it would be necessary to divide this product by the cross-sectional area of the other beam. But the objective brightness of the field is not required. When the glass plate is removed, the subjective brightness of the field becomes 23 photons at the current in question. Arrangement 3 was standardized in a different manner.

Some workers prefer to measure objective brightness of a surface in metre-candles, a brightness of ten metre-candles being equal to one millilambert. The millilambert

is to be preferred, however, as a unit of brightness, since the metre-candle is strictly speaking a unit of illumination. The millilambert suffers from the disability that we are unaware how far magnesium oxide fulfils the requirements of a perfectly diffusing surface.

It will be observed that the maxima of our two best curves lie at antilogs 2·1 and 2·45, say a mean of 2·3. How much of the difference is real we are as yet unable to say; the results are by different observers with different apparatus standardized in different ways, the standardization involving the difficult process of heterochromatic photometry. Now, the maxima of König and Brodhun's curves lie at 3·5 on their scale of intensities. To change their unit to log photons it seems that we must subtract 1·2.

We cannot reconcile this with the definition of their unit. The latter is the brightness of a magnesium oxide surface illuminated by one-tenth of a Violle standard at a distance of 1 metre and viewed through a 1 sq. mm. artificial pupil. The brightness of the surface is therefore 0·2 millilambert. In their work on Fechner's law they used an aperture of 1 sq. mm. area. So their unit was one-fifth photon. Thus the maxima of their curves should lie at 3·5 − log 5 = 2·8, and there is a discrepancy of 0·5 between their results and ours. The Violle standard was difficult to work with, and the standardization of their field was done apparently by viewing the standard and the field one after the other, not simultaneously with the comparison surfaces touching. This is not an accurate method.

The value of König's unit has already been considered by Blanchard * and by Hecht †. Blanchard made a determination of $\Delta I/I$ for white light for a part of the range, and decided that, if his contrast sensibility was the same as König's, the latter's unit should be multipled by 0·004 to bring it to photons. Hecht arrives at the same conclusion in another way. He divides 0·2 photon by 50, which he takes as the normal pupil aperture at this intensity; this gives 0·004. The position of the maximum is thus at 3·5 + log 0·004 = 1·1. Blanchard did not reach the maximum in his determination, so we do not know that his contrast sensibility is the same as König's. Since König

* Phys. Rev. xi. p. 81 (1918).
† Journ. Gen. Physiol. vii. p. 235 (1924–25).

worked with an aperture of 1 sq. mm., there is no justification for bringing in the factor 50 as Hecht does ; moreover, for the intensity in question the factor should be nearer 35 than 50.

In comparing series IV. and V. for red and blue it will be noticed that the maxima occur at the same place, but that the maximum sensibility is higher for blue. This second result is doubtful, because the point was not specifically investigated. The eye may have been in a more sensitive condition when the blue observations were made. To be certain on this point it would be necessary to take the red and blue readings alternately on the same days.

It will be noticed that at low intensities the sensibility in the blue is higher. This is due to so-called rod vision coming into play. In taking V. the eye was intentionally kept in the same state of partial dark adaptation throughout. If the eye is carefully dark adapted $I/\Delta I$ becomes greater throughout this region, and it is also possible to observe at much lower intensities. For example, at antilog -1 photons $I/\Delta I$ is 3·0 under the conditions of the experiment. On observing immediately after entering the room from daylight it is 3·5 ; after 10 minutes in the dark it was 2·4, and after another 20 minutes it was 1·6. After another 10 minutes it was possible to observe down to approximately antilog -5 photons. There is doubt, however, about the exact value of this limit, as it was obtained by exterpolating the calibration curve.

§ 2. Experiments investigating the relation between visual acuity and intensity of illumination have been carried out by Uhthoff (1886, 1890), König (1897), and others, but the results obtained by König * are so comprehensive, and the range of illumination he used was so great, that the more recent researches may be regarded as merely corroborating his work.

As object he employed Snellen's test figure E in various sizes, painted in black on a white background, and he altered the illumination by (1) using different sources—a candle, a petroleum lamp, and an electric arc, (2) varying the distance of the source from the object, and (3) interposing neutral glasses between the source and object. When working with white light he took as his unit of

* *Sitzungsber. d. Akad. d. Wissensch. zu Berlin*, p. 559 (1897)

illumination that which was produced by a Hefner lamp at a distance of 1 metre.

He made the observations himself, and assumed that his eye had unit acuity if it could approximately recognize the open side of the figure when the latter was at such a distance that it subtended an angle of 5′, and the lines and spaces each subtended 1′. His values are thus higher than if expressed in ophthalmologist's units, which may be regarded as the reciprocal of the angle subtended in minutes by the breadths of the lines and spaces when they are clearly distinguishable. It was in order to avoid fatigue that he renounced certainty in favour of approximation, and he gave the factor $\frac{3}{4}$ for the conversion of his results to ophthalmologists' units.

To investigate the effect of colour he cut out the black test figures and pasted them on red, green, or blue paper. The light from the above-mentioned sources was then made to pass through glasses of the appropriate colour before falling on the object.

Unfortunately, he did not state definitely his unit of intensity in these latter cases. He exhibited his results as four curves (one for each colour), showing the variation of the acuity with the logarithm of the illumination, and regarded each curve as made up of three straight lines, the one for low values having a low gradient, the intermediate one being fairly steep, and the one for high values being almost flat. Since he stated that if the curves for the colours had been plotted for the same unit of intensity as for white the four intermediate lines would have been coincident, we have been able to reduce all his results to absolute units with fair accuracy, and they are shown in the following table. His unit of intensity for white is equivalent to 0·072 millilamberts if we assume the reflexion coefficient of his paper to have been 0·8, and his units for red, green, and blue, derived as explained above, are 0·0072, 0·00018, and 0·000018 millilamberts respectively. In the table the log of the intensity I has been expressed in log photons. König did not use an artificial pupil in this work, so the area of the pupil at each intensity has been calculated from the data of Reeves.

As the observations were very numerous they have been averaged in threes for white, in fives for red, in threes for green, and in fours for blue :—

White.		Red.		Green.		Blue.	
Log I.	Acuity.	Log I.	Acuity.	Log I.	Acuity.	Log I.	Acuity.
$\bar{3}$·124	0·038	$\bar{2}$·26	0·023	$\bar{4}$·41	0·016	$\bar{4}$·23	0·022
·32	·046	·55	·034	·76	·034	·52	·031
·81	·065	·74	·044	$\bar{3}$·16	·050	·625	·032
$\bar{2}$·09	·072	·85	·060	·49	·061	$\bar{3}$·13	·049
·36	·084	·95	·074	·88	·081	·235	·054
·49	·095	$\bar{1}$·03	·094	$\bar{2}$·15	·088	·415	·062
·77	·101	·15	·095	·37	·101	·67	·069
$\bar{1}$·045	·126	·26	·127	·70	·115	$\bar{2}$·19	·092
·28	·147	·47	·192	$\bar{1}$·04	·128	·47	·099
·56	·201	·68	·275	·505	·188	·88	·126
·64	·214	·87	·319	·63	·195	1·46	·155
·71	·226	·97	·344	·75	·246	·83	·176
·79	·293	0·16	·451	·86	·257	0·09	·199
·84	·277	·23	·463	·97	·302	·27	·226
·955	·325	·38	·527	0·10	·391	·42	·232
0·02	·386	·57	·664	·415	·550	·48	·251
·06	·395	·67	·700	·615	·595	·61	·280
·17	·449	1·08	·913	·75	·741	·67	·300
·315	·565	·22	·971	·91	·845	·77	·311
·385	·545	·31	1·027	1·12	1·025	·88	·361
·42	·605	·49	1·137	·32	1·131	1·22	·422
·50	·596	·58	·242	·68	·267	·63	·516
·66	·744	·68	·331	2·23	·516	·99	·607
·71	·821	·93	·452				
·89	·693	2·15	·528				
1·08	1·000	·30	1·538				
·30	0·994	·69	·686				
·34	0·939						
·38	1·146						
·54	1·116						
·73	1·333						
·89	·313						
2·05	·420						
·25	·532						
·46	·650						
·64	1·695						
·73	·672						
·94	·693						
3·22	·686						
·525	·708						
·99	1·750						

Fig. 3 expresses the results in graphical form, the axes being in their correct positions for white, but the other curves are displaced one, two and four units of the log I scale to the right respectively to avoid superposition. It will be noticed that the blue curve extends further to the left than the green and that the green extends further to the left than the red. This is due to "rod vision" coming into operation.

Before attempting to explain König's results we thought it better to verify them for the case of white light. As test-object we chose the simplest possible—viz., a series of parallel lines, the widths of the lines and the intervening spaces being equal.

Fig. 3.

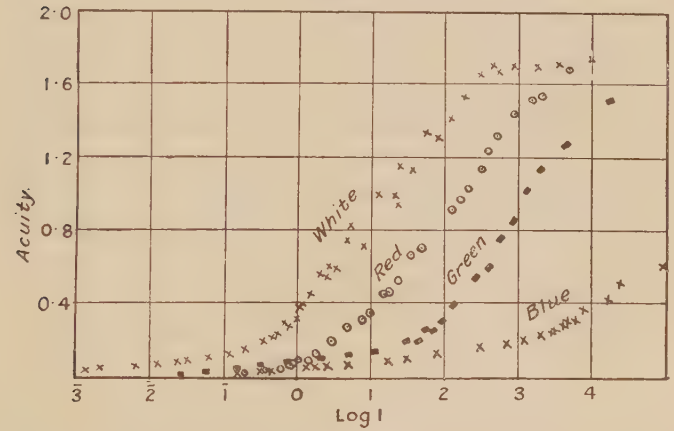

Among various preliminary attempts may be mentioned one which utilized the rhomb and sliding apparatus described above. A series of pairs of parallel lines separated by spaces of the same width as the lines, with the widths increasing from pair to pair, was drawn and photographed so that they all appeared on the one negative. The latter was placed just over the rhomb, and the intensity of the beam was changed until each pair in turn was just resolvable. The values of log I were obtained from those of the currents through the lamp. But this was abandoned in favour of the following arrangement :—

Two positives, one dense and "contrasty" and the other thin, were prepared of a drawing of a large number of

parallel lines. One of them was set up in front of a Fullolite lamp, the current through which could be varied and noted; and for different values of the current, and consequently of the intensity, the observer moved nearer to or farther from the object until the lines just appeared separate. His distance from the object was measured by means of a tape which was fixed in a convenient position, and this distance was proportional to his acuity at that intensity. The latter was determined in millilamberts and in photons from the calibration curve of the lamp, in much the same way as has been described earlier. An artificial pupil was not used, but one of a series of prepared apertures was always in position in front of the object, so that the angle subtended by the diameter of the "available" object was constant—approximately 2°.

Then the other positive was used as the object, and the series of observations repeated. The whole arrangement was characterized by extreme simplicity, the one source and the one object being used throughout for each test.

The results obtained are shown in the following table, each value being the mean of six observations. The acuity is taken as the reciprocal of the angle subtended by the breadth of a line or the breadth of a space in minutes, and I is expressed in photons in log I.

Dense Positive.		Thin Positive.	
Log I.	Acuity.	Log I.	Acuity.
3·44	1·564	3·48	1·280
·13	·517	·17	·260
2·79	·413	2·82	·179
·46	·329	·49	·097
·13	·241	·17	0·984
1·72	·174	1·76	·858
·35	·036	·39	·764
0·96	0·856	·00	·642
·54	·687	0·58	·508
·16	·502	·18	·345
$\bar{1}$·80	·341	$\bar{1}$·84	·292
·51	·230	·56	·171
·19	·126	$\bar{2}$·99	·087
$\bar{2}$·75	·079	·60	·054
·27	·051		

The results are shown graphically in fig. 4. On the same diagram König's results for white light are plotted as black disks for the purpose of comparison. König's intensity was the intensity of the white part of the test-object, ours the average intensity of the whole test-object, and the agreement of his results with the results for our dense object would be improved by shifting all our results 0·2 to the right. It is also obvious that the units of acuity have not been equivalent, for the agreement would be improved by increasing our ordinates by one eighth. König's curve has a corner near the top which ours lack.

Fig. 4.

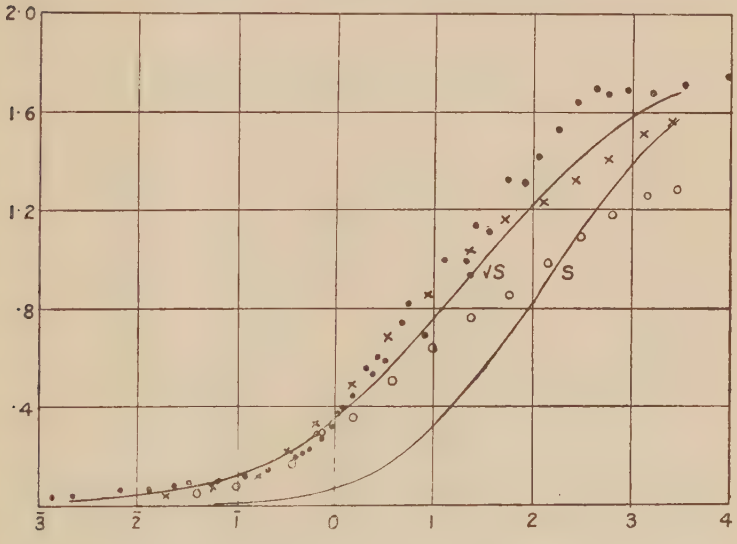

This may be due to his object being contrastier than ours, but the point requires further investigation.

Let us now consider the theoretical interpretation of the results. König describes his curves as being composed of three straight lines. This is hardly accurate, and gives us no clue as to the mechanism. Hecht suggested that the acuity is proportional to the number of percipient elements per unit area in the retina, and in a former paper Houstoun put forward the view that instead of this quantity we should take the number of percipient elements per unit length modified by a contrast factor. Since we are assuming that the sensation of brightness S is proportional

to the number of percipient elements stimulated, this would mean that the acuity should be proportional to $\sqrt{S}$ modified by a contrast factor or to $\sqrt{S}$ alone if the contrast factor is left out.

This hypothesis was tested in fig. 5 of the previous paper just referred to without success, owing to using the commonly accepted value of König's intensity unit, which we have found to be wrong. Let us now test it in the light of our own results. The observations on acuity were all made by J. F. Shearer. He also made the observations recorded in the lower curve of fig. 2. The integral curve corresponding to the latter, that is $y=\int_{-\infty}^{x} e^{-x^2} dx$, has been entered on fig. 4, choosing a suitable scale of ordinates.

Fig. 5.

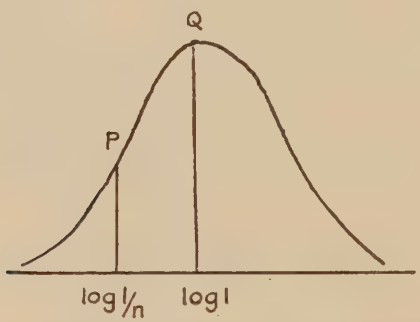

It represents S for Mr. Shearer's eye. Alongside is graphed $\sqrt{S}$, and it will be observed it fits the "dense" results reasonably well. It is also obvious that S does not fit the results.

In order to introduce the effect of contrast suppose that the brightness of the transparent strips is I, and that the black strips transmit one nth of the light incident upon them. Let us suppose that the intensity of light falling upon the black strips is, to begin with, I, and the intensity of light falling upon the clear strips is I/n. Then the whole test object appears one uniform hue. Throughout the area involved the elements are stimulated up to the level P in fig. 5. Increase the intensity in the clear strips to the level I. Then the additional elements represented by the area PQ come into action, and it is upon them alone that

the discrimination of detail depends. As the intensity rises this area moves across the curve. It has a constant breadth, log n. It is the root of this area which determines the number of active elements per unit-length, and we suggest that the acuity is proportional to this quantity. In the case of a very contrasty test object log n is large numerically, and the area to the left of P may be neglected.

By proceeding on these lines the difference between our "dense" and "thin" results may be explained, but a detailed discussion of this part of the work is postponed until we have more observations at our disposal. No matter what further results accrue it is clear that our hypotheses enable us to connect successfully the hitherto unrelated fields of acuity and intensity discrimination.

§ 3. We have suggested that the brightness of the image of a surface is proportional to the number of nerve-fibres stimulated by that image, and that each nerve-fibre transmits impulses only at a constant rate. This requires that if point sources are unequally bright one must stimulate more fibres than the other ; is this consistent with the process of image formation by the eye ?

The stars have been graded from ancient times into six classes, and are recognized as point sources. Thus a point is capable of six different brightnesses. This question seemed worthy of detailed investigation, so an artificial star was formed by setting up a circular hole of diameter one-tenth millimetre in the window of a light-tight room, and focussing the image of the filament of a half-watt lamp outside the room on this hole. The latter was viewed by an observer inside the room, from a distance of 4 metres, while an assistant decreased the intensity of the image by putting resistance in series with the lamp. This resistance was increased in steps, each step being adjusted to produce a just perceptible diminution in the brightness of the image. It will be noticed that in this method of experimenting the observer sees nothing but the point source, and we have to consider nothing but the area directly involved ; spatial induction is eliminated. Observations were made both with the unfiltered light of the lamp and also with Wratten tricolour filters in front of the hole. To the degree of accuracy attained in the experiments the hole could be regarded as infinitely small.

When white or red light was used extinction was reached in about 16 or 17 steps from the highest intensity. At the

highest intensity the image had a definite area of irregular outline, its breadth subtended perhaps 3 or 4 mm. at the eye, and it had streamers ; only for the last six steps was it a point. The last step was colourless. Over the last six steps with red the intensity increased one hundred times, and the increase in the logarithm of the intensity was approximately the same from each step to the one above it ; the other colours gave similar results, though not quite so regular. Thus the steps correspond roughly to the magnitudes of the stars, for an average star of the first magnitude is just about one hundred times as bright as one of the sixth, and the stars of each magnitude are approximately two and one-half times as bright as those of the next fainter.

The image of a point on the retina is not a point but an Airy disk surrounded by rings. With a pupil of 4 mm. and yellow light the radius of the first dark ring subtends 0·61′, and the radii of the second and third dark rings subtend respectively 1·12′ and 1·62′. 0·839 of the total light goes to form the central disk. 0·071 to form the first bright ring, and 0·028 to form the second bright ring. Now, while the pupillary diameter during the observations was considerably greater than 4 mm., owing to other aberrations there would be no gain in definition ; so we may take the above distribution of light in the image as fairly accurate. We notice at once that the average density of illumination over the central disk is twenty-eight times the average density of illumination over the first bright ring.

A point source is just visible when it gives as much light as one-tenth candle at 1 kilometre. Let us suppose that the light is distributed uniformly over the Airy disk in the retina. Then the same image would be formed if we assumed that the object was a disk the radius of which subtended 0·61′ and the laws of geometrical optics strictly held. If the brightness of a small area is B lamberts, and its area is S, it radiates as much light in the direction of the normal as a source of BS/π candles. We have thus

$$\frac{BS}{\pi} = \frac{1}{10},$$

$$S = \pi\left(\frac{0{\cdot}61\pi \times 10^5}{60 \times 180}\right)^2 \text{cm.}^2,$$

$$= 988 \text{ cm.}^2,$$

and $$B = 0{\cdot}318 \text{ millilamberts.}$$

The maximum area of the pupil ot the eye is about 45 sq. mm. Hence the brightness of the image on the retina is

$$45 \times 0{\cdot}318 = 14{\cdot}3 \text{ photons.}$$

This may be taken as the average intensity of illumination of the Airy disk at the limit of visibility. It is a comparatively high illumination. At this intensity four-tenths of the cones are above the threshold. The Airy disk covers five or six cones and the first bright ring about fourteen. Hence at the limit of visibility two cones on the disk should be above the threshold.

If we increase the intensity by six just perceptible steps, *i. e.*, raise it to the limit when the image ceases to appear

Fig. 6.

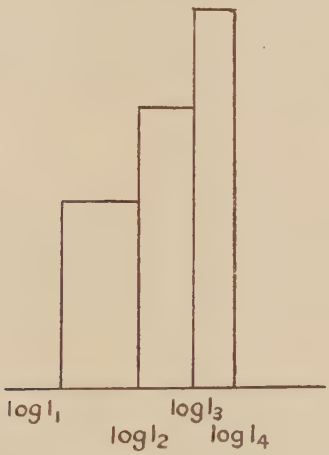

a point, the intensity of illumination on the disk goes up to 1430 photons, and on the first bright ring to 51 photons. At these intensities four-fifths and two-fifths of the cones respectively are above the threshold, *i. e.*, about ten should be stimulated.

The calculation is only approximate, but it shows that the increase in brightness of a point source can be quite reasonably explained on the assumption that each step in intensity is due to an additional nerve-fibre going into action.

§ 4. When $I/\Delta I$ is graphed as a function of log I the area of the curve to the left of any intensity represents the sensation at that intensity. It may be shown that this

holds not only for the limit, when ΔI is infinitesimal, but also for the case of finite steps. For (fig. 6) let I_2-I_1 be the just appreciable increase in intensity when the intensity is I_1, let I_3-I_2 be the just appreciable increase when the intensity is I_2, and so on. At the points whose abscissæ are $\log I_1$, $\log I_2$, etc., erect ordinates equal to

$$\frac{1}{\log I_2-\log I_1}, \quad \frac{1}{\log I_3-I_2}, \quad \frac{1}{\log I_4-\log I_3}, \text{ etc.},$$

and complete the rectangles as shown. Then their areas are equal. By definition the sensation increases by one unit from I_1 to I_2 and by one unit from I_2 to I_3. Thus each rectangle corresponds to one unit of sensation. If we wish to be rigorously accurate the smoothed curves we have hitherto dealt with should be replaced by a stepped curve as shown in fig. 6. But the accuracy attainable in the experimental work is not sufficient to make this refinement necessary.

XLII. *On some Problems of Nuclear Physics treated according to Wave-Mechanics.* *By* A. C. Banerji, *M.A. (Cantab.), M.Sc. (Cal.), Professor of Mathematics, Allahabad University* *.

In a previous paper † the author treated the problem of scattering of α-particles by light (not heavy) atoms according to Schrödinger's form of wave-mechanics, and showed that the assumption of the law of force,

$$F=\frac{2Ze^2}{r^2}\left(1-\frac{r_0}{r}\right),$$

leads to results which are in good agreement with experimental data. In the present paper an attempt has been made to extend the same consideration to some problems of nuclear physics. It is first necessary to give a brief survey of these problems.

According to modern theories of atomic structure, all atoms are composed of protons and electrons. The electrons are arranged in definite shells about the nucleus, according

* Communicated by Dr. M. N. Saha, F.R.S.

† Phil. Mag. ix. p. 273 (1930).

to the principles successively elaborated by Bohr *, Stoner and Mainsmith, and Pauli. The nucleus, whose dimension is of the order 10^{-13} cm., consists of an excess of protons, the electrons acting as binding material. We have to explain why, in spite of the preponderance of positive particles, the nucleus does not ordinarily explode. The assumption is made (Rutherford and Chadwick, Bieler †, and Debye ‡ and Hardemeier) that the usual repulsive forces between positively-charged particles change into attractive forces when the distance between them is of the order 10^{-13} cm. The assumption of these attractive forces gives a general explanation of abnormal scattering, and Rutherford and Thibaud § have attempted to explain the origin of nuclear γ-rays on the assumption of these forces. But more problems on the principle of nucleus construction have been suggested by the investigations of Aston ‖ on the packing effect of atoms. Possibly successive theoretical treatment of these problems will enable us to evolve the principles of nuclear construction (Kern-auf-bau-prinzip) ; hence it will be profitable to give a brief account of the problems suggested by Aston's experimental results.

Aston showed that, even if the weight of oxygen nucleus be taken as 16, the weight of the other nuclei differ markedly from whole numbers. To take the simplest case—the weight of the H-atom is found to be 1·00778, while the weight of the neutral H-particle (or neutron) in the nucleus is found to be unity. The reality of this neutron is rendered very plausible because we have got isotopes like Li_6 and Li_7, the different isotopes of Kr, which differ in weight exactly by unity on the oxygen scale. Since the nuclear charges are exactly the same, we have to suppose that the isotope Li_7 is simply Li_6 with a neutron attached to it. Hence we come to the following interesting problem :—According to Bohr's theory, the electron can be at best at a distance of $10^{-9} \times 5{\cdot}32$ cm. from the proton (Bohr's first orbit); it cannot approach nearer. The mass is 1·00778 (proton + electron). But in the nucleus a new proton-electron combination is formed in which the distance is $< 10^{-13}$ cm., resulting in a loss of mass of amount ·00724 from the proton. It has been pointed out that $\cdot 00724 = \alpha$, where α = Sommer-

* See 'Atomic Structure and Spectral Lines,' by Sommerfeld.
† Proc. Camb. Phil. Soc. xxi. p. 686 (1923).
‡ *Phys. Zs.* xxvii. p. 181.
§ *Journ. de Phys.* vi. p. 82 (1925)
‖ Proc. Roy. Soc. cxxiii. p .383.

feld's fine structure constant $\frac{2\pi e^2}{ch}$; hence in such a close combination the system loses the energy $M\alpha c^2 + mc^2$, where M = mass of the proton, m = mass of the electron. The existing theories (Bohr, Schrödinger, Dirac) seem incapable of explaining this fact.

We can also refer to the explanation of the packing effect observed in the formation of other heavier nuclei; but these problems can be tackled only after the neutron problem has been successfully solved.

Radioactivity.

In finding out the principles of nuclear construction, our knowledge of the phenomena of radioactivity will be a great guiding factor. It is well known that the phenomenon of spontaneous disintegration cannot be explained from mechanical principles. Recently Gamow * and Gourney and Condon † suggested explanations from the wave-mechanical point of view which have been further elucidated by von Laue ‡, Kudar, Th. Sexl, Möller, and Born.

From the works of Rutherford, Chadwick, and Bieler, it transpires that, if we plot the value of the potential from the centre of the atom outwards, it starts from negative infinity in the centre, passes through the zero value and rises to a steep positive maximum value, and gradually falls down to zero asymptotically (*vide* curve A).

This steep maximum of potential prevents the constituents in the inside from getting out, thus preventing explosion, and is known as the potential barrier. But, according to wave-mechanics, the α-particle is a wave, and though as a particle it cannot jump over the barrier unless it has an amount of energy which is never observed, as a wave it can occasionally get over the barrier. Gamow worked out the rate of leakage of the α-particle wave, and identified the process with the radioactive process of disintegration. He was thus able to offer a general explanation of the Geiger-Nutall relationship, connecting life with velocity of emission; but subsequent more rigorous work by von Laue, Kudar, Sexl, and Möller § has shown that the agreement is not as good as was at first

* Gamow, *Zs. f. Phys.* li. p. 204 (1928); lii. p. 501 (1929); liii. p. 601 (1929).

† Gourney and Condon, 'Nature,' cxxii. p. 439 (1928).

‡ Laue, *Zs. f. Phys.* lii. p. 726 (1929). Kudar, *Zs. f. Phys.* liii. pp. 61, 95 (1929). Sexl, *Zs. f. Phys.* liv. p. 445 (1929). Möller, *Zs. f. Phys.* lv. p. 451 (1929). Born, *Zs. f. Phys.* lviii. p. 306 (1929).

§ *Locc. citt.*

supposed. In particular, none of these workers have been able to show why α-particles emerge with *discrete positive* values.

Curve A.

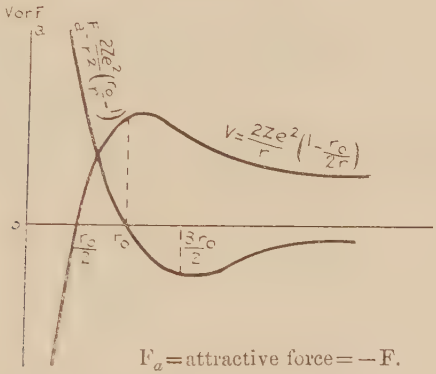

F_a = attractive force = $-F$.

Origin of Nuclear γ-Rays and Cosmic Rays.

The success of the law $V=2e^2Z\left(\frac{1}{r}-\frac{r_0}{2r}\right)$ in explaining the main results of scattering by light elements encourages the belief that it may also give us some clue regarding the origin of nuclear γ-rays. Recently some lively controversy has taken place on this question.

*Methods of Measuring the Wave-length of the γ-Ray Spectrum *.*

It is necessary to know how far the wave-lengths of the γ-rays have been correctly determined. The method which has been universally used by Ellis, M. de Broglie, Black, Meitner, and others † is that of photo-electric ionization. As the γ-ray which originates from the nucleus traverses the atom, it is absorbed by the electrons in the K, L_I, L_{II}, L_{III}, ... layers. Hence, in the resulting $\mathcal{E}$-ray spectrum the known differences $K-L_I$, $K-L_{II}$, L_I-L_{II} occur, and from an analysis of them it is possible to find out the frequency of the original γ-ray. The wave-lengths have been directly

* See 'Handbuch der Experimental Physik'—XV. Radioaktivitat, pp. 47, 56, 57.

† See Ellis and Wooster, Proc. Camb. Phil. Soc. 1925, p. 849. Ellis, Proc. Camb. Phil. Soc. 1924, p. 376. Black, Proc. Roy. Soc. 1924, p. 633; Proc. Camb. Phil. Soc. 1925, p. 838.

determined by Thibaud *, using ruled glass gratings at glancing-angle. The results of Thibaud are in fair agreement with those of the earlier workers.

L. Meitner † showed from such analysis that the γ-ray emission follows a process of radioactive disintegration, and does not precede it, as has been formerly thought. An example will suffice: RadAct (atomic No. 90) breaks up with ejection of α-rays. It has also got a γ-ray activity. Analysis of γ-rays, according to the methods sketched above, shows that the γ-ray spectrum excites β-rays with characteristic energy-level differences of the atomic No. 88, and not of 90. Hence it is concluded that the γ-ray emission takes place after ejection of α-rays. After the ejection the atomic shells are rearranged, according to the displacement law of Fajans and Soddy, as they would be in the element 88; and as the γ-ray traverses the atom, the β-rays are excited with the characteristic energy-level differences of element No. 88. Ellis ‡ has established the same fact in the case of a β-ray transformation.

The emission of γ-rays is therefore due to some rearrangement in the nucleus after either the α- or the β-ray has left it, and is therefore unconnected with the main causes leading to disintegration. It is still an open question whether they are due to the vibration of electrons, protons, α-particles, or some neutral particles which are supposed to exist in the neucleus. Ellis § has shown that the different γ-rays are homogeneous at least one in a thousand, *i. e.*, they are almost monochromatic; and from this and certain other arguments Kuhn ‖ concludes that they cannot be due to the vibrations of electrons, but are due to vibrations of heavier particles, the proton or the α-particle, as otherwise, owing to radiation damping, the line would be drawn into a broad band.

The damping factor due to radiation is

$$\alpha = \frac{8\pi^2 e^2 \nu^2}{3c^3 m},$$

where m = mass of the vibrating particle

* Thibaud, *Journ. de Phys.* vi. p. 82 (1925); 'Handbuch der Physik,' xxiii. chap. ii. D.

† Meitner, *Zs. f. Phys.* xxvi. p. 169 (1924); 'Handbuch der Physik,' xxii. chap. ii. D.

‡ Ellis and Wooster, Proc. Camb. Phil. Soc. xxii. p. 844 (1924).

§ See the recent discussion in Proc. Roy. Soc. cxxiii. p. 353.

‖ Kuhn, *Zs. f. Phys.* xliii. p. 56; xliv. p. 32.

Since $\nu = 3 \times 10^{21}$ for γ-rays, α would be too large, unless m were large. The half-breadth of the emitted line would be too great.

At present we may suppose that the γ-ray emission is due to any one of the following causes :—

(1) The α-particle or any charged positive particle may be describing quantum orbits with definite energy values about the nucleus. The γ-rays may be due to change of levels as in the optical spectrum.

Ellis has established the presence of discrete energy levels in the γ-spectrum of Ra B and Ra C, but the data are yet too fragmentary.

(2) The γ-ray spectrum may be similar to vibration or rotation spectra of molecules. The outer α-particle and the nucleus may be rotating about the common C.G. like a molecular dipole, and give rise to γ-rays ; or it may be due to similar processes in discrete entities like $\alpha - \alpha$, neutron-neutron oscillating in the field of the nucleus.

We have only explored the possibility No. 1. Let the potential energy be given by

$$V = \frac{2e^2 Z}{r}\left(1 - \frac{r_0}{2r}\right). \quad . \quad . \quad . \quad . \quad . \quad (1)$$

Case I. :

When discrete *quantized negative* values of energy are observed.

The Schrödinger equation is now

$$\nabla^2\psi + \frac{8\pi^2 M}{h^2}\left(E - \frac{2e^2 Z}{r} + \frac{e^2 Z r_0}{r^2}\right)\psi = 0. \quad . \quad . \quad (2)$$

Put * $\psi = R.\theta.\Phi$, and the equation in R is

$$\frac{d^2R}{dr^2} + \frac{2}{r}\frac{dR}{dr} + \left\{\frac{8\pi^2 ME}{h^2} - \frac{16\pi^2 MZe^2}{h^2 r} + \frac{8\pi^2 e^2 MZr_0}{h^2 r^2} - \frac{k(k+1)}{r^2}\right\} R = 0. \quad (2\text{A})$$

Putting $R = e^{\frac{1}{2}a_1 r}.S$, where the negative value of a_1 is to be taken, we have

$$\frac{d^2S}{dr^2} + \left(a_1 + \frac{2}{r}\right)\frac{dS}{dr} + \left(\frac{a_0}{r} + \frac{b_0}{r^2}\right)S = 0, \quad . \quad . \quad (2\text{B})$$

* See 'Wave Mechanics,' by H. T. Flint, chap. iii.

where

$$\left.\begin{aligned} \tfrac{1}{4}a_1^2 &= -\frac{8\pi^2 \mathrm{ME}}{h^2}, \\ a_0 &= a_1 - \frac{16\pi^2 \mathrm{MZ}e^2}{h^2}, \\ b_0 &= -k(k+1) + \frac{8\pi^2 e^2 \mathrm{MZ}r_0}{h^2}. \end{aligned}\right\} \quad . \quad . \quad . \quad (3)$$

Our equation now reduces to

$$f\left(r\frac{d}{dr}\right)\mathrm{S} + \frac{1}{r}g\left(r\frac{d}{dr}\right)\mathrm{S} = 0, \quad . \quad . \quad . \quad . \quad (4)$$

where

$$f(z) = a_1 z + a_0,$$
$$g(z) = z^2 + z + b_0.$$

Let α_1 be one of the roots of

$$z^2 + z + b_0 = 0,$$

so that

$$\alpha_1 = -\tfrac{1}{2} + \tfrac{1}{2}\sqrt{1 - 4b_0}$$
$$= -\tfrac{1}{2} + \sqrt{(k+\tfrac{1}{2})^2 - \frac{8\pi^2 e^2 \mathrm{ZM}r_0}{h^2}}.$$

One of the series will terminate after n_r terms if

$$a_1(\alpha_1 + n_r) + a_0 = 0,$$

from which we get, after substituting the values of a_1, a_0, α_1, the discrete quantized values of E:

$$\mathrm{E} = -\frac{8\pi^2 e^4 \mathrm{Z}^2 \mathrm{M}}{h^2} \frac{1}{\left\{(n_r + \tfrac{1}{2}) + \sqrt{(k+\tfrac{1}{2})^2 - \frac{8\pi^2 e^2 \mathrm{ZM}r_0}{h^2}}\right\}^2}.$$

. . . (5)

The quantity

$$\frac{8\pi^2 e^2 \mathrm{ZM}}{h^2} r_0 = \frac{r_0}{\frac{am}{2\mathrm{MZ}}}, \quad . \quad . \quad . \quad . \quad (6)$$

where a = radius of the Bohr orbit $= \dfrac{h^2}{4\pi^2 e^2 m}$,

m = mass of the electron,

M = mass of the α-particle

$$\frac{am}{2\mathrm{MZ}} = \frac{3{\cdot}66 \times 10^{-13}}{\mathrm{Z}} \text{ cm.}$$

For RadAct, Z=90, this equals 4×10^{-15} cm.
As r_0 is certainly of the order $10^{-13}\sim10^{-12}$ cm.*,

$$\frac{r_0}{\frac{\hbar}{am}}{\frac{}{2MZ}} = n_0^2,$$

where n_0 is a quantity of the order of 10 to 12.
Hence we have

$$E = -4Rh Z^2\left(\frac{M}{m}\right)\left\{\frac{1}{n_r+\frac{1}{2}+\sqrt{(k+\frac{1}{2})^2-n_0^2}}\right\}^2, \quad . \quad (7)$$

where R is the Rydberg's constant, and for real values of E $(k+\frac{1}{2})$ must be greater than n_0.

If we use Dirac's form, the half-values will probably disappear, and moreover if we put $n_r=0$, we get

$$E = -\frac{4Rh Z^2\left(\frac{M}{m}\right)}{k^2-n_0^2}, \quad k>n_0. \quad . \quad . \quad . \quad (7\text{A})$$

We have

$$\nu = Rh Z^2\left(\frac{M}{m}\right)\left[\frac{1}{k^2-n_0^2}-\frac{1}{k'^2-n_0^2}\right], \quad . \quad . \quad (8)$$

where $k'\geq k$.
If we take

$$k = n_0+1, \qquad k' = n_0+2,$$

$$\nu = 4Rh Z^2\frac{M}{m}\frac{2n_0+3}{(4n_0+4)(2n_0+1)} \quad . \quad . \quad . \quad (8\text{A})$$

$$= Rh Z^2\frac{M}{m}\frac{1}{n_0+1} \quad \text{approximately.}$$

Since $\frac{M}{m}=4\times1836$, these rays become about 600 times harder than the K-spectrum of the element, and even if they exist, they can only be compared to the cosmic rays. Hence we cannot explain the ordinary nuclear γ-ray spectrum on the basis of the existence of negative energy values. Wave-lengths of cosmic rays have been estimated by Millikan to range from ·004 cm. to $\cdot00013\times10^{-8}$ cm. (about 1000 times harder than γ-rays) from the values of absorption-coefficients. The relation of absorption-coefficients to wave-length, which is the basis of Millikan's measurements of wave-lengths, is,

* See discussion in Proc. Roy. Soc. cxxiii. p. 353.

however, not definitely settled. Klein and Nishina * have worked out a new formula of dispersion from Dirac's theory according to which the wave-length may be several times smaller than hitherto thought. The negative energy values, however, afford a clue to the origin of cosmic rays which may be identified as those arising from vibrations in the intra-nuclear space.

Case II.:

When discrete *quantized positive* values of energy are observed.

We take the Schrödinger equation in the form

$$\nabla^2\Psi = -\frac{4\pi i M}{h}\frac{\partial\Psi}{\partial t} - \frac{8\pi^2 M}{h^2}V\Psi = 0. \quad . \quad . \quad (9)$$

Put

$$\Psi = e^{-\frac{\mu}{2}t}.e^{\frac{2i\pi E}{h}t}\psi. \quad . \quad . \quad . \quad . \quad . \quad (10)$$

We get

$$\nabla^2\psi + \frac{8\pi^2 M}{h^2}(E-V)\psi + \frac{i.2\pi M\mu}{h}\psi = 0. \quad . \quad (9\,A)$$

Putting the value of V, we have

$$\nabla^2\psi + \frac{8\pi^2 M}{h^2}\left(E - \frac{2Ze^2}{r} + \frac{Ze^2 r_0}{r^2}\right)\psi + \frac{i.2\pi M\mu}{h}\psi = 0. \quad . \quad (9\,B)$$

Put

$$\psi = R.\theta.\Phi,$$

and the equation in R is found to be

$$\frac{d^2R}{dr^2} + \frac{2}{r}\frac{dR}{dr} + \left\{\frac{8\pi^2 ME}{h^2} + \frac{i.2\pi M\mu}{h} - \frac{16\pi^2 ZMe^2}{h^2}\frac{1}{r} + \frac{8\pi^2 MZe^2 r_0}{h^2}\frac{1}{r^2} - \frac{k(k+1)}{r^2}\right\}R = 0. \quad . \quad (9\,C)$$

Put

$$R = e^{\frac{1}{2}(a_1+ip)r}.S.$$

We have

$$\frac{d^2S}{dr^2} + \left(a_1 + ip + \frac{2}{r}\right)\frac{dS}{dr} + \left(\frac{a_0}{r} + \frac{b_0}{r^2}\right)S = 0, \quad . \quad (9\,D)$$

* Klein and Nishina, *Z. f. Phys.* lii. p. 853; 'Nature,' Sept. 15, 1928.

where

$$\left.\begin{aligned} \tfrac{1}{4}(p^2-a_1^2) &= \frac{8\pi^2 \mathrm{M E}}{h^2}, \\ a_1 p &= -\frac{4\pi \mathrm{M}\mu}{h}, \\ a_0 &= a_1 + ip - \frac{16\pi^2 \mathrm{MZ}e^2}{h^2}, \\ b_0 &= -k(k+1) + \frac{8\pi^2 \mathrm{MZ}e^2 r_0}{h^2}. \end{aligned}\right\} \quad . \quad . \quad (11)$$

Our equation now reduces to

$$f\left(r\frac{d}{dr}\right)\mathrm{S} + \frac{1}{r}g\left(r\frac{d}{dr}\right)\mathrm{S} = 0, \quad . \quad . \quad . \quad . \quad (9\,\mathrm{E})$$

where

$$f(\mathrm{Z}) = (a_1+ip)\mathrm{Z} + a_0,$$
$$g(\mathrm{Z}) = \mathrm{Z}^2 + \mathrm{Z} + b_0.$$

Let α_1 be one of the roots of

$$\mathrm{Z}^2 + \mathrm{Z} + b_0 = 0,$$

so that

$$\begin{aligned} \alpha_1 &= -\tfrac{1}{2} + \tfrac{1}{2}\sqrt{1-4b_0} \\ &= -\tfrac{1}{2} + \sqrt{(k+\tfrac{1}{2})^2 - \frac{8\pi^2 e^2 \mathrm{MZ}r_0}{h^2}}. \quad . \quad . \quad . \quad (12) \end{aligned}$$

The series will terminate after n_r terms if

$$(a_1+ip)(\alpha_1+n_r) + a_0 = 0$$

or

$$a_1 + ip = \frac{16\pi^2 e^2 \mathrm{MZ}}{h^2} \frac{1}{n_r + \tfrac{1}{2} + \sqrt{(k+\tfrac{1}{2})^2 - \frac{8\pi^2 e^2 \mathrm{MZ}r_0}{h^2}}}. \quad (12)$$

In order that the above equation may be possible, $\frac{8\pi^2 e^2 \mathrm{MZ}r_0}{h^2}$ must be greater than $(k+\frac{1}{2})^2$ or $r_0 > f_0(k+\frac{1}{2})^2$, where

$$f_0 = \frac{h^2}{8\pi^2 e^2 \mathrm{MZ}} = \frac{am}{2\mathrm{MZ}}.$$

Then we have from (12), after some calculations,

$$a_1 = \frac{16\pi^2 e^2 \mathrm{MZ}}{h^2} \frac{n_r + \tfrac{1}{2}}{(n_r+k+1)(n_r-k) + \dfrac{r_0}{f_0}}, \quad . \quad (13)$$

$$p = -\frac{16\pi^2 e^2 \mathrm{MZ}}{h^2} \frac{\sqrt{\frac{r_0}{f} - (k+\frac{1}{2})^2}}{(n_r - k)(n_r + k + 1) + \frac{r_0}{f_0}}. \quad . \quad (14)$$

For the quantized discrete values of E we get

$$\mathrm{E} = \frac{8\pi^2 \mathrm{MZ}^2 e^4}{h^2} \frac{\left\{\frac{r_0}{f_0} - (k+\frac{1}{2})^2 - (n_r+\frac{1}{2})^2\right\}}{\left\{(n_r+k+1)(n_r-k) + \frac{r_0}{f_0}\right\}^2}$$

$$= 4\mathrm{R}h\mathrm{Z}^2\left(\frac{\mathrm{M}}{m}\right) \frac{\left\{\frac{r_0}{f_0} - (k+\frac{1}{2})^2 - (n_r+\frac{1}{2})^2\right\}}{\left\{(n_r+k+1)(n_r-k) + \frac{r_0}{f_0}\right\}^2}, \quad (15)$$

where R is Rydberg's constant.

We get also

$$\mu = \frac{8\pi \mathrm{E}}{h} \frac{(n_r+\frac{1}{2})\sqrt{\frac{r_0}{f_0} - (k+\frac{1}{2})^2}}{\frac{r_0}{f_0} - (k+\frac{1}{2})^2 - (n_r+\frac{1}{2})^2}. \quad . \quad . \quad (16)$$

E is positive when $r_0 > f_0\{(k+\frac{1}{2})^2 + (n_r+\frac{1}{2})^2\}$.

If we put $n_0 = 0$, we get discrete quantized *positive* energy values, provided $r_0 > f_0\left[(k+\frac{1}{2})^2 + \frac{1}{4}\right]$.

If we now take

$$\frac{r_0}{f_0} = n_0^2 + \tfrac{1}{4} \quad \text{approximately,}$$

we get

$$\mathrm{E} = 4\mathrm{R}h\mathrm{Z}^2\left(\frac{\mathrm{M}}{m}\right) \frac{1}{\left[n_0^2 - (k+\frac{1}{2})^2\right]} \quad \text{approximately.}$$

When $k < n_0$, the frequency is given by

$$\nu = 4\mathrm{R}\mathrm{Z}^2\left(\frac{\mathrm{M}}{m}\right)\left[\frac{1}{n_0^2 - (k+\frac{1}{2})^2} - \frac{1}{n_0^2 - (k'+\frac{1}{2})^2}\right].$$

If n_0 is sufficiently large, and k' and k are taken as 1 and 2 respectively, we get

$$\nu = 4\mathrm{R}\mathrm{Z}^2\left(\frac{\mathrm{M}}{m}\right).\frac{4}{n_0^4} \quad \text{approximately.}$$

We come within the γ-ray region if we take $n_0 = 10$, which is not an improbable value*.

* Rutherford has used as large a quantum number as 30 for accounting for γ-rays on the Debye-Hardemeir theory. See Volta Centenary Volume.'

This type of solution has been obtained by Thibaud *, using the elementary Bohr theory. He gets

$$\nu = 4\mathrm{R}Z\left(\frac{\mathrm{M}}{m}\right)\left[\frac{1}{n_0^2-k^2}-\frac{1}{n_0^2-k'^2}\right],$$

where $k'<k$ and k, $k'<n_0$. He shows that this formula accounts in a fairly satisfactory way for the nuclear γ-ray of RadAct.

The energy of α-rays emitted from radioactive bodies varies in range from $6{\cdot}6\times10^{-6}$ erg (α-rays from Ur) to $1{\cdot}4\times10^{-5}$ erg (α-rays from ThC′) †. But the energy of γ-rays is much less than this, *e. g.* in RadAct the wave-length of γ-rays varies from 40×10^{-11} cm. to 400×10^{-11} cm., corresponding to energy-values 5×10^{-7} erg to 5×10^{-8} erg ‡. This is easily explained on the theory given here. The energy of the α-particle is

$$\frac{\mathrm{R}h\mathrm{Z}^2}{n_0^2-(k+\frac{1}{2})^2}\cdot\frac{\mathrm{M}}{m}=\frac{1{\cdot}24\times10^{-3}}{n_0^2-(k+\frac{1}{2})^2}\ \mathrm{erg},$$

$$\mathrm{Z}=90 \text{ for RadAct.}$$

If we put $k=0$ and $n_0=14$, the energy becomes $6{\cdot}6\times10^{-6}$ erg; for $n_0=9$, $\mathrm{E}=1{\cdot}40\times10^{-5}$ erg. So the order of energy of α-rays is of the same dimensions as is actually observed. The energy of γ-rays is then for the transition $k'\rightarrow k$, $1\rightarrow2$ of the order 4×10^{-8} erg, *i. e.* of the same order as is observed for the softest γ-rays. For transitions involving larger values of k, the energy becomes of the same order as of the harder γ-rays.

The above results, viz. existence of discrete and quantized positive energy values, of α-rays within the potential barrier, and agreement in the order of dimensions of the calculated energy values for α-particles and nuclear γ-rays with those actually observed, are distinctly new.

In Tables I. to VI. I have tried to account for the nuclear γ-rays of six elements: RaB, RaC, —ThC′+C″, MesTh 2, RadAct, Act X; the data have been taken from the 'Handbuch der Experimental Physik,' xv. p. 56.

In the first column are given the wave-lengths in Siegbahn units, viz. 10^{-11} cm. The second column gives the energy

* Thibaud, *Compt. Rend.* clxxxi. p. 857 (1925).

† See Enskog, *Zs. Phys.* lii. p. 207.

‡ See 'Handbuch der Experimental Physik'—XV. Radioaktivität, pp. 56–57.

$h\nu$ in ergs. In the third column values of P as deduced from observations are given, where

$$P = \frac{(n_0^2 - k^2)(n_0^2 - k'^2)}{k^2 - k'^2}$$

The values of n_0, k, and k' have been chosen by trial. In the last column calculated values of P from trial values of n_0, k, and k' are given. Z stands for atomic number.

TABLE I.

Radium B, Z=81.

X. E.	Ergs.	Values of P deduced from observations.	$n_0=19$.	Calculated values of P.
230·3	$8{\cdot}5\times10^{-8}$	$1{\cdot}22\times10^{4}$	$k=5,\ k'=4$	$1{\cdot}29\times10^{4}$
62·7	$3{\cdot}1\times10^{-7}$	$\cdot34\times10^{4}$	$k=6,\ k'=1$	$\cdot33\times10^{4}$
59·9	$3{\cdot}3\times10^{-7}$	$\cdot32\times10^{4}$	$k=6,\ k'=0$	$\cdot32\times10^{4}$
50·7	$3{\cdot}9\times10^{-7}$	$\cdot27\times10^{4}$	$k=7,\ k'=3$	$\cdot28\times10^{4}$
47·5	$4{\cdot}1\times10^{-7}$	$\cdot25\times10^{4}$	$k=7,\ k'=2$	$\cdot25\times10^{4}$
44·7	$4{\cdot}4\times10^{-7}$	$\cdot24\times10^{4}$	$k=7,\ k'=1$	$\cdot23\times10^{4}$
41·6	$4{\cdot}7\times10^{-7}$	$\cdot22\times10^{4}$	$k=7,\ k'=0$	$\cdot23\times10^{4}$
34·9	$5\ \times10^{-7}$	$\cdot21\times10^{4}$	$k=8,\ k'=0$	$\cdot21\times10^{4}$
26·2	$7{\cdot}5\times10^{-7}$	$\cdot14\times10^{4}$	$k=9,\ k'=3$	$\cdot14\times10^{4}$
25·6	$7{\cdot}7\times10^{-7}$	$\cdot13\times10^{4}$	$k=9,\ k'=2$	$\cdot13\times10^{4}$

TABLE II.

Radium C, Z=81.

X. E.	Ergs.	Values of P deduced from observations.	$n_0=19$.	Calculated values of P.
44·9	$4{\cdot}3\times10^{-7}$	$\cdot24\times10^{4}$	$k=7,\ k'=2$	$\cdot25\times10^{4}$
37·1	$5{\cdot}3\times10^{-7}$	$\cdot20\times10^{4}$	$k=8,\ k'=4$	$\cdot21\times10^{4}$
31·7	$6{\cdot}2\times10^{-7}$	$\cdot17\times10^{4}$	$k=8,\ k'=1$	$\cdot17\times10^{4}$
28·8	$6{\cdot}8\times10^{-7}$	$\cdot15\times10^{4}$	$k=9,\ k'=4$	$\cdot15\times10^{4}$
20·2	$9{\cdot}2\times10^{-7}$	$\cdot11\times10^{4}$	$k=10,\ k'=3$	$\cdot10\times10^{4}$
13·1	$1{\cdot}5\times10^{-6}$	$\cdot69\times10^{3}$	$k=12,\ k'=7$	$\cdot70\times10^{3}$
10·9	$1{\cdot}8\times10^{-6}$	$\cdot58\times10^{3}$	$k=12,\ k'=4$	$\cdot58\times10^{3}$
9·9	$2\ \times10^{-6}$	$\cdot52\times10^{3}$	$k=13,\ k'=8$	$\cdot53\times10^{3}$
8·66	$2{\cdot}1\times13^{-6}$	$\cdot50\times10^{3}$	$k=13,\ k'=7$	$\cdot50\times10^{3}$
6·94	$2{\cdot}8\times10^{-6}$	$\cdot37\times10^{3}$	$k=14,\ k'=8$	$\cdot37\times10^{3}$
5·56	$3{\cdot}5\times10^{-6}$	$\cdot30\times10^{3}$	$k=14,\ k'=1$	$\cdot30\times14^{3}$

TABLE III.

Thorium C + C′, Z = 81.

X. E.	Ergs.	Values of P deduced from observations.	$n_0 = 19$.	Calculated values of P.
303	$6{\cdot}5\times10^{-8}$	$1{\cdot}6\times10^{4}$	$k=4,\ k'=3$	$1{\cdot}73\times10^{4}$
85·4	$2{\cdot}2\times10^{-7}$	$\cdot47\times10^{4}$	$k=5,\ k'=1$	$\cdot50\times10^{4}$
58·6	$3{\cdot}3\times10^{-7}$	$\cdot32\times10^{4}$	$k=6,\ k'=0$	$\cdot32\times10^{4}$
52·9	$3{\cdot}7\times10^{-7}$	$\cdot28\times10^{4}$	$k=7,\ k'=3$	$\cdot28\times10^{4}$
48·8	$4{\cdot}0\times10^{-7}$	$\cdot26\times10^{4}$	$k=7,\ k'=2$	$\cdot25\times10^{4}$
47·7	$4{\cdot}1\times10^{-7}$	$\cdot25\times10^{4}$	$k=7,\ k'=1$	$\cdot23\times10^{4}$
44·3	$4{\cdot}4\times10^{-7}$	$\cdot24\times10^{4}$	$k=7,\ k'=0$	$\cdot23\times10^{4}$
42·3	$4{\cdot}9\times10^{-7}$	$\cdot21\times10^{4}$	$k=8,\ k'=4$	$\cdot21\times10^{4}$
23·8	$8{\cdot}2\times10^{-7}$	$\cdot13\times10^{4}$	$k=9,\ k'=2$	$\cdot13\times10^{4}$
18·8	$1{\cdot}1\times10^{-6}$	$\cdot95\times10^{3}$	$k=10,\ k'=1$	$\cdot95\times10^{3}$
4·7	$4{\cdot}2\times10^{-6}$	$\cdot25\times10^{3}$	$k=15,\ k'=8$	$\cdot25\times10^{3}$

TABLE IV.

Mesothorium 2, Z = 90.

X. E.	Ergs.	Values of P deduced from observations.	$n_0 = 19$.	Calculated values of P.
214	$8{\cdot}9\times10^{-8}$	$1{\cdot}4\times10^{4}$	$k=3,\ k'=0$	$1{\cdot}45\times10^{4}$
95·6	$2{\cdot}1\times10^{-7}$	$\cdot59\times10^{4}$	$k=5,\ k'=2$	$\cdot58\times10^{4}$
67·2	$2{\cdot}9\times10^{-7}$	$\cdot43\times10^{4}$	$k=6,\ k'=3$	$\cdot42\times10^{4}$
38·8	$5{\cdot}1\times10^{-7}$	$\cdot24\times10^{4}$	$k=7,\ k'=2$	$\cdot25\times10^{4}$
36·5	$5{\cdot}3\times10^{-7}$	$\cdot23\times10^{4}$	$k=7,\ k'=1$	$\cdot23\times10^{4}$
26·7	$7{\cdot}3\times10^{-7}$	$\cdot17\times10^{4}$	$k=8,\ k'=1$	$\cdot17\times10^{4}$
13·5	$1{\cdot}5\times10^{-6}$	$\cdot83\times10^{3}$	$k=11,\ k'=5$	$\cdot84\times10^{3}$
12·7	$1{\cdot}6\times10^{-6}$	$\cdot78\times10^{3}$	$k=11,\ k'=4$	$\cdot79\times10^{3}$

TABLE V.

Radio-actinium, Z = 90.

X. E.	Ergs.	Values of P deduced from observations.	$n_0 = 19$.	Calculated values of P.
41·1	$4{\cdot}8\times10^{-7}$	$\cdot26\times10^{4}$	$k=7,\ k'=2$	$\cdot25\times10^{4}$
43·8	$4{\cdot}5\times10^{-7}$	$\cdot28\times10^{4}$	$k=7,\ k'=3$	$\cdot28\times10^{4}$
48·6	4×10^{-7}	$\cdot31\times10^{4}$	$k=6,\ k'=0$	$\cdot32\times10^{4}$
63	$3{\cdot}1\times10^{-7}$	$\cdot40\times10^{4}$	$k=6,\ k'=3$	$\cdot42\times10^{4}$

TABLE V. (*cont.*).

Radio-actinium, Z=90.

X. E.	Ergs.	Values of P deduced from observations.	$n_0=19$.	Calculated values of P.
82·8	$2{\cdot}4\times10^{-7}$	$\cdot52\times10^4$	$k=5,\ k'=1$	$\cdot5\ \times10^4$
123	$1{\cdot}6\times10^{-7}$	$\cdot78\times10^4$	$k=5,\ k'=3$	$\cdot74\times10^4$
201	$9{\cdot}7\times10^{-7}$	$1{\cdot}28\times10^4$	$k=5,\ k'=4$	$1{\cdot}29\times10^4$
232	$8{\cdot}4\times10^{-7}$	$1{\cdot}47\times10^4$	$k=3,\ k'=0$	$1{\cdot}45\times10^4$
282	$7{\cdot}0\times10^{-8}$	$1{\cdot}77\times10^4$	$k=4,\ k'=3$	$1{\cdot}73\times10^4$
390	$5{\cdot}0\times10^{-8}$	$2{\cdot}48\times10^4$	$k=3,\ k'=2$	$2{\cdot}51\times10^4$

TABLE VI.

Actinium X, Z=88.

X. E.	Ergs.	Values of P deduced from observations.	$n_0=17$.	Calculated values of P.
86	$2{\cdot}3\times10^{-7}$	$\cdot53\times10^4$	$k=4,\ k'=1$	$\cdot52\times10^4$
80·4	$2{\cdot}4\times10^{-7}$	$\cdot50\times10^4$	$k=4,\ k'=0$	$\cdot49\times10^4$
79	$2{\cdot}5\times10^{-7}$	$\cdot48\times10^4$	$k=5,\ k'=3$	$\cdot47\times10^4$
62	$3{\cdot}2\times10^{-7}$	$\cdot38\times10^4$	$k=5,\ k'=2$	$\cdot36\times10^4$
46	$4{\cdot}3\times10^{-7}$	$\cdot28\times10^4$	$k=6,\ k'=3$	$\cdot26\times10^4$

It is to be seen that in most cases the agreement is extremely good. We expect, in each case, that if all the intermediate values of k and k' are to be allowed, a much larger number of γ-rays should exist. Such a number is not observed. Probably there may be a selection principle restricting the transitions from $k'\to k$, or certain weak γ-rays have not yet been observed. It may be pointed out that k has been chosen in place of $k+n_r$, and such transitions as $k'=3$ to $k'=7$ denote changes in the total quantum number. I hope to treat the problem further from the standpoint of Dirac's theory of the electron on a future occasion.

I have great pleasure in thanking my colleague Prof. M. N. Saha, F.R.S., of the Physics Department of the Allahabad University, for much help and many suggestions in preparing this paper.

Department of Mathematics,
Allahabad University.
Dec. 10, 1929.

XLIII. *The Reduction of Observations.*

By A. F. Dufton, *M.A., D.I.C.* *

1. IN the reduction of observations, the possibilities of a graphical solution are not always realized. The determination of the function $R = 46{\cdot}3465 + 0{\cdot}181600\ t$ (with a mean deviation of $2{\cdot}4 \times 10^{-4}$) from observations with values of t ranging from 14 to 28, which would appear at first sight beyond the scope of a graph, is a typical example †.

In a recent paper on "Reducing Observations by the Method of Minimum Deviations" ‡, Dr. Rhodes calls attention to the necessity for methods alternative to that of Least Squares and discusses the fitting of a parabola to a series of points. The method he describes is stated to be simpler than that of Edgeworth but undoubtedly more laborious than that of Least Squares.

It may perhaps be of interest to show the application of a simple graphic method to Dr. Rhodes' data, which are reproduced below.

2. This method, which was briefly described in 'Nature' two years ago §, is for the determination of a linear function of X approximating to Y for a range of corresponding values (X, Y). The plotted values are divided into two classes by the median of X and the required straight line divides each class into equal numbers.

In the description given in 'Nature,' the straight line is unique when the number of values of (X, Y) is $4n+2$ or $4n+3$. In other cases, to avoid ambiguity, the following procedure is suggested: when there are $4n+1$ values, include the median in each class into which it divides the values; when there are $4n$ values, include the two "medians" in each class.

3. In the problem of the parabola stated by Dr. Rhodes, if the required equation is

$$y = a + b(x+c)^2,$$

it follows that $\Delta = 2b(n+c)$,

where $\Delta = \frac{1}{2}(y_{(n+1)} - y_{(n-1)})$

or $y_{(n+\frac{1}{2})} - y_{(n-\frac{1}{2})}$.

* Communicated by the Director of Building Research, Department of Scientific and Industrial Research.

† Proc. Phys. Soc. xliii. p. 103 (1930).

‡ Phil. Mag. ix. p. 974 (1930).

§ 'Nature,' cxxi. p. 866 (1928).

and a linear function of Δ approximating to n can be determined as in fig 1.

x $(=n)$	y	Δ
-8	28	
$-7\frac{1}{2}$		-67
-7	-39	-34
$-6\frac{1}{2}$		-1
-6	-40	19
$-5\frac{1}{2}$		39
-5	-1	$31\frac{1}{2}$
$-4\frac{1}{2}$		24
-4	23	$17\frac{1}{2}$
$-3\frac{1}{2}$		11
-3	34	1
$-2\frac{1}{2}$		-9
-2	25	3
$-1\frac{1}{2}$		15
-1	40	9
$-\frac{1}{2}$		3
0	43	$-5\frac{1}{2}$
$\frac{1}{2}$		-14
1	29	$-14\frac{1}{2}$
$1\frac{1}{2}$		-15
2	14	$-8\frac{1}{2}$
$2\frac{1}{2}$		-2
3	12	-15
3		-28
4	-16	-13
$4\frac{1}{2}$		2
5	-14	-15
$5\frac{1}{2}$		-32
6	-46	-26
$6\frac{1}{2}$		-22
7	-68	11
$7\frac{1}{2}$		44
8	-24	

The graph shows that when $\Delta=0, n=-\frac{1}{2}$, so that the value of c is $\frac{1}{2}$.

The parabola, therefore, is

$$y=a+b(x+\tfrac{1}{2})^2$$

and a linear function of $(x+\frac{1}{2})^2$ approximating to y can be determined as shown in fig. 2.

The function is

$$y=33-1{\cdot}7(x+\tfrac{1}{2})^2,$$

which is the parabola required.

Fig. 1.

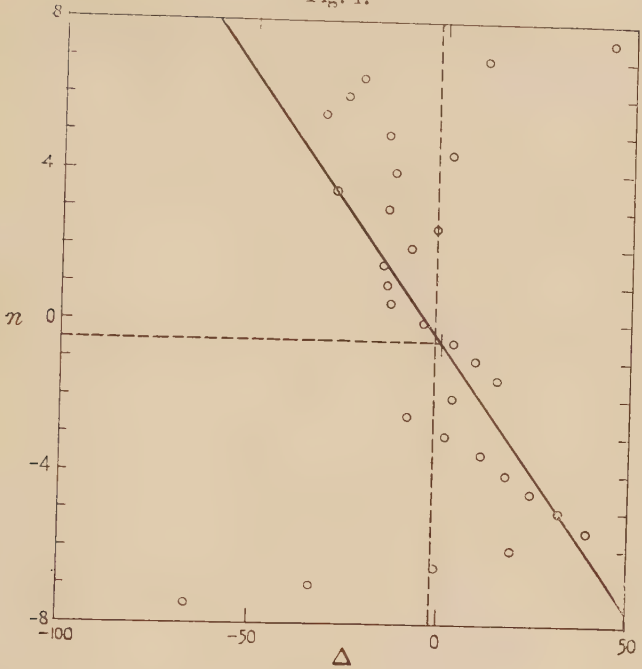

Fig. 2.

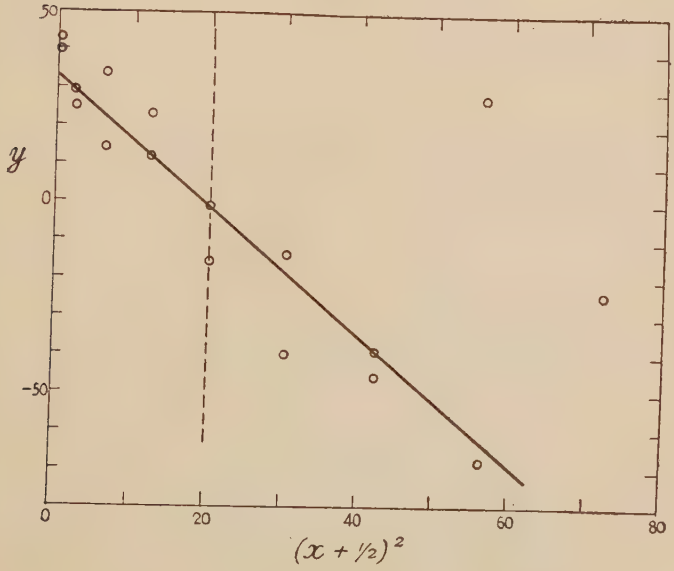

This parabola is shown with the original data in fig. 3. The mean deviation of y from the parabola is 15·4, which may be compared with 17·2 from the "least square" parabola and with the minimum value of 15·3.

Fig. 3.

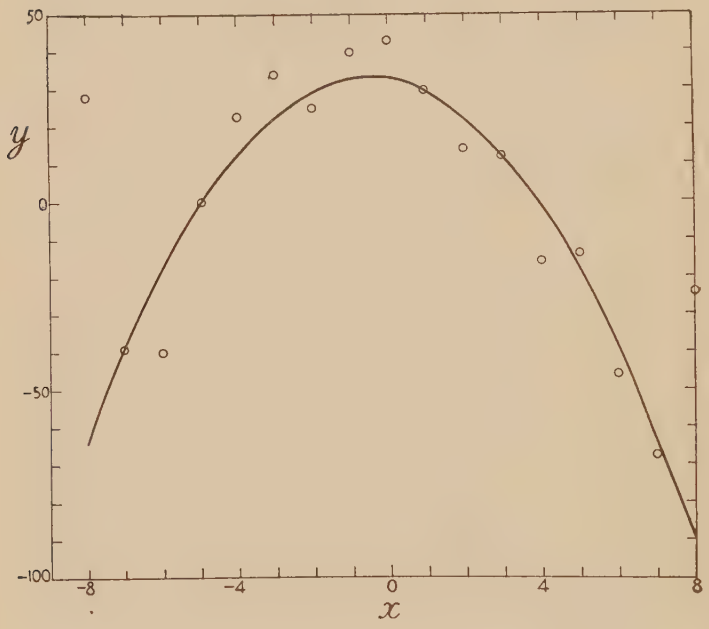

4. The second of Dr. Rhodes' examples deals with the fitting of the curve $y = Bx^a$ to the following data :—

x.	y.	x.	y.
68	192	102	105
75	135	103	91
79	169	107	121
81	141	108	114
85	116	109	94
90	123	110	100
93	103	112	82
94	123	113	77
96	120	113	93
96	101	114	86
97	109	116	86
98	130	118	89
100	102	118	89

DATA (*cont.*).

x.	y.	x.	y.
119	99	123	96
120	106	124	90
120	109	133	93
120	82	137	60
121	85	140	66
122	79	147	93
123	79		

Fig. 4.

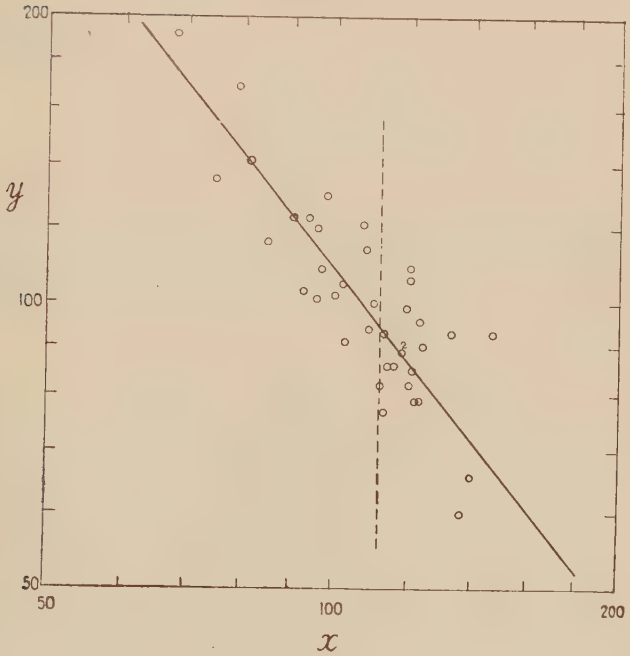

A graph on logarithmic paper (fig. 4) shows that on each side of the straight line joining the points (90, 123) and (113, 93) there are nine points on each side of the median $x=112$.

The points (90, 123) and (113, 93) lie on

$$y=3{\cdot}0953x^{-1{\cdot}2285},$$

which is the curve required.

The mean deviation of y from this curve is 10·2, which may be compared with the minimum value of 10·1.

5. The examples discussed illustrate incidentally the expedience of anamorphosis: by a suitable transformation the fitting of a curve to a series of points is reduced to the simpler problem of fitting a straight line to a corresponding series. In each case the graphical solution compares favourably with that obtained by the method of Minimum Deviations.

Building Research Station,
Garston, Herts.

XLIV. *An X-Ray Investigation of the Lead-Antimony Alloys.* *By* D. Solomon, *B.Sc.* (*Wales*) *and* W. Morris Jones, *M.A.*, *M.Sc.*, *F.Inst.P.* (*Department of Physics, University College of Swansea*) *.

Introduction.

THE equilibrium diagram of the lead-antimony system, and the physical properties of the alloys, have occupied the attention of many workers. The most recent investigations are those of R. S. Dean [1], Broniewski and Sliwowski [2], and Stephens [3].

Dean [1], by thermal analysis and microscopic examination of lead alloys of low antimony content, found that antimony is soluble in solid lead up to between 2 per cent. and 3 per cent. by weight of antimony at the eutectic temperature of 247° C. In a further paper, Dean, Hudson, and Fogler [4] measured the electrical conductivities, at various temperatures, of lead alloys of low antimony content, and concluded that the solid solubility of antimony in lead varies from 2·45 per cent. at the eutectic temperature to ·8 per cent. at room temperature. They added a note to the effect that the alloy containing ·8 per cent. of antimony breaks down, and the solubility of antimony in lead may be brought at least as low as ·5 per cent. antimony.

Later work, in 1928, of Broniewski and Sliwowski [2], who examined the complete system, agrees with that of previous investigators as to the absence of definite compounds, but shows evidence of two solid solutions in the neighbourhood of the two constituent elements, of about 8 atomic per

* Communicated by W. Morris Jones, Senior Lecturer in Physics, University College, Swansea.

cent. (13 per cent. by weight) of lead in antimony, and 2 atomic per cent. (1·2 per cent. by weight) of antimony in lead.

E. Stephens[3], working in this laboratory, has examined the galvanomagnetic effects in the lead-antimony alloys, and the curves obtained by him, being continuous and containing no irregularities, offer no evidence for the formation of solid solutions or compounds.

Since the alloys made and annealed by Stephens[3] were at hand, an investigation of their crystal structures was undertaken, as a knowledge of the structures would be of interest, and should also serve to identify the phases of the system.

Method of Experiment.

The crystal structures were examined by the X-ray powder method. The precautions taken to ensure accuracy of measurement have been described in previous papers[5]. The copper target used gave rise to two radiations, K_α and K_β, the latter being absorbed, as far as possible, by a thin filter of nickel.

TABLE I.

Antimony.

Radiation.	Plane.	Intensity.	Observed d/n.	Calculated d/n.
K_α	100 (2)	St.	3·103	3·111
K_α	211	M.	2·636	2·637
K_α	110 (2)	M.	2·250	2·250
K_α	221	M.	2·154	2·159
K_α	111	W.	1·874	1·880
K_α	320	M.	1·771	1·755
K_α	100 (4)	W.	1·557	1·555
K_α	210 (2)	W.	1·417	1·416
K_α	332	W.	1·370	1·385
K_α	431	W.	1·259	1·261
K_α	100 (5)	V.W.	1·244	1·245
K_α	432	V.W.	1·196	1·203

Structure :—Face-centred rhombohedral.
Dimension of unit cell :—a_0=6·235 Å.U.
Angle of rhombohedron=87° 24′.

Results.

To obtain the crystal structures of the system, powder photographs were taken of the two metals (lead and antimony), and of the alloys 70 per cent. antimony 30 per cent. lead, and 20 per cent. antimony 80 per cent.

TABLE II.

Alloy of 70 per cent. Antimony and 30 per cent. Lead.

Radiation.	Plan.	Intensity.	Observed d/n.	Calculated d/n.
*K_α	100 (2)	St.	3·101	3·111
K_α	111	M.	2·840	2·846
*K_α	211	M.	2·636	2·637
K_α	100 (2)	M.	2·457	2·465
*K_α	110 (2)	W.	2·245	2·250
*K_α	221	W.	2·149	2·159
K_β	110 (2)	V.W.	1·745	1·743
*K_α	111	W.	1·869	1·880
*K_α	320	W.	1·765	1·755
K_α	110 (2)	M.	1·746	1·743
*K_α	100 (4)	W.	1·549	1·555
K_α	131	M.	1·486	1·484
*K_α	210 (2)	W.	1·417	1·416
*K_α	332	W.	1·375	1·385
*K_α	431	W.	1·255	1·261
K_α	100 (4)	V.W.	1·237	1·232
K_α	331	W.	1·129	1·129
K_α	120 (2)	W.	1·101	1·099
K_α	112 (2)	W.	1·009	1·006
K_α	151	W.	·949	·947
K_α	110 (4)	V.W.	·870	·871
K_α	531	W.	·834	·833

Mixture of face-centred cubic lattice, dimensions :—$a_0 = 4{\cdot}93$ Å.U. ; and a face-centred rhombohedral lattice, dimensions :—$a_0 = 6{\cdot}240$ Å.U., and angle of rhombohedron 87° 24′.

Note :—The lines of the face-centred rhombohedral lattice of antimony are denoted by *.

lead, the results being tabulated in Tables I. to IV. The first column states the quality of the copper radiation ; the second, the Miller indices of the reflecting planes ; the third, the intensities of the lines on the photograph ;

the fourth, the plane spacings obtained from measurements on the film ; and the fifth, the calculated spacings for the structure found.

Antimony is known to have a face-centred rhombohedral structure. The side of the unit cell deduced in the present investigation is $a_0 = 6{\cdot}235$ A.U., and the angle of the rhomb 87° 24′. The result is identical with the value found by Morris Jones and Howells[6], and closely agrees also with that found by Persson and Westgren[7].

Table II. gives the spacings from the powder photograph of the alloy 70 per cent. antimony 30 per cent. lead. The

TABLE III.

Lead.

Radiation.	Plane.	Intensity.	Observed d/n.	Calculated d/n.
K_α	111	M.	2·840	2·846
K_α	100 (2)	M.	2·461	2·465
K_β	110 (2)	V.W.	1·747	1·743
K_α	110 (2)	St.	1·742	1·743
K_α	131	St.	1·486	1·484
K_α	111 (2)	M.	1·423	1·423
K_α	100 (4)	W.	1·229	1·232
K_α	331	M.	1·130	1·129
K_α	120 (2)	M.	1·102	1·099
K_α	112 (2)	M.	1·005	1·006
K_α	151	M.	·948	·947
K_α	110 (4)	W.	·870	·871

Structure :—Face-centre cubic.
Dimension of unit cell :—$a_0 = 4{\cdot}93$ Å.U.

lines on the film show that the crystal structure of the alloy consists of a mixture of the face-centred rhombohedral lattice of antimony and the face-centred cubic lattice of lead, the lattice constants being the same as those for pure antimony and pure lead. The atomic diameter of antimony is 2·80 Å.U., and that of lead 3·80 Å.U. An expansion of the antimony cell would, therefore, be expected if lead was soluble to any extent in solid antimony. The results give no measurable change in the size of the antimony cell—hence the solution of lead in antimony

is very small, and does not exceed ·5 per cent. by weight of lead.

Lead has a face-centred cubic lattice, earlier investigation giving the edge as $a_0=4{\cdot}91$ Å.U. Powder photographs of Phebus and Blake [8], however, resulted in the determination $a_0=4{\cdot}93$ Å.U. In the present investigation the side of the lattice was calculated to be $a_0=4{\cdot}93$ Å.U.

TABLE IV.

Alloy of 80 per cent. and Lead 20 per cent. Antimony.

Radiation.	Plane.	Intensity.	Observed d/n.	Calculated d/n.
*K_α	100 (2)	M.	3·107	3·111
K_α	111	M.	2·848	2·846
*K_α	211	W.	2·650	2·637
K_α	100 (2)	M.	2·455	2·465
*K_α	110 (2)	W.	2·246	2·250
*K_α	221	W.	2·149	2·159
K_β	110 (2)	V.W.	1·747	1·743
*K_α	111	V.W.	1·870	1·880
*K_α	320	W.	1·761	1·755
K_α	110 (2)	St.	1·747	1·743
*K_α	100 (4)	W.	1·553	1·555
K_α	131	St.	1·490	1·484
K_α	111(2)	M.	1·427	1·423
*K_α	332	V.W.	1·377	1·385
*K_α	431	V.W.	1·257	1·261
K_α	100 (4)	W.	1·235	1·232
K_α	331	M.	1·133	1·129
K_α	120 (2)	M.	1·104	1·099
K_α	151	M.	·950	·947
K_α	110 (4)	W.	·872	·871
K_α	531	M.	·834	·833
K_α	100 (6)	M.	·822	·822

Mixture of a face-centred cubic lattice, dimensions :—$a_0=4{\cdot}93$ Å.U., and a face-centred rhombohedral-lattice, dimensions :—$a_0=6{\cdot}240$ Å.U., and angle of rhombohedron 87° 24′.

Note :—The lines of the face-centred rhombohedral lattice of antimony are denoted by *.

The results obtained from the powder photograph of the alloy 80 per cent. lead 20 per cent. antimony are given in Table IV.

An examination of the spacings deduced from this film shows a mixture of the lattice spacings of pure lead and pure antimony, the size of the lattice in each case being unchanged. Thus, the X-ray analysis offers no evidence for the formation of a solid solution at the lead end of the equilibrium diagram.

Table II., which shows that in alloy 70 per cent. antimony 30 per cent. lead the lead lattice is unchanged, also indicates this result. If any solid solution of antimony in lead exists, therefore, at room temperature, the solubility cannot be more than about ·5 per cent. by weight of antimony.

The present work shows that there are no definite compounds in the lead-antimony system of alloys, and that if lead is soluble in antimony, or antimony in lead, the degree of solubility of either metal in the other is very small at room temperature: and in no case does it exceed ·5 per cent. by weight.

These results agree with Dean's [1] work on the lead end of the equilibrium diagram, but do not confirm the existence of the solid solutions found at both ends by Broniewski and Sliwowski [2].

As the atomic diameters of lead and antimony are 3·80 Å.U. and 2·80 Å.U. respectively, the solid solution of 13 per cent. by weight of lead in antimony, and the solid solution of 1·2 per cent. by weight of antimony in lead, should produce measurable changes in the size of the respective unit cells.

No such changes were observed in the present investigation, the structures obtained being those of antimony and lead.

References.

(1) J. Ann. Chem. Soc. xlv. p. 1683 (1928).
(2) *Revue de Met.* xxv. p. 392 (1928).
(3) Phil. Mag., April 1930.
(4) Ind. and Engin. Chem. p. 1246 (1925).
(5) Phil. Mag. vii. (Jan. 1929).
(6) Phil. Mag. (May 1930).
(7) *Zeit. für Phys. Chem.* cxxxvi. p. 208 (Sept. 1928).
(8) Phys. Rev. (ii.) xxv. p. 107 (1925).

May 1930.

XLV. *Corona Discharge in Hydrogen.*

By J. H. Bruce, *B.A., Balliol College, Oxford* *.

1. THE study of the corona discharge yields data bearing on problems of theoretical interest in connexion with the motion of positive ions, and this paper contains an account of experiments which I have made on the discharge between coaxial cylinders in hydrogen at low pressures.

2. The apparatus used by Huxley in his researches on helium and neon † was used in these experiments. It consisted of two quartz tubes each containing a nickel cylinder 4·6 cm. in diameter and 12 cm. long, with guard-rings 8 cm. long. A nickel wire 1·65 mm. in diameter was fixed along the axis of one cylinder and a wire 3·16 mm. in diameter along the axis of the other cylinder. The pressure-gauge and the pump for exhausting the apparatus were connected to the quartz cylinders through mercury vapour taps cooled with liquid air. The hydrogen was prepared by the electrolysis of barium hydrate and admitted to the apparatus through heated palladium. The apparatus was heated and washed out several times with fresh gas, while a high-frequency discharge was passed between the electrodes. This process was repeated until all traces of impurities were removed.

3. The starting-potentials for discharges between the wires and the cylinders are shown in fig. 1, in which the ordinates are the starting-potentials measured in volts and the abscissæ the pressures in mm. of mercury.

It will be observed that at pressures above that corresponding to the minimum starting-potential, the discharge passes more readily when the wire is negative than when it is positive, while at lower pressures the positive discharge passes more readily than the negative. The positive and negative discharges differ greatly in character, the positive consisting of a glow distributed uniformly along the wire, while the negative is generally concentrated at various parts of the wire. In the positive discharge the current increases continuously with the applied potential when the pressure is large, while the negative discharge is disruptive.

* Communicated by Prof. J. S. Townsend, F.R.S.

† Phil. Mag. v. p. 74 (1928).

The electric force X at the surface of the wire required to start a discharge is found from the potential difference between the electrodes.

The relation

$$aX = f(ap),$$

where a is the radius of the wire and p is the pressure of the gas, is found to hold except at the lower pressures (as with

Fig. 1.

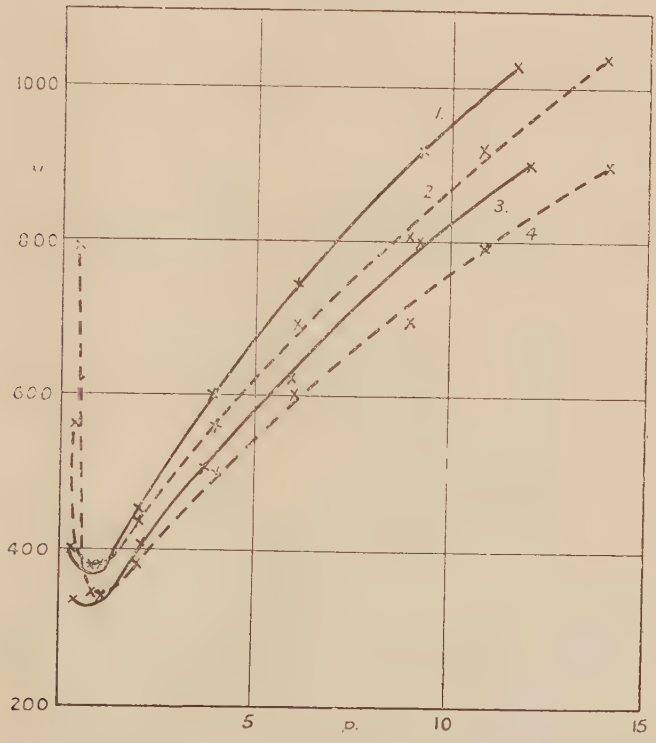

Potential required to start a discharge between the wire and the cylinder, as a function of the pressure. Curves 1 and 3 refer to the wire 3·16 mm. in diameter, curves 2 and 4 to the wire 1·65 mm. in diameter. Curves 1 and 2 refer to positive discharges and curves 3 and 4 to negative discharges.

other gases). In fig. 2 aX is represented as a function of ap, the ordinates being aX measured in volts and the abscissæ the product ap, a being measured in cm. and p in mm. of mercury.

Impurities, when present in small quantities, lower the starting-potentials ; in large quantities they raise them and make them ill defined, the current being maintained by a lower potential than is required to start it. This effect is specially marked when the wire is negative ; thus, when the tube containing the wire 3·15 mm. in diameter was being cleaned out, the values found for the starting-potentials were those given in the second column of the following table. The potentials required to maintain the current were those given in the third column. This potential was nearly con-

Fig. 2.

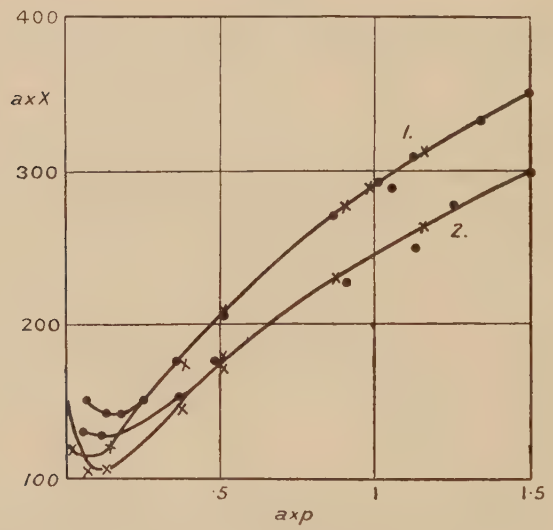

aX as a function of ap. Points marked with crosses refer to the wire 1·65 mm. in diameter, those with circles to the wire 3·15 mm. in diameter. In curve 1 the wire is positive, in curve 2 it is negative.

stant for currents ranging from about 1 microampere to about 100 microamperes.

p.	Starting potential.	Potential to maintain current.
8·35 mm.	790 volts.	700 volts.
6·5 „	665 „	610 „
3·6 „	515 „	485 „

4. The current in pure hydrogen between the wire and cylinder when the wire was positive was measured for various

values of the applied potential. A curve giving the current as a function of the applied potential is shown in fig. 3, where the abscissæ (V) are the applied potential in volts and the ordinates (i) are the currents in microamperes.

Fig. 3.

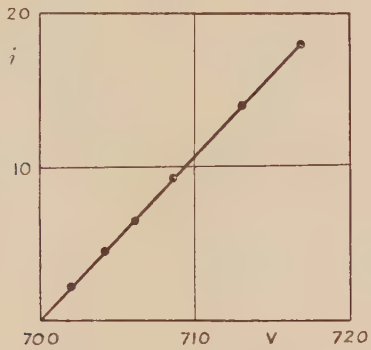

Relation between current i and applied potential V.

Fig. 4.

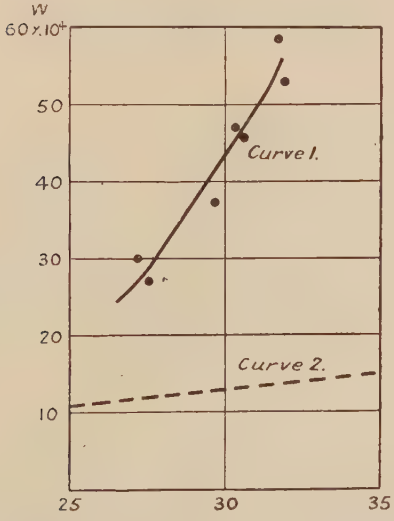

Velocities of the positive ions in the direction of the electric force as a function of X/p. The ordinates are W in cm. per sec. and the abscissæ X/p, X being in volts per cm. and p in mm. of mercury.

5. The velocity W of the positive ions in the direction of the electric force may be found from a formula of

Townsend's *, from the curve fig. 3. The values of W in terms of the ratio X/p thus obtained are given by curve 1 of fig. 4, X being the mean electric force in the space between the cylinders and p the pressure.

For small values of X/p it is known that W is proportional to X/p, and the velocity under a force of 1 volt per cm. at 1 mm. pressure is given by Van de Graaff † as 4300 cm. per sec. If the ratio of W to X/p were constant and equal to 4300 X/p for all values of X/p, the velocities for values of X/p from 25 to 35 would be given by curve 2 of fig. 4.

It will be seen that as X/p is increased W increases very rapidly. Thus the increases in W found by Huxley ‡ in the monatomic gases are equally present in hydrogen.

In conclusion I wish to thank Professor Townsend for his constant advice and criticism.

XLVI. *The Heat-loss from a Plate embedded in an Insulating Wall.* *By* F. H. Schofield, *B.A., B.Sc., Physics Department, National Physical Laboratory, Teddington, Middlesex* §.

Abstract.

A mathematical treatment of the two-dimensional problem of the steady flow of heat from a rectangular isothermal plate embedded in an insulating wall with rectangular isothermal boundaries. The use of measurements of the electrical resistance of sheet metal as a means for checking and extending the theoretical results is described, and consideration is given to the three-dimensional case of a finite plate within a finite wall as the basis of a simplified apparatus for testing thermal insulators.

I. *Introduction.*

THIS problem arises in connexion with the design of apparatus for measuring the thermal conductivity of heat-insulating materials. Theoretically the best type of apparatus for this purpose is one in which the specimen

* Phil. Mag. xxviii. p. 83 (1914).
† Phil. Mag. vi. p. 210 (1928).
‡ *Loc. cit.*
§ Communicated by the Author.

takes the form of a spherical shell, having a constant source of heat applied internally and means for measuring the steady gradient of temperature maintained between the inner and outer surfaces. A method of this description has, in fact, been used *, and lends itself to the case of powders or other materials readily adaptable to the spherical form ; but where, as is often the case, the material is made up in the form of a flat slab, it becomes necessary to adopt another form of apparatus. One commonly used for the purpose † (see fig. 1) consists of an electrically-heated plate (Q) and guard-ring (R) sandwiched between two layers of the test material, the whole being contained between the water-cooled plates (PP).

The use of the guard-ring is based on the analogy of Kelvin's electrometer ; but whereas in the electrical case the plate R must be at a constant potential which is easily adjusted to equality with that of Q, it is not possible in the thermal case to do more than adjust the heat supply to Q and R, so that the contiguous edges of the plates show,

Fig. 1.

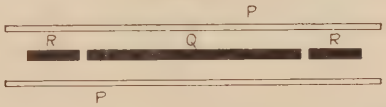

on the average, as small a difference of temperature as possible. The heat transfer due to any temperature difference between the hot plate and guard-ring is inversely proportional to the width of the gap between them, and can therefore be reduced by increasing this width. On the other hand, an increased width means a departure from normal flow near the edges of the plate, and a resulting uncertainty as to its "effective" area.

It is proposed to consider whether it is feasible, without serious loss of accuracy, to simplify the apparatus by dispensing with the guard-ring and using a single hot plate. For this purpose account must be taken of the departures from normal flow due to the edges, thickness, and corners of the plate. The treatment below is strictly two-dimensional ; but, when taken in conjunction with similar experimental work in three-dimensions, would appear to give the desired heat-loss to a fair degree of accuracy.

* Nusselt, *Forsch. Ver. d. Ing.* 1909, pp. 63, 64.

† See, *e.g.*, Poensgen, *Zs. d. Ver. Deutsch. Ing.* lvi. p. 1653 (1912), or Special Report No. 35 of Food Investigation Board (H.M. Stationery Office, 1929).

II. *Edge Effect of Thin Plate.*

First consider a thin plate of section ABC (fig. 2) surrounded by insulation, with an isothermal boundary DEFG, etc., the whole being infinitely broad in the plane perpendicular to the paper. The flow lines BE and CG, from the

Fig. 2.

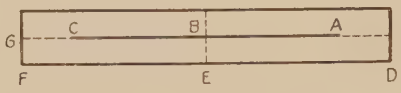

centre and edge of the plate respectively, will be straight, and hence it is only necessary to treat the rectangle EFGB. This can be done on the lines previously adopted by the author * in a similar case, by means of the Christoffel-Schwarz transformation. Since we shall require to deal also with the case in which the length of the rectangle becomes infinite, it is convenient to use a transformation which will allow of the deduction of this case from that of the finite rectangle. Such a transformation is represented in fig. 3. Here the linear dimensions of the z and w planes

Fig. 3.

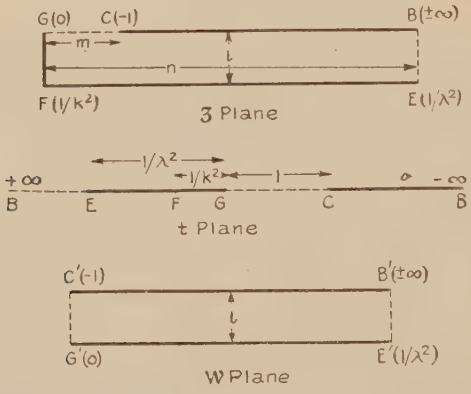

are as indicated, and the lettering in brackets represents the lengths of the corresponding points along the real axis in the t plane. We follow also the convention previously adopted of showing the boundary isothermals and flow lines as full and dashed lines respectively.

* Phil. Mag. v. p. 567 (1928).

For the transformation from the z to the t plane we have

$$\frac{dz}{dt} = \frac{A}{(t)^{1/2}(t-1/k^2)^{1/2}(t-1/\lambda^2)^{1/2}}.$$

By the substitution $t=r^2/k^2$ this yields on integration *

$$z = P\,\mathrm{sn}^{-1}\{k(t)^{1/2},\ \lambda/k\} + Q.$$

If G is the origin and GF the real axis in the z plane, we have $Q=0$ and $P=l/K$, and hence by inversion

$$\mathrm{sn}\{zK/l,\ \lambda/k\} = k(t)^{1/2}. \quad . \quad . \quad . \quad . \quad . \quad (1)$$

The constants λ and k are given in terms of the linear dimensions l, m, and n by means of the following relations derived from (1):

$$\frac{l}{n} = \frac{K}{K'}(\mathrm{mod}\ \lambda/k), \quad . \quad . \quad . \quad . \quad . \quad (2)$$

$$ik = \mathrm{sn}\{imK/l,\ \lambda/k\}$$

$$= i\,\frac{\mathrm{sn}}{\mathrm{cn}}\left\{\frac{mK}{l},\ \left(1-\frac{\lambda^2}{k^2}\right)^{1/2}\right\}. \quad . \quad . \quad . \quad (3)$$

Similarly, for the transformation from the w to the t plane,

$$\frac{dw}{dt} = \frac{B}{(t)^{1/2}(t+1)^{1/2}(t-1/\lambda^2)^{1/2}}.$$

Hence, by substituting $(t+1)=r^2$, and calling C′ the origin, and C′G′ the real axis in the w plane,

$$\mathrm{sn}\left\{\frac{wK}{l},\ \frac{\lambda}{(1+\lambda^2)^{1/2}}\right\} = (t+1)^{1/2}. \quad . \quad . \quad . \quad (4)$$

Now eliminating t and k, except when it appears in the modulus, between (1), (3), and (4),

$$\mathrm{sn}\left\{\frac{zK}{l},\ \frac{\lambda}{k}\right\} = i\,\mathrm{cn}\left\{\frac{wK}{l},\ \frac{\lambda}{(1+\lambda^2)^{1/2}}\right\} \times \frac{\mathrm{sn}}{\mathrm{cn}}\left\{\frac{mK}{l},\ \left(1-\frac{\lambda^2}{k^2}\right)^{1/2}\right\}. \quad (5)$$

Then, since λ and k are known in terms of l, m, and n, it is clear that equation (5) gives the coordinates $(x+iy)$ of any point of the z plane in terms of the coordinates $(u+iv)$ of the corresponding point of the w plane, and so gives the distribution of flow lines and isothermals of the former plane

* Since the integral is to be inverted, it is here written sn^{-1} in place of Legendre's F.

in terms of the rectilinear distribution of the latter. The calculation of the distribution would involve the troublesome process of splitting (5) into real and imaginary parts*. However, it will be shown below that, provided the semi-length of the plate $(n-m)$ is somewhat greater than the thickness (l) of the insulation, the distribution in a finite rectangle corresponds closely with that in an infinite rectangle. The latter may be calculated as follows:—Putting $\lambda=0$, n becomes infinite and equation (5) reduces † to

$$\sin(z\pi/2l)=i\cos(w\pi/2l)\sinh(m\pi/2l). \quad . \quad . \quad (6)$$

Here the imaginary axes are infinite, *i.e.*, axis of y in the z plane and v in the w plane, and in order to bring the case into line with others to be dealt with below, it is convenient to turn the axes in both planes through a right angle. Equation (6) then reads

$$\sinh(z\pi/2l)=\cosh(w\pi/2l)\sinh(m\pi/2l). \quad . \quad . \quad (7)$$

The complete distribution of flow lines and isothermals may be calculated from (7) by use of tables or graphs ‡ of trigonometric functions of a complex variable. Thus for the intersection of any flow line (u=constant) with any isothermal (v=constant), the real and imaginary parts of $\cosh[(u+iv)\pi/2l]$ could be read off and, after multiplying by the constant $\sinh(m\pi/2l)$, the inverse sinh-function would give the coordinates x and y. Alternatively (7) can be split into real and imaginary parts and solved for x and y respectively. This would yield:

$$\frac{\cosh^2(u\pi/2l)\cos^2(v\pi/2l)}{\cosh(x\pi/l)-1}+\frac{\sinh^2(u\pi/2l)\sin^2(v\pi/2l)}{\cosh(x\pi/l)+1}=\frac{1}{2\sinh^2(m\pi/2l)} \quad . \quad (8)$$

$$-\frac{\cosh^2(u\pi/2l)\cos^2(v\pi/2l)}{1+\cos(y\pi/l)}+\frac{\sinh^2(u\pi/2l)\sin^2(v\pi/2l)}{1-\cos(y\pi/l)}=\frac{1}{2\sinh^2(m\pi/2l)} \quad . \quad (9)$$

* See method suggested in previous paper, p. 570.

† K(mod 0)$=\pi/2$, sn $(u,0)=\sin u$, cn $(u,0)=\cos u$, sn $(u,1)/\mathrm{cn}(u,1)=\tanh u/\mathrm{sech}\, v=\sinh u$. See, *e.g.*, Dixon's 'Elliptic Functions,' p. 69 (Macmillan & Co.).

‡ Johnston, Proc. Phys. Soc. xxiii. p. 344 (1911); Kennelley's 'Tables of Complex Hyperbolic and Circular Functions.' Also 'Chart Atlas' of same (Harvard Univ. Press, 1914).

These equations are quadratics in $\cos(y\pi/l)$ and $\cosh(x\pi/l)$ respectively, and taking a value of $m=l$ we have calculated the points of intersection of the flow lines $u=l/4,\ 2l/4,\ 3l/4$ ..... with the isothermals $v=l/4,\ 2l/4,\ 3l/4$ ..... The result is shown on the left-hand side of fig. 4. For purposes of comparison, on the right hand of fig. 4 is shown the distribution when the boundary GF is moved to infinity. This case was originally treated by Clerk-Maxwell * without the aid of the Christoffel-Schwarz transformation, but the data can readily be obtained from equation (7). Thus, transferring the origin in the z plane to C, so that z is replaced by $(z'+m)$, we have

$$\cosh(w\pi/2l) = \sinh\{(z'+m)\pi/2l\} \div \sinh(m\pi/2l)$$
$$= \sinh(z'\pi/2l)\coth(m\pi/2l) + \cosh(z'\pi/2l\,;$$

so that, when m is infinite,

$$\cosh(w\pi/2l) = e^{z'\pi/2l}. \quad . \quad . \quad . \quad . \quad . \quad (10)$$

Hence by taking the logarithms and splitting into real and imaginary parts,

$$y = (2l/\pi)\tan^{-1}\{\tanh(u\pi/2l)\tan(v\pi/2l)\}, \quad . \quad (11)$$

$$x' = (l/\pi\log\{\cosh^2(u\pi/2l)\cos^2(v\pi/2l)$$
$$+\sinh^2(u\pi/2l)\sin^2(v\pi/2l)\}. \quad (12)$$

Comparing the two halves of fig. 4, it will be observed that the effect of moving the boundary GF to infinity only produces a slight displacement in the lines of flow from the plate, and that in each case the spacing of the isothermals and flow lines becomes practically normal at a short distance from the edge. Since the effect of the edge dies rapidly away, it is clear that the total heat-loss from a finite rectangle of moderate length will not differ greatly from that of the same length of an infinite rectangle. The difference between the two cases can be calculated as follows:—

The total heat flow across a strip of width l and length BC (see fig. 3, z plane) is equal to the flow across a strip of the same width and length B′C′ in the w plane, where the flow is entirely normal. If there were no edge at C, so that the side of the rectangle extended indefinitely in the direction BC, the flow from BC would also be normal. Hence we

* ‘Electricity and Magnetism,’ i. para. 195 and fig. xi.

may regard the effect of the edge on the heat-flow across the strip as adding a length X, which is given by

$$X = B'C' - BC$$
$$= m - l\{K'/K \,(\mathrm{mod}\, \lambda/k) - K'/K \,(\mathrm{mod}\, \lambda/(1+\lambda^2)^{1/2}\}. \quad (13)$$

Fig. 4.

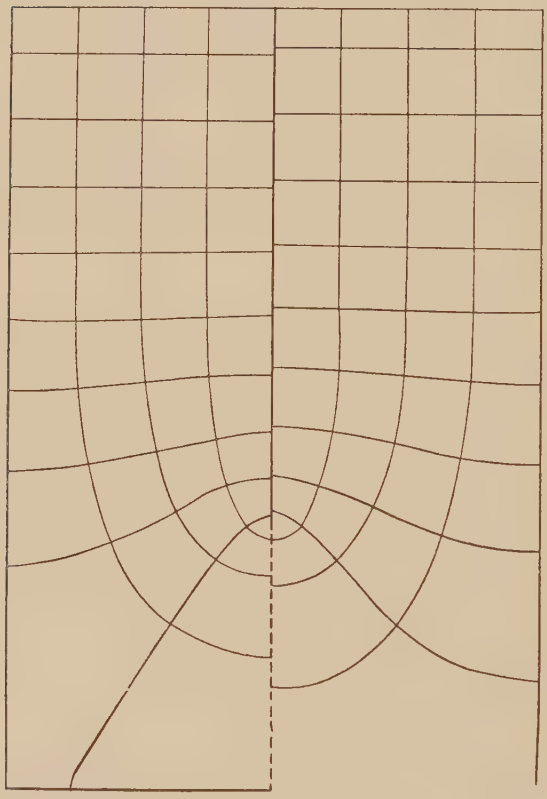

The corresponding effect of the edge in the case of a rectangle extending to infinity in the direction CB (fig. 3) is obtained by putting $\lambda = 0$. Hence

$$[X]_{n=\infty/2} = m - (2l/\pi)\, \mathrm{Lt}_{\lambda=0} [\log 4k/\lambda - \log 4(1+\lambda^2)^{1/2}/\lambda]$$
$$= m - (2l/\pi)\, \mathrm{Lt}_{\lambda=0} [\log k],$$

or substituting for k the value given by (3) and the footnote to (6),

$$[X]_{n=\infty/2} = m - (2l/\pi) \log \sinh (m\pi/2l). \quad (14)$$

If, further, we make m infinite, we have

$$[X]_{n=2m=\infty} = \mathrm{Lt}_{m=\infty}\,[m-(2l/\pi)\log\tfrac{1}{2}(e^{m\pi/2l}-e^{-m\pi/2l})]$$
$$= (2l/\pi)\log 2. \quad . \quad . \quad . \quad . \quad . \quad . \quad . \quad . \quad . \quad (15)$$

The expression (15) agrees with J. J. Thomson's * solution for this marginal case.

In calculating X for the finite rectangle from (13), we first obtain the modulus $\lambda\,k$ from (2) and the value of k from (3), and hence the second modulus. The calculations indicated would be somewhat troublesome, but they can be simplified by taking another transformation in place of that shown in fig. 3. This transformation was not originally adopted because it does not lend itself to the deduction of equation (6). Thus, if the values of t for the points BCGFE (fig. 3) are taken as 0, 1, $1/\mu^2$, $1/\nu^2 \pm \infty$, it can be shown that

$$n/l = \mathrm{K}/\mathrm{K}'\,(\mathrm{mod}\,\nu/\mu),$$
$$\frac{n-m}{l} = \frac{\mathrm{sn}^{-1}(\mu,\,\nu/\mu)}{\mathrm{K}'},$$
$$\frac{\mathrm{C'B'}}{l} = \frac{\mathrm{K}}{\mathrm{K}'}\,(\mathrm{mod}\,\mu),$$
$$\mathrm{X} = m - l\,[\mathrm{K}/\mathrm{K}'\,(\mathrm{mod}\,\nu/\mu) - \mathrm{K}/\mathrm{K}'\,\mathrm{mod}\,\mu)].$$

From these expressions X may easily be calculated by use of Legendre's Tables. We set out below the values of X/l for a series of values of $(n-m)/l$, taking the two cases where m/l are 1 and 2.

TABLE I.

2X is the "Added Length" for complete edge.

$(n-m)/l$.	X/l for	
	$m=l$.	$m=2l$.
0·5	0·465	0·439
1·0	0·469	0·442
1·5	0·470	0·442
∞	0·470	$0·442_5$

It will be seen that, when the semi-length $(n-m)$ of the plate is equal to the thickness (l) of the insulation, the edge correction is practically the same as for a plate of infinite length.

* 'Notes on Recent Researches in Electricity and Magnetism,' p. 218 (Clarendon Press, 1893).

III. *Comparison of Thin and Square Edge.*

In the preceding section it was shown that the disturbing effect of a thin edge rapidly dies away. The effect in the case of a thick plate might be expected to be even more restricted. To obtain a more precise idea of the limits of disturbance, we may compare the extreme cases of an infinitely thin and infinitely thick plate. For the latter a convenient transformation * is that shown in fig. 5. Here the two boundary flow lines are wholly at infinity,

Fig. 5.

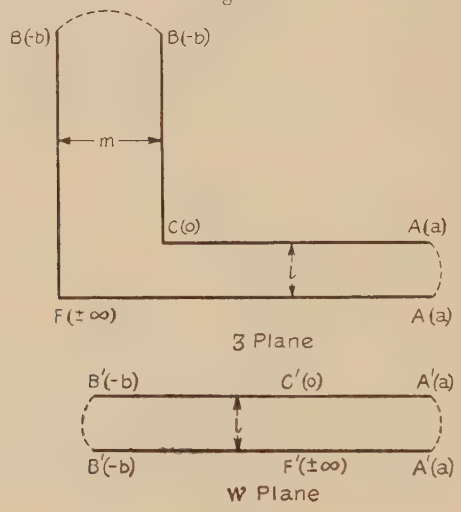

and are shown as curved dashed lines, following the convention previously used by the author. The transformation yields

$$dz/dt = \mathrm{M}(t)^{1/2}(t-a)^{-1}(t+b)^{-1}, \quad . \quad . \quad . \quad (16)$$

$$dw/dt = \mathrm{N}(t-a)^{-1}(t+b)^{-1}. \quad . \quad . \quad . \quad . \quad (17)$$

Integrating, we have

$$z = \frac{2\mathrm{M}}{(a+b)} \left\{ (b)^{1/2} \tan^{-1}\left(\frac{t}{b}\right)^{1/2} - (a)^{1/2} \tanh^{-1}\left(\frac{t}{a}\right)^{1/2} \right\} + \mathrm{P}, \quad . \quad . \quad . \quad (18)$$

$$w = \frac{\mathrm{N}}{(a+b)} \log \frac{(t-a)}{(t+b)} + \mathrm{Q}. \quad . \quad . \quad . \quad . \quad . \quad . \quad . \quad . \quad . \quad (19)$$

* For the particular purpose required here this transformation is perhaps more convenient than that given in Jeans's 'Electricity and Magnetism' (4th edition), p. 277.

If the origins are C and C′ and the real axes are CA and C′A′ in the respective planes,

$$l=\frac{M\pi a^{1/2}}{(a+b)},\quad m=\frac{M\pi b^{1/2}}{(a+b)},\quad P=0 \quad . \quad . \quad (20)$$

$$l=\frac{N\pi}{(a+b)},\quad Q=-\frac{N}{(a+b)}\log\left(-\frac{a}{b}\right), \quad . \quad (21)$$

and (18) may be written

$$z=+(2m/\pi)\tan^{-1}(t/b)^{1/2}-(2l/\pi)\tanh^{-1}(t/a)^{1/2}. \quad (22)$$

Now the spacing of the flow lines or flux density at any point $(x, 0)$ along the real axis is given by

$$\frac{\partial u}{\partial x}=\frac{N}{M(t)^{1/2}}=\left(\frac{a}{t}\right)^{1/2} \quad . \quad . \quad . \quad . \quad . \quad (23)$$

At an infinite distance along the x-axis $\partial u/\partial x=1$. If we wish to find the position of a point P of coordinates $(p, 0)$, such that the flux density at this point differs by a certain amount, say 1 per cent. from its final value of 1 at infinity, we express p in terms of $(a/t)^{1/2}$, for which the value 1·01 is then substituted. Thus

$$p=(2l/\pi)\tanh^{-1}(1/1{\cdot}01)-(2m/\pi)\tan^{-1}(l/m\times 1{\cdot}01). \quad (24)$$

For the thin plate we have from (7), putting y and $v=0$,

$$\sinh(x\pi/2l)=\cosh(u\pi/2l)\sinh(m\pi/2l), \quad . \quad (25)$$

and hence by differentiation

$$\cosh(x\pi/2l)=-\sinh(m\pi/2l)\sinh(u\pi/2l)[\partial u/\partial x]. \quad (26)$$

On eliminating $u\pi/2l$ between (25) and (26),

$$\sinh^2(x\pi/2l)-\cosh^2(x\pi/2l)[\partial x/\partial u]^2=\sinh^2(m\pi/2l).$$

$$\therefore \quad \cosh(x\pi/2l)=\cosh(m\pi/2l)\div[1-(\partial x/\partial u)^2]^{1/2}. \quad (27)$$

x is measured from G (fig. 3), and hence, if p is the distance from the edge C at which $\partial u/\partial x=1{\cdot}01$, we have

$$p+m=\frac{2l}{\pi}\cosh^{-1}\left\{\frac{\cosh(m\pi/2l)}{0{\cdot}1404}\right\}. \quad . \quad . \quad (28)$$

Comparing the formulæ (24) and (28), we have the following values for the thin edge and square edge.

TABLE II.

p is the distance from the edge beyond which the flux density is within 1 per cent. of its final value.

m/l.	p/l.	
	Thin edge.	Square edge.
0	1·69	1·69
0·5	1·37	1·34
1·0	1·28	1·19
2·0	1·25	1·10
3·0	1·25	1·08
∞	1·25	1·06

IV. *Edge Correction for Thick Plate.*

It is clear from the argument above that a plate of finite thickness may, if of moderate length, be assumed to be

Fig. 6.

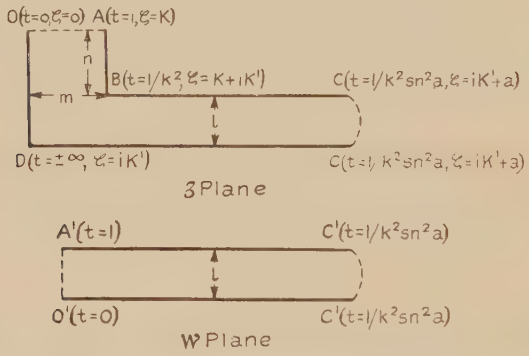

infinitely long. This case, of an infinitely long thick plate (figs. 6 or 8), has already been treated by Cockcroft *, but for our present purpose it is convenient to develop an alternative solution, using for the z-plane transformation one already employed by the author †. We treat one half of the figure as divided by the line of symmetry AO (see fig. 6), $2n$ being the thickness of the plate. Then, as already shown, the several dimensions are given by

$$\frac{m}{l} = \frac{2K}{\pi}\left\{\int \frac{\mathrm{sn}\,a\,\mathrm{dn}\,a}{\mathrm{cn}\,a} - Z(a)\right\}, \quad . \quad . \quad . \quad (29)$$

* Journ. Inst. Elect. Eng. lxvi. p. 403 (1928).
† *Loc. cit.* pp. 578–580 and 591.

$$\frac{n}{l}=\frac{2\mathrm{K}'}{\pi}\left\{\frac{\mathrm{sn}\,a\,\mathrm{dn}\,a}{\mathrm{cn}\,a}-\mathrm{Z}(a)\right\}-\frac{a}{\mathrm{K}}. \quad . \quad (30)$$

$$\mathrm{BC}=\frac{l}{\pi}\log\left\{\frac{\mathrm{sn}\,2a\,\Theta(2a)}{\Theta(0)}\right\}-m\left(1-\frac{a}{\mathrm{K}}\right)-\frac{l}{\pi}\mathrm{Lt}_{\epsilon=0}[\log\mathrm{sn}\,\epsilon]. \quad . \quad . \quad . \quad (31)$$

Here the infinite length BC is obtained by putting $t=1/k^2\,\mathrm{sn}^2(a+\epsilon)$ and taking the limit for $\epsilon=0$.

For the transformation from the w to the t plane

$$dw/dt=\mathrm{P}t^{-1/2}(t-1)^{-1/2}(t-1/k^2\,\mathrm{sn}^2\,a)^{-1}, \quad . \quad (32)$$

which, on integration and evaluation of the constants, O′ being the origin and O′C′ the real axis in the w plane, gives

$$w=\frac{l}{\pi}\log\left\{\frac{t^{1/2}-k\,\mathrm{sn}\,a+\mathrm{dn}\,a(t-1)^{1/2}}{-t^{1/2}-k\,\mathrm{sn}\,a+\mathrm{dn}\,a(t-1)^{1/2}}\times\frac{t^{1/2}k\,\mathrm{sn}\,a+1}{t^{1/2}k\,\mathrm{sn}\,a-1}\right\}. \quad . \quad . \quad . \quad (33)$$

To obtain the infinite length O′C′, we proceed in the manner already adopted for the z plane :

$$\mathrm{O'C'}=\mathrm{Lt}_{\epsilon=0}\left[\frac{l}{\pi}\log\left\{\frac{1-k^2\,\mathrm{sn}\,a\,\mathrm{sn}\,(a+\epsilon)+\mathrm{dn}\,a\,\mathrm{dn}\,(a+\epsilon)}{-1-k^2\,\mathrm{sn}\,a\,\mathrm{sn}\,(a+\epsilon)+\mathrm{dn}\,a\,\mathrm{dn}\,(a+\epsilon)}\times\frac{\mathrm{sn}\,a+\mathrm{sn}\,(a+\epsilon)}{\mathrm{sn}\,a-\mathrm{sn}\,(a+\epsilon)}\right\}\right],$$

which can be shown to reduce to

$$\mathrm{O'C'}=\frac{l}{\pi}\log\left\{\frac{2\,\mathrm{dn}\,a}{k^2\,\mathrm{sn}\,a\,\mathrm{cn}\,a}\right\}-\frac{l}{\pi}\mathrm{Lt}_{\epsilon=0}[\log\mathrm{sn}\,\epsilon]. \quad (34)$$

We may consider the effect of the edge as follows :— If the heat flow from AB and BC had been normal, it would have been equivalent to the flow across a strip of width l and length $(\mathrm{BC}+nl/m)$. Actually the flow from AB plus BC is equal to the normal flow across a strip of width l and length O′C′, since the latter is the length in the w plane equivalent to AB plus BC in the z plane. Hence the effect of the edge is equivalent to the addition, to a strip of width l, of a length X given by

$$\mathrm{X}=\mathrm{O'C'}-\mathrm{BC}-nl/m$$
$$=\frac{l}{\pi}\log\left\{\frac{2\,\mathrm{dn}\,a\,\Theta(0)}{k^2\,\mathrm{sn}\,a\,\mathrm{cn}\,a\,\mathrm{sn}\,2a\,\Theta(2a)}\right\}+m\left(1-\frac{a}{\mathrm{K}}\right)-\frac{nl}{m}. \quad . \quad . \quad . \quad (35)$$

The problem treated above involves three finite dimensions, and its solution as given by equations (29), (30), and (35) may be checked by degenerating it to obtain the solutions for three marginal cases, each involving two finite dimensions.

Case 1: $n/l=0$.

This is obtained by putting $k=1$, which gives the following degenerations:

$$\mathrm{K}=\infty, \quad \mathrm{K}'=\pi/2, \quad \mathrm{sn}\,a=\tanh a, \quad \mathrm{cn}\,a=\mathrm{dn}\,a=\mathrm{sech}\,a,$$
$$\mathrm{Z}(a)=(\tanh a-a/\mathrm{K}), \quad \Theta(2a/\Theta(0)=\cosh 2a;$$

so that

$$m/l=2a/\pi,$$
$$n/l=0,$$
$$\mathrm{X}=m+\frac{l}{\pi}\log\left(\frac{2}{\tanh a\tanh 2a\cosh 2a}\right),$$
$$=m-(2l/\pi)\log\sinh(m\pi/2l), \quad . \quad . \quad . \quad . \quad (36)$$

which agrees with (14) above.

Case 2: $m/l=\infty$.

This is obtained by putting $k=1$ and $a=\mathrm{K}-\beta$, where β is a finite quantity, K of course being infinite. Then

$$\mathrm{Z}(\mathrm{K}-\beta)=\beta/\mathrm{K}=0,$$
$$\frac{\mathrm{sn}\,(\mathrm{K}-\beta)\,\mathrm{dn}\,(\mathrm{K}-\beta)}{\mathrm{cn}\,(\mathrm{K}-\beta)}=\frac{\mathrm{cn}\,\beta}{\mathrm{sn}\,\beta\,\mathrm{dn}\,\beta}=\frac{1}{\tanh\beta};$$

so that

$$\frac{m}{l}=\frac{2\mathrm{K}}{\pi}\left(\frac{1}{\tanh\beta}-\frac{\beta}{\mathrm{K}}\right)=\infty,$$
$$\frac{n}{l}=\frac{1}{\tanh\beta}-1,$$

and hence

$$\tanh\beta=l/(n+l)$$

or

$$\beta=\frac{1}{2}\log\left(\frac{2l+n}{n}\right).$$

In dealing with the expression for X, we have

$$\frac{\mathrm{dn}\,(\mathrm{K}-\beta)}{\mathrm{sn}\,(\mathrm{K}-\beta)\,\mathrm{cn}\,(\mathrm{K}-\beta)}=\frac{\mathrm{dn}\,\beta}{\mathrm{sn}\,\beta\,\mathrm{cn}\,\beta}=\frac{1}{\tanh\beta},$$
$$\Theta\,(2\mathrm{K}-2\beta)/\Theta\,(0)=\cosh 2\beta,$$

and hence

$$\begin{aligned} X &= \frac{l}{\pi}\log\left\{\frac{2}{\tanh\beta\tanh 2\beta\cosh 2\beta}\right\} + m\left(1-\frac{K-\beta}{K}\right) \\ &= \frac{2l}{\pi}\log\left(\frac{1}{\sinh\beta}\right) + \frac{2l\beta}{\pi\tanh\beta} \\ &= \frac{2l}{\pi}\log\left(\frac{2l+n}{l}\right) + \frac{n}{\pi}\log\left(\frac{2l+n}{n}\right). \quad . \quad . \quad . \quad . \quad (37) \end{aligned}$$

which agrees with J. J. Thomson's * solution for this marginal case.

Case 3: $n/l=\infty$.

This is obtained by putting $k=0$, which gives

$$\mathrm{sn}\,a=\sin a,\ \mathrm{cn}\,a=\cos a,\ \mathrm{dn}\,a=1,\ Z(a)=0,\ \Theta(2a)/\Theta(0)=1,$$

$$K=\pi/2,\ \ K'=\log(4/k)=\infty;$$

so that

$$m/l=\tan a,$$

$$n/l=(2K'/\pi)\tan a-a/K=\infty.$$

From these two latter

$$\frac{nl}{m}=\frac{2l}{\pi}K'-\frac{2l^2}{m\pi}\tan^{-1}\left(\frac{m}{l}\right),$$

$$m\left(1-\frac{a}{K}\right)=\frac{2m}{\pi}\left[\frac{\pi}{2}-\tan^{-1}\left(\frac{m}{l}\right)\right]=\frac{2m}{\pi}\tan^{-1}\left(\frac{l}{m}\right).$$

Further,

$$\begin{aligned} \frac{l}{\pi}\log\frac{2\,\mathrm{dn}\,a\,\Theta(0)}{k^2\,\mathrm{sn}\,a\,\mathrm{cn}\,a\,\mathrm{sn}\,2a\,\Theta(2a)} &= \frac{l}{\pi}\log\frac{1}{k^2\sin^2 a\cos^2 a} \\ &= \frac{2l}{\pi}\log\left(\frac{4}{k}\right)+\frac{2l}{\pi}\log\left(\frac{m^2+l^2}{4ml}\right). \end{aligned}$$

Hence,

$$X=\frac{2l}{\pi}\left\{\log\left(\frac{l^2+m^2}{4lm}\right)+\frac{m}{l}\tan^{-1}\frac{l}{m}+\frac{l}{m}\tan^{-1}\frac{m}{l}\right\}, \quad (38)$$

which agrees with J. J. Thomson's † solution for this marginal case.

* *Loc. cit.* p. 219.

† *Loc. cit.* p. 222, or see form given in Jeans's 'Electricity and Magnetism' (4th edition), p. 277.

V. *Calculation of "Edge" or "Peripheral" Correction.*

For the purpose of calculation from equations (29), (30), and (35) use may be made of the tables of Θ and allied functions due to Greenhill and Hippisley *. The equation (35) gives the correction (X) for the "edge" proper, *i.e.*, the total heat-flow less that which would be given by the normal flow from AB plus BC (fig. 6). Since we

Fig. 7.

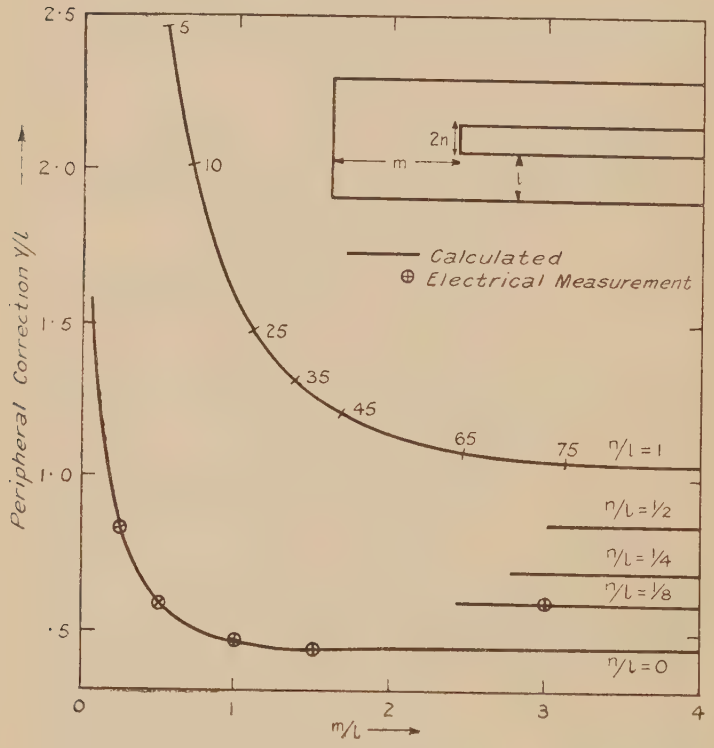

are concerned mainly with comparatively thin plates, it is convenient to use a correction, which may be called the "peripheral correction," representing the total heat-flow less the normal flow from BC only. This peripheral correction (Y) is obtained from (35) by omission of the last

* 'Smithsonian Mathematical Formulæ and Tables of Elliptic Functions' (Publication No. 2672, Washington, 1922).

term, and can be expressed as follows, in the notation used in the tables, the argument r being equal to $90a/\mathrm{K}$:

$$\frac{\mathrm{Y}}{l} = \frac{1}{\pi}\log\left\{\frac{2(k')^{3.2}\mathrm{C}(r)\mathrm{D}(r)}{k^2\mathrm{A}(r)\mathrm{B}(r)\mathrm{A}(2r)}\right\} + \frac{m}{l}\left(1-\frac{r}{90}\right). \quad (39)$$

When $2r$ is greater than 90°, $\mathrm{A}(2r)$ is replaced by $\mathrm{B}(s)$, where $s=2r-90$.

Similarly, equations (29) and (30) become

$$\frac{m}{l} = \frac{2\mathrm{K}}{\pi}\left\{\frac{\mathrm{A}(r)\mathrm{C}(r)}{\mathrm{B}(r)\mathrm{D}(r)} - \mathrm{E}(r)\right\}, \quad . \quad . \quad . \quad (40)$$

$$\frac{n}{l} = \frac{2\mathrm{K}'}{\pi}\left\{\frac{\mathrm{A}(r)\mathrm{C}(r)}{\mathrm{B}(r)\mathrm{D}(r)} - \mathrm{E}(r)\right\} - \frac{r}{90}. \quad . \quad . \quad (41)$$

If, for example, we wish to obtain for a constant n the variation of Y with m, we can from (40), using any modulus k, get the value of r to give the required value for n/l, and hence calculate m/l and Y/l. This has been done for the case $n=l$ with the result shown in fig. 7, the figures written against the curve being the respective angles of modulus. It will be seen that the value of the correction is rapidly asymptotic to its final value, given by equation (37), for an infinite value of m. The curve for the thin plate ($n/l=0$), calculated for (14), is even more rapidly asymptotic.

VI. *Electrical Determination of Effect of Shape, etc.*

It has been pointed out in a former paper * that the effect on the flow of heat of shape and other complexities of structure may be determined by measurements based on electrical analogy. Thus, in the case of three-dimensional problems, the measurement of the capacity of an air-condenser of the correct shape or of the resistance of an electrolyte contained within cells reproducing the appropriate boundary conditions can be made to give the required information. In the paper referred to, two-dimensional cases were treated by the simple plan of measuring the resistance of a sheet of metal cut to the required shape.

The main difficulty in carrying out this plan consists in so attaching the electrodes as to reproduce accurately the boundary conditions. Theoretically the electrodes should be of negligible resistance, as compared with the sheet, and make perfect contact with it along the desired lines. The

* J. H. Awbery and F. H. Schofield, "Effect of Shape on Heat-loss through Insulation" (5th Internat. Congress on Refrigeration, 1928).

lines in question may correspond either with the boundary isothermals or the boundary flow lines—since in any particular problem the two sets of lines are interchangeable—the choice being made so as to reduce to a minimum the errors due to failure to comply with the ideal requirements set out above.

If we take as an example the heat-flow from a thick plate to a rectangular isothermal boundary, a semi-section of which is shown in fig. 8, the isothermals ABCD and EFGH are seen to be of considerable length, and any failure to attach electrodes accurately and in good contact along them, particularly near BC, would be likely to give rise to serious error. Inverting the problem, however, the electrodes could be attached along the lines EA and DH, which are comparatively short and are situated in a region of normal flow.

Fig. 8.

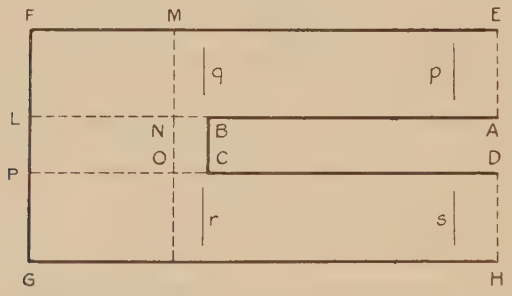

The resistance of the sheet between these lines is then directly proportional, instead of inversely proportional as in the other case, to the required heat-flow.

In the experiments previously described, the metal sheet consisted of thin lead foil, which allowed of the making of very rapid measurements of moderate accuracy. For our present purpose the attempt has been made to increase considerably the accuracy, and to this end a number of modifications have been introduced. Brass sheet was used, 1·6 mm. in thickness, so as to reduce errors due to inequalities of a very thin sheet, and about 40×120 cm. in area. The contacts at EA and DA were made by clamping the brass sheet between heavy copper bars with an interleaving of lead foil. The resistance measurements were made by comparing the potential drop on the strip and on a standard resistance in series with it, a steady current of 10 amps. being passed through the two. The usual precautions were adopted of

taking readings before and after reversals of the current and potential leads. The potential contacts were needle-points resting on the lines p and s, taken at such a distance from the electrodes that a traverse of the lines showed variations of E.M.F. not exceeding 0·1 per cent. After a measurement of resistance, taken from the mean of a number of readings across the potential lines, had been made, the strip was cut through on a line parallel to FG and the process repeated. Finally, after the measurement for the line through M (near BC), cuts were made along BN and CO and the normal resistance of the sides was determined between the respective pairs of potential lines pq and rs. Throughout the experiments the temperature of the sheet was measured by means of a thermocouple soldered to a thin copper disk which could be pressed on to the sheet. A number of readings were taken along the central flow line, and the mean temperature so obtained was used to reduce all resistance values to a common temperature.

The results of the determinations of edge correction for a thin plate (see fig. 2, or fig. 8 with BC=0) are given in the following Table, together with the theoretical values calculated from equation (14) :—

TABLE III.

Edge Correction for Thin Plate.

m/l.	X/l by	
	Electrical measurement.	Calculation.
∞	—	0·442
1·5	0·447	0·447
1	0·470	0·470
0·5	0·587	0·590
0·25	0·822	0·831

It will be seen that there is a good agreement between the experimental and theoretical values. The former were obtained as the differences between two comparatively large quantities, and the maximum error, of the order of 1 per cent., shown in the above Table is only equivalent to an uncertainty of about 1 part in 1000 on the resistance measurements.

An example of the use of resistance measurements on a sheet of metal to determine corrections not amenable to calculation is afforded by the following case :—Suppose a hot plate ABCD (fig. 8) to be surrounded by two slabs of

material ALFE and HGPD, the conductivity of which is required, and that it is not convenient to cut the slab material so as to fill with it the gap LBCP. It is proposed to ascertain the effect of inserting into the gap material of somewhat different conductivity. Taking relative dimensions such as might be met with in practice, viz., 5 cm. for EA (l), 1·25 cm. for BC ($2n$), 15 cm. for LB (m), and 15 cm. for AB, a specimen was made up of this size in sheet brass 0·6 cm. thick. After measurement of its resistance, as above described, the area LBCP was milled out to about $\frac{3}{4}$ and then $\frac{1}{2}$ of its previous thickness, corresponding to the thermal conductivity of this portion, being respectively 25 and 50 per cent. greater than that of the remainder. The reverse case of a material of less conductivity than the rest could be reproduced by milling away the whole of the strip except LBCP, but as a simpler plan, though one of less accuracy, a sheet of tinned iron was taken with an extra thickness, lightly soldered along the edges, over the area in question. The results of the experiments are given in the Table below.

TABLE IV.

Peripheral Correction for Fig. 8 when Area LBCP is t times the Thickness of Remainder.

t.	$Y_t \div l$.	
	Electrical measurement.	Equation (42).
∞	—	**0·442**
2	$0{\cdot}54_3$	$0{\cdot}51_7$
1	$0{\cdot}58_5$	**0·592**
0·69	$0{\cdot}63_9$	$0{\cdot}65_9$
0·44	$0{\cdot}70_5$	$0{\cdot}78_3$

For purposes of comparison a theoretical estimate of the correction may be attempted. Thus, calling Y_t the peripheral correction when the thickness of LBCP is t times that of the remainder, we have Y_1 given generally by equation (35), or where, as in the present case, LB is large, by equation (37). Further, when $t = \infty$, corresponding to the case of a perfect thermal insulator in the gap LBCP, it is clear that the correction becomes identical with that for a thin edge, and is, therefore, given by equations (14) or (15), as the case may be. Hence we try the following simple formula for the case taken above, in which $Y_\infty = 0{\cdot}442\,l$ and $Y_1 = 0{\cdot}592\,l$:

$$Y_t = Y_\infty + (Y_1 - Y_\infty)/t. \quad . \quad . \quad . \quad . \quad (42)$$

It will be seen that there is a rough agreement between the formula and experiment. In the case of the interpolated value the divergence would be near its maximum for the position taken, and for most cases of interpolation, *i. e.*, with the space LBCP having a material of less conductivity than the rest, the formula (42) could apparently be used with sufficient accuracy for practical purposes.

VII. *Application of Results to Finite Rectangular Plate.*

In considering the bearing of the two-dimensional results given above on the problem of a finite rectangular plate contained within a finite wall, reference may be made of the experiments of Langmuir, Adams, and Meikle*. By measuring the resistance of an electrolyte of the appropriate shapes they were able to make an analysis of the corrections applicable to the case of one rectangular parallelopiped contained within another, the gap between the two being constant. It was shown that the departure from normal flow was divisible into two parts, namely, the two-dimensional edge corrections and the three-dimensional corner corrections. As regards the former, it is interesting to note that the correction for a thin edge was given as 0·93, as against the theoretical value of 0·940 † found in the present investigation, while for a square edge the value was 0·54, as against the theoretical value of 0·558 ‡. The correction for the total eight corners was relatively small, being given as $0{\cdot}35\,l$ for a thin plate and $1{\cdot}2\,l$ for a thick plate. For a single plate embedded in a uniform thickness of insulation the formulæ of Langmuir could be used, or, as an alternative for the edge corrections, those given in this paper. Such an apparatus could very well be employed for testing thermal insulators, but would have the disadvantage that the four end plates FG (fig. 8) would have to be maintained strictly isothermal with the main plates FE and GH, *e. g.*, by water-cooling, However, by increasing the overlap of the main plates so that the length LB(m) becomes considerably greater than the length EA(l), the edge correction becomes independent of m, and the need for accurate temperature control of the end plates becomes less important.

Thus it has been shown above for a moderately thin plate that, if the overlap m and the semi-width ($a/2$) of the plate are each of the order of $2l$ the peripheral correction Y

* Trans. Electrochem. Soc. xxiv. p. 53 (1913).
† *I. e.* twice the value shown in line 3 of Table III.
‡ Jeans, 'Electricity and Magnetism,' p. 279.

will be given by (37). The correction X for the four short square edges, each of length $2n$, would be given by (38), and, assuming the corner correction to be unaltered, we should have for the complete shape-factor S,

$$S=(2a^2/l)+(8a\,Y/l)+8n\,X/l)+0{\cdot}35\,l.$$

Taking the following as a numerical example, viz., 40 cm. for the side a of the plate, 6 cm. for the thickness l of the insulation, 1·5 cm. for $2n$ the thickness of the plate, and 18 cm. for the overlap m, we should find that Y was $0{\cdot}592\,l$ and X $0{\cdot}762\,l$, and hence

$$S=533+189+5+2.$$

We observe that the fourth, or three-dimensional, term of the equation is very small, and that a large error in its coefficient could be tolerated without appreciably affecting the total.

As to the construction of the hot plate, the usual procedure of clamping an electric heater between thick metal plates could be followed, but in view of the increased flux-density towards the edges (see fig. 4), it would be as well to have independent heating elements for the marginal and central portions of the plate. By this device, and the use of plates of sufficient thickness and conductivity, it should be possible to secure a reasonable uniformity of temperature over the hot plate.

In conclusion, the author wishes to acknowledge the assistance received from Mr. C. R. Barber, Junior Observer at the National Physical Laboratory, in the electrical measurements and calculations.

XLVII. *Electrical Conductivity Measurements at low Temperatures.* *By* Prof. J. C. McLennan, *F.R.S.*, J. F. Allen, *M.A.*, *and* J. O. Wilhelm, *M.A.**

DURING the course of an investigation on superconductivity, a number of elements, alloys, and compounds were examined which did not show this phenomenon over the temperature range available. The substances on which the measurements were made do not fall into any definite group. The measurements represent, however, the result of following up various lines of attack which suggested themselves during the investigation.

* Communicated by the Authors.

It has been found * that alloys composed of a superconductor and an element of the fifth group have a higher superconducting point than that of the superconductor alone. With this in mind, various metals alloyed with those of the fifth group were examined in the hope that their superconducting point which existed would be raised sufficiently so as to fall within our temperature range. These alloys were Ag–Bi, Cu–Bi, Cd–Bi, Mn–Bi, Ag–Sb, Cd–Sb, Cu–As, and Au–As. The radioactive element Po was also examined. It was expected that this substance would show signs of superconductivity, since it degenerates into an isotope of lead. The rare earth elements Ce and La were then studied, since their position in the periodic table of the elements lies close to several of the superconductors. Also alloys of these rare earth metals with lead were examined in order to determine their effect on its superconductivity.

The discovery of the superconductivity of CuS by Meissner † recently led us to examine other common sulphides, namely, PbS, AgS, FeS, and Bi_2S_3. The result of the investigation on PbS showed that it became superconducting at 1°·2 K. This was the only sulphide to show the phenomenon. Other substances Cd–Zn, Ag–Cl_2, and a Heusler alloy were also examined.

Various methods were used in the preparation of samples for measurement. Many of the alloys were made by fusion in a pyrex tube, the molten mixture then being strained through glass wool and allowed to solidify in a capillary tube. When the glass was cracked off, current and potential leads of fine copper wires were soldered or fastened with copper clips to the rod thus formed. Other substances of higher melting-point were fused and cast in a carbon tube resistance furnace. Several metals such as Ce, La, and the Heusler alloys were in the form of blocks or large rods, from which small rods suitable for measurement were sawn. The results obtained are given in Tables I. to XX. and plotted in figs. 1 to 5.

I.—Ag–Bi, Cu–Bi, Cd–Bi, Mn–Bi.

The first three of these were prepared in pyrex tubes and the fourth, Mn–Bi, being of higher melting-point was

* McLennan, Allen, and Wilhelm, Trans. Roy. Soc. Can. xxiv. Sect. III. (1930).

† Meissner, *Zeit. für Phys.* lviii. p. 570 (1929).

fused in a carbon furnace. Ag–Bi, Cd–Bi, and Mn–Bi are eutectic alloys, while Cu–Bi is a solid solution. Ag and Cu were expected to show signs of superconductivity on being alloyed with Bi since Au–Bi is known to be a superconductor. However, at a temperature of 1°·9 K., none of the alloys had become superconducting. Cd, which was at one time thought to be superconducting, was also expected to exhibit this phenomenon on alloying with Bi. The alloy, however, does not, although its curve bends down sharply towards the temperature axis as though

Fig. 1.

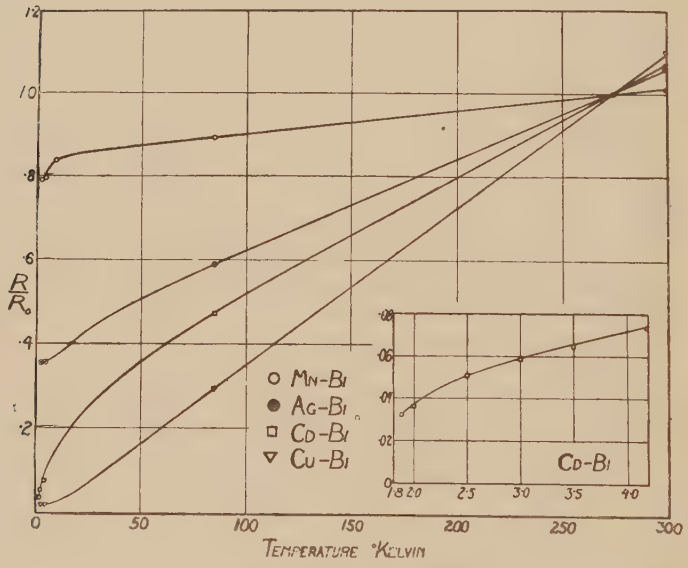

it would become superconducting between 1°·0 and 1°·5 K. The Mn–Bi also shows quite a pronounced drop in resistance near the low-temperature end of the curve, and a further extension of the curve down to lower temperatures might prove it to become superconducting. The readings for these alloys are given in Tables I., II., III., and IV. and curves for them are plotted in fig. 1.

II.—Ag–Sb, Cd–Sb, Cu–As, Au–As.

These again were all eutectics with the exception of Cd–Sb, which was a 60 per cent. Sb alloy. Being alloys containing a member of the fifth group of elements, it was

TABLE I.—Mn–Bi.

T° K.	R (microhms).	R/R_0.
300°	1303	1·015
273	1285	1·000
85	1149	·894
9	1067	·838
4·2	1027	·799
2·0	1020	·794

TABLE II.—Ag–Bi.

T° K.	R (microhms).	R/R_0.
300°	3581	1·060
273	3380	1·000
85	1990	·589
4·2	1199	·354
2·0	1190	·352

TABLE III.—Cd–Bi.

T° K.	R (michrohms).	R/R_0.
300°	2055	1·070
273	1920	1·000
85	910	·474
4·2	142	·0739
3·5	125	·0652
3·0	113	·0589
2·5	98	·0510
2·0	70	·0635
1·9	64	·0345
1·88	60	·0325

TABLE IV.—Cu–Bi.

T° K.	R (microhms).	R/R_0.
300°	513	1·103
273	465	1·000
85	138	·296
4·2	8	·0172
1·9	8	·0172

expected that some of them might exhibit superconductivity. Ag–Sb and Cd–Sb were prepared in pyrex, Cu–As in a carbon furnace, and Au–As in a quartz tube. Difficulty was experienced in obtaining the Au-As alloy, since the As sublimed at a much lower temperature than the Au melted. However, by melting the gold and dropping some crystals of As on the molten metal an alloy was successfully obtained. Neither of the Sb alloys showed any tendency to lose their resistance at very low temperatures, but both of the As alloys exhibited sharp

Fig. 2.

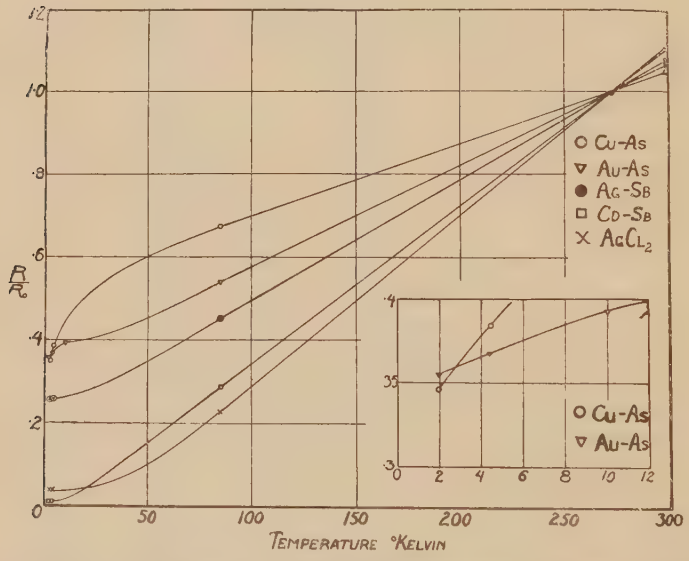

drops at the lower end of the resistance curves. This indicated that if lower temperatures were available, they might be found superconducting. It is, of course, impossible to predict the onset of the superconducting state, since the transition usually takes place within a few hundredths of a degree and the shape of the curve above the transition-point is no real criterion for superconductivity. The measurements obtained from these alloys are given in Tables V. to VIII. and plotted in fig. 2.

III.—Ce, La, Pb–Ce, Pb–La.

The results of observations made on these substances are given in Tables X. to XIII. and plotted in fig. 3. The

Table V.—Cu–As.

T° K.	R (microhms).	R/R_0.
300	1314	1·051
273	1250	1·000
85	840	·673
4·2	480	·384
2·2	434	·347

Table VI.—Au–As.

T° K.	R (microhms).	R/R_0.
300	291	1·067
273	273	1·000
85	147	·538
10	107	·392
4·2	100	·367
1·9	97	·355

Table VII.—Ag–Sb.

T° K.	R (microhms).	R/R_0.
300	1354	1·080
273	1252	1·000
85	579	·451
4·2	324	·258
1·9	320	·255

Table VIII.—Cd–Sb.

T° K.	R (microhms).	R/R_0.
300	4690	1·096
273	4280	1·000
85	1192	·280
4·2	42	·0093
1·9	35	·0070

two metals Ce and La were pure samples obtained from Hopkin and Williams. Situated as they are in the periodic system surrounded by a group of superconductors it was hoped that they would prove to be superconductors. Neither one showed this property down to 1°·9 K., although

the curve for Ce takes a considerable drop at that temperature. Having made this test we desired to know the effect of alloying these metals with lead. Accordingly, the constituents were melted together in a pyrex tube. Difficulty was encountered in obtaining the alloys, since a violent exothermic reaction took place on fusion. However, fairly good samples were finally obtained and measurements made. The resistance-curves for the alloys were much the same as those for the pure metals, except that they had a greater slope. Also in the region

Fig. 3.

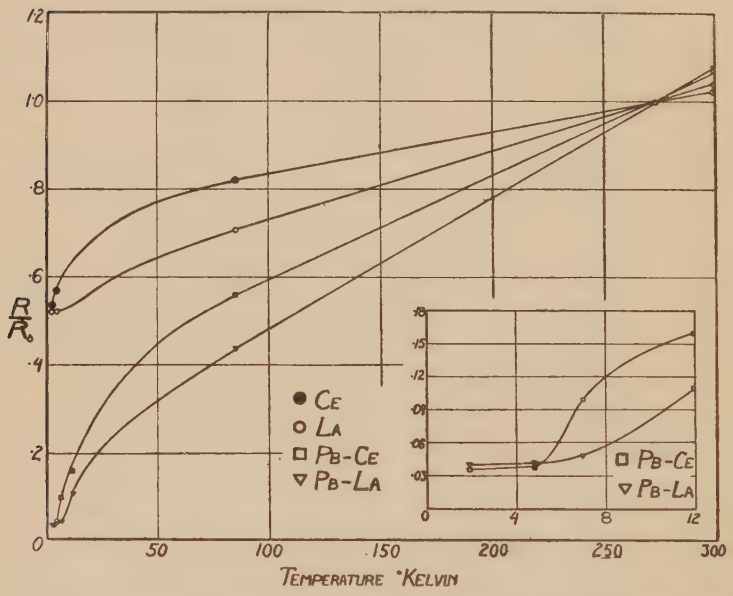

of the superconducting point of lead, both alloys and especially the Pb–Ce showed pronounced drops in resistance. This, however, might be due to a certain amount of free lead in the alloy.

IV.—FeS, AgS, Bi_2S_3.

The fact that CuS becomes superconducting is very peculiar, since Cu on being alloyed with a superconductor in nearly every case has the property of rendering the alloy non-superconducting. However, as it was our purpose to test other common sulphides for this phenomenon, AgS and FeS being easily made came under our

TABLE IX.—$AgCl_2$.

T° K.	R (microhms).	R/R_0.
300°	1837	1·114
273	1649	1·000
84	375	·228
4·2	66	·040
1·9	65	·0395

TABLE X.—Ce.

T° K.	R (microhms).	R/R_0.
300°	2860	1·025
273	2792	1·000
85	2295	·820
4·2	1590	·568
2·0	1493	·535

TABLE XI.—La.

T° K.	R (microhms).	R/R_0.
300°	4200	1·040
273	4015	1·000
85	2825	·706
4·2	2095	·522
1·9	2093	·520

TABLE XII.—Pb–Ce.

T° K.	R (microhms).	R/R_0.
300°	1139	1·075
273	1060	1·000
85	593	·559
12	169·5	·160
7	105	·099
5	42	·0396
1·9	41	·0387

TABLE XIII.—Pb–La.

T° K.	R (microhms).	R/R_0.
300°	488	1·077
273	453	1·000
85	198	·437
12	50	·1102
7	22	·0485
4·8	19	·0419
1·9	18	·0398

scrutiny. The sulphide in both cases consisted of a coating on the surface of a wire (and was formed by heating the wire) in a vapour of sulphur. From the measurements given in Tables XIV. and XV. and plotted in fig. 4, it can be seen that neither compound became superconducting above 1°·9 K. A single crystal of Bi_2S_3, a naturally occurring mineral known as Bismuthenite, was also examined, but no irregularities were observed in the resistance-curve, which is given in fig. 5 from data in Table XX.

Fig. 4.

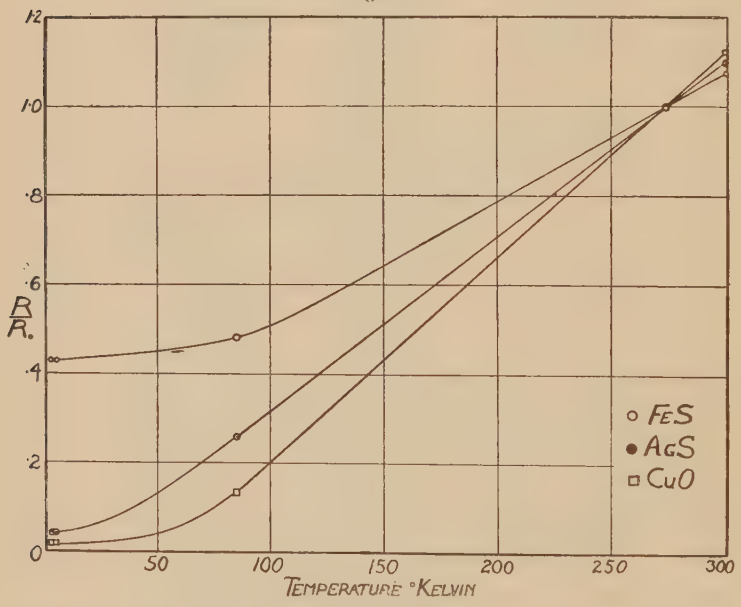

V.—CuO.

We desired in this case to find out if oxygen, which is the first member of the sixth group, had the effect of rendering Cu superconducting. The oxide was in the form of a film coated on the surface of copper ribbon. The curve which is shown in fig. 4 and Table XVI. shows no irregular features.

VI.—$AgCl_2$.

A film of the chloride was coated on a silver wire by allowing the wire to stand in a vapour of chlorine for

several hours. The curve obtained is given in Table IX. and fig. 2 and shows no peculiarities. The curve, instead, followed the usual silver temperature resistance curve.

Table XIV.—FeS.

T° K.	R (microhms).	R/R_0.
300	2531	1·083
273	2365	1·00
85	1140	·481
4·2	1016	·428
1·9	1000	·422

Table XV.—AgS.

T° K.	R (microhms).	R/R_0.
300	1915	1·102
273	1740	1·000
85	450	·258
4·2	73	·042
1·9	70	·04

Table XVI.—CuO.

T° K.	R (microhms).	R/R_0.
300	2765	1·130
273	2445	1·000
85	328	·134
4·2	34	·0138
1·9	33	·0135

Table XVII.—Heusler Alloy.

T° K.	R (microhms).	R/R_0.
300	725	1·075
273	696	1·000
85	311	·447
4·2	208	·299
2·0	203	·292

VII.—Heusler Alloy.

A rod sawn from a sample of this alloy which possesses marked magnetic properties was subjected to measurement at very low temperatures. Nothing abnormal was observed. The measurements are given in Table XVII.

VIII.—Cd–Zn.

The eutectic alloy of these two metals was formed in the usual way in a pyrex tube. Aside from having an extremely small residual resistance, no irregularities were observed. The curve is shown in fig. 5 and the data given in Table XVIII.

Fig. 5.

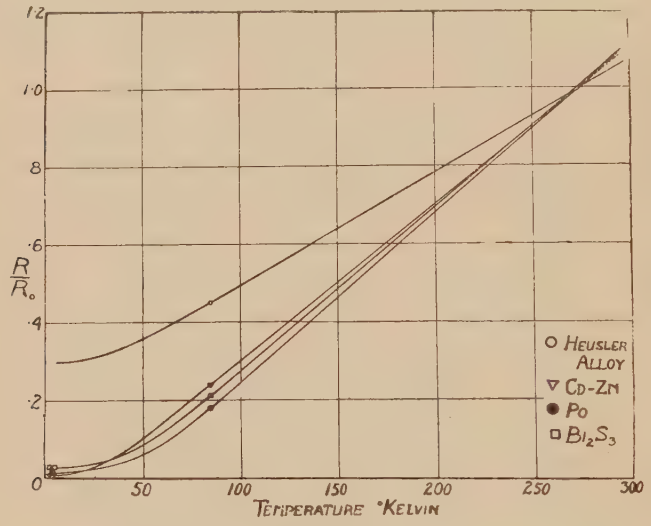

TABLE XVIII.—Cd–Zn.

T° K.	R (microhms).	R/R_0.
300	1208	1·113
273	1085	1·000
86	254	·234
4·2	10·5	·0096
2·0	8·76	·0081

TABLE XIX.—Po.

T° K.	R (microhms).	R/R_0.
300	510	1·118
273	456	1·000
85	81	·178
4·2	6	·0132

TABLE XX.—Bi_2S_3.

T° K.	R (microhms).	R/R_0.
300°	530	1·126
273	472	1·000
85	100	·212
4·2	11	·0233
2·0	11	·0233

IX.—Po.

This was a sample precipitated in 1922 and plated on copper. It was expected that since Po degenerates into an isotope of lead and has a half life of 136 days, it would become superconducting. This was not the case, however, the resistance-curve being the characteristic curve for copper. The surface of the Po, however, appeared badly oxidized, so that quite possibly there was no metallic lead on the plate. The curve is given in fig. 5 from data in Table XIX.

The Physical Laboratory,
University of Toronto,
June 18, 1930.

XLVIII. *Reducing Observations by the Method of Minimum Deviations.*

To the Editors of the Philosophical Magazine.

GENTLEMEN,—

IN your journal for May 1930 there is a paper by Dr. Rhodes on reducing observations by the method of Minimum Deviations, on which I should like to make some remarks.

(1) In practice it is often necessary to draw smooth curves through the plotted observations of two variables where there is a good deal of scatter of the plotted points and the exact theoretical relation between the variables is not known. The experience of the Physical Department is that in these cases it is rarely worth the labour of fitting algebraic curves, and it is usually enough to draw free-hand curves through the points. In some cases the drawing of the curves is assisted by dividing the observations into groups and finding the centre of gravity of each group.

(2) The first example given in Dr. Rhodes's paper seems

to be of the above type, as the observations show considerable variations.

Dividing the observations into five groups of 4, 3, 3, 3, 4 observations, the curve shown in the attached diagram is obtained, and is a good fit.

(3) If it is desired to fit a curve of particular algebraic type, *i. e.*, a parabola, the quickest way to do this is the method of Zero Sum described by Dr. Norman Campbell in the Philosophical Magazine, 1920, vol. xxxix. p. 177, and 1924, vol. xlvii. p. 816.

By this method the problem is reduced in a few minutes to the solution of three normal equations. The method of

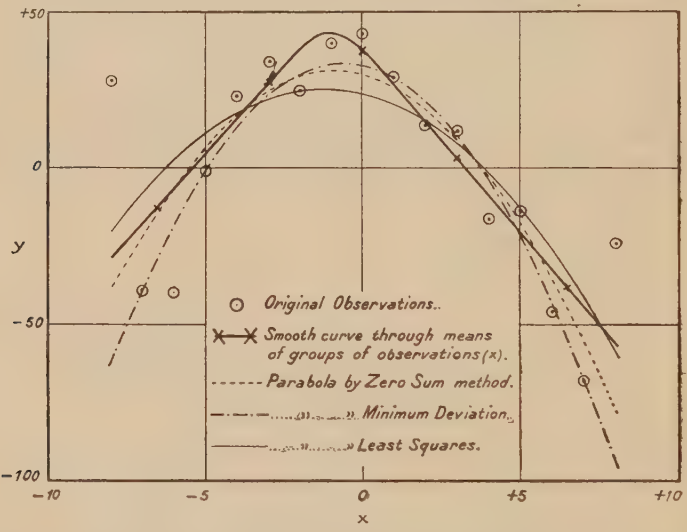

least squares only arrives at its normal equations after much computation, and Dr. Rhodes's method of minimum deviations requires still more computation to arrive at the normal equations. In fact the amount of labour is prohibitive.

The parabola obtained by the method of Zero Sum is given in the diagram, as well as those obtained by Dr. Rhodes from Least Squares and Minimum Deviations. The most commonly occurring case in practice is the fitting of a straight line, and this is very quickly done by the method of Zero Sum. A justification of the method is given by Dr. Norman Campbell in the above papers.

Ministry of Public Works,
Physical Department, Cairo.
June 14th, 1930.

Yours faithfully,
H. E. Hurst.
Director General, Physical Department.

XLIX. *The Effect of Stratification on the Gravity Gradient and the Curvature of the Level Surface.* *By* Edith A. Nelson, *M.A., M.Sc., Natural Philosophy Laboratory, University of Melbourne**.

IT is found, on examination of the values of the gravity gradient and of the curvature of the level surface obtained in a gravity survey with the Eötvös balance, that in certain instances the curvature changes sign when the gradient is a maximum, while in other cases this does not hold. It will be shown that there is no general relation between these quantities, and that this phenomenon is evidence of the stratification of the earth's crust in the region under survey.

Let V be the gravity potential. The equation to the level surface is then $V(xyz) = 0$.

Since the plane XOY is a tangent plane at the origin,

$$\frac{\partial V}{\partial x} = \frac{\partial V}{\partial y} = 0, \qquad \frac{\partial z}{\partial x} = \frac{\partial z}{\partial y} = 0.$$

Let A, B, F, G, H, respectively, denote the values at the origin of the quantities

$$\frac{\partial^2 V}{\partial x^2}, \quad \frac{\partial^2 V}{\partial y^2}, \quad \frac{\partial^2 V}{\partial y \partial z}, \quad \frac{\partial^2 V}{\partial z \partial x}, \quad \frac{\partial^2 V}{\partial x \partial y};$$

then

$$g = \frac{\partial V}{\partial z}.$$

$$\text{Gradient along OX} = \frac{\partial g}{\partial x} = \frac{\partial^2 V}{\partial x \partial z} = G.$$

$$\text{Gradient along OY} = \frac{\partial g}{\partial y} = \frac{\partial^2 V}{\partial y \partial z} = F.$$

$$\therefore \quad \text{Gradient} = (F^2 + G^2) = \Gamma.$$

If k_1, k_2, respectively, denote the maximum and minimum curvatures of the level surface at O, and ϕ the angle between the section of minimum curvature and OX, then

$$\tan 2\phi = -2 \frac{\partial^2 V}{\partial x \partial y} \Big/ \left(\frac{\partial^2 V}{\partial y^2} - \frac{\partial^2 V}{\partial x^2} \right) = -2H/(B-A),$$

$$g(k_1 - k_2) = -\left(\frac{\partial^2 V}{\partial y^2} - \frac{\partial^2 V}{\partial x^2} \right) \sec 2\phi = -\{(B-A)^2 + 4H^2\}^{\frac{1}{2}} = T.$$

T is called the Curvature Vector of the level surface.

* Communicated by Prof. T. H. Laby.

It is desired to find the nature of the relation, if any, between Γ and T.

Differentiating $V(xyz) = 0$ with respect to the independent variables x and y, and substituting the values of the differential coefficients at the origin, we have

$$A + g\frac{\partial^2 z}{\partial x^2} = 0, \quad . \quad . \quad . \quad . \quad . \quad . \quad . \quad . \quad (1)$$

$$H + g\frac{\partial^2 z}{\partial x \partial y} = 0, \quad . \quad . \quad . \quad . \quad . \quad . \quad . \quad . \quad (2)$$

$$B + g\frac{\partial^2 z}{\partial y^2} = 0, \quad . \quad . \quad . \quad . \quad . \quad . \quad . \quad . \quad (3)$$

$$\Gamma = (F^2 + G^2)^{\frac{1}{2}}, \quad . \quad . \quad . \quad . \quad . \quad . \quad . \quad (4)$$

$$T = \{(B - A)^2 + 4H^2\}^{\frac{1}{2}}. \quad . \quad . \quad . \quad . \quad (5)$$

Fig. 1.

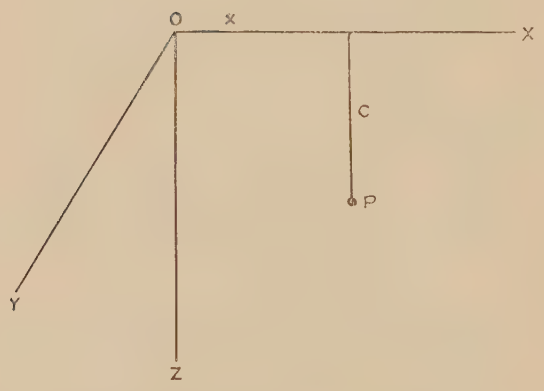

In order to obtain a relation between Γ and T it is necessary to eliminate the quantities A, B, F, G, H, $\frac{\partial^2 z}{\partial x^2}$, $\frac{\partial^2 z}{\partial x \partial y}$, $\frac{\partial^2 z}{\partial y^2}$ from the above equations. This is clearly impossible without a knowledge either of the form of the function V or of the values of A, B, F, G, H. Each case must therefore be treated as an individual problem.

Two special cases will be considered :—

1. The disturbing body a sphere with centre at $P(x, o, c)$.

Let γ = constant of gravitation,

M = mass of sphere ;

then $$B-A = -3\gamma M x^2/(x^2+c^2)^{5/2},$$
$$H = F = 0,$$
$$G = 3\gamma M c x/(x^2+c^2)^{5/2},$$

whence

$$T = 3\gamma M x^2/(x^2+c^2)^{5/2},$$
$$\Gamma = 3\gamma M c x/(x^2+c^2)^{5/2}.$$

Fig. 2.

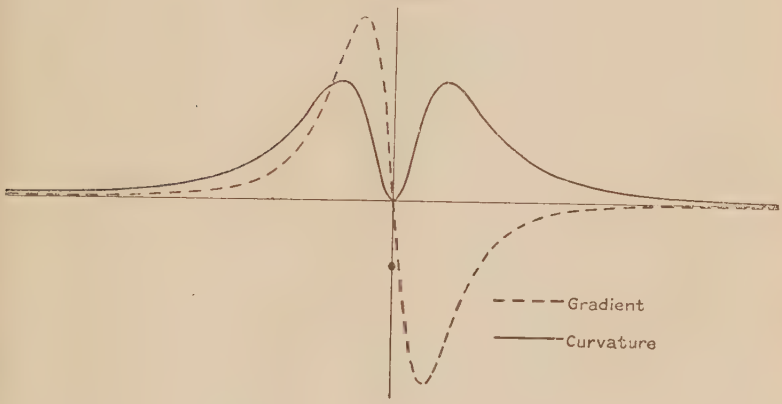

Fig. 3.

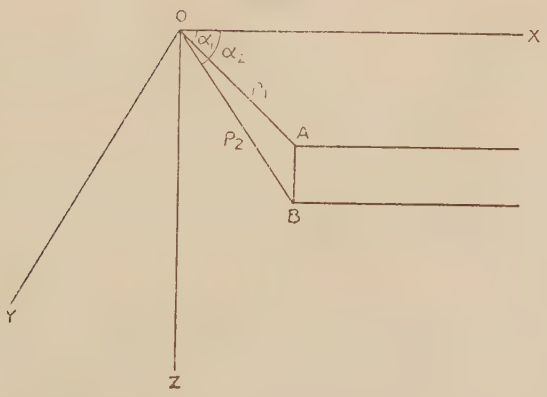

If, in a gravity survey in which T and Γ are determined, a traverse be taken in the direction OX, the values obtained are given by the curves in fig. 2. The gradient and the curvature vanish together above the centre of the sphere. The maximum value of the gradient is given at $x=0{\cdot}5c.$, and that of the curvature vector at $x = 0{\cdot}82\,c$.

2. The disturbing body a semi-infinite slab.

Let σ = density of the material of the slab,

$$\mathrm{OA} = \rho_1, \quad \mathrm{OB} = \rho_2,$$

$$\mathrm{XOA} = \alpha_1, \quad \mathrm{XOB} = \alpha_2;$$

then
$$\mathrm{B} - \mathrm{A} = 2\gamma\sigma(\alpha_1 - \alpha_2),$$

$$\mathrm{F} = \mathrm{H} = 0,$$

$$\mathrm{G} = 2\gamma\sigma \log_e \rho_2/\rho_1,$$

whence

$$\mathrm{T} = 2\gamma\sigma(\alpha_2 - \alpha_1),$$

$$\sigma = 2\gamma\sigma \log \rho_2/\rho_1.$$

Fig. 4.

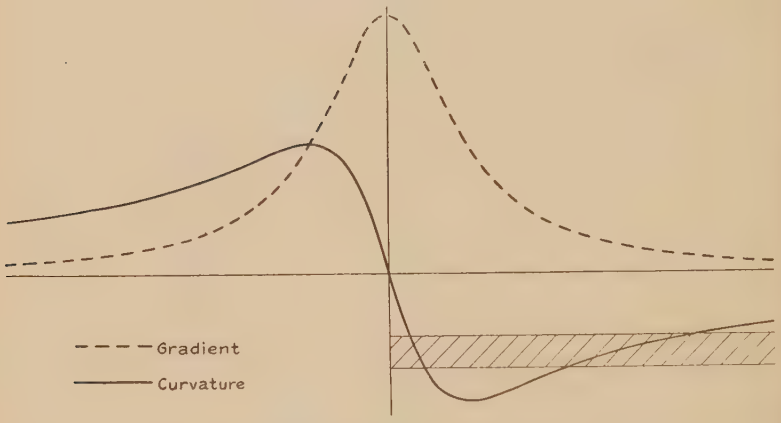

The curves corresponding to a transverse in the direction OX are given in fig. 4. The curvature vector changes sign immediately over the edge of the slab, while the gradient has a maximum at the same point.

It may be concluded that when, in a survey of a region with the Eötvös balance, the curvature vector changes sign where the gradient is a maximum, the earth's crust in that region is stratified, the edge of the stratum being situated below the point of the maximum gradient.

In conclusion, I desire to express my thanks to Professor T. H. Laby, who suggested this problem.

Melbourne,
November 1929.

L. *Notices respecting New Books.*

Statistical Methods for Research Workers. By R. A. Fisher, Sc.D., F.R.S. (Biological Monographs and Manuals, No. V.). Third Edition. [Pp. xv+ 284, with tables.] (Edinburgh : Oliver and Boyd, 1930. Price 15*s.* net.)

THE need for a new edition of this book, at an interval of only two years after the publication of the previous edition, is an indication—if such were needed, in view of the excellence of the work—that it has met a real want. The present edition differs only slightly from the second edition, which was reviewed in these pages, and detailed notice is therefore unnecessary. The chapter on the principles of statistical estimation, added to the second edition to provide practical illustrations of a subject which had received only general discussion in the first edition, has been enlarged by the addition of two new sections illustrating the applicability of the method of maximum likelihood and of the quantitative evaluation of information. The principal other addition is the generalized expression for the series of orthogonal polynomials used in connexion with the fitting of curved regression lines ; these expressions are useful in cases in which polynomials of a high order require to be employed.

It may be mentioned that the numbers of sections, tables, and examples have been unaltered by the addition of fresh material in the later editions, so that references to them (but not to pages) are valid for any edition.

The book can be strongly recommended to all those who have occasion to use statistical methods but are not concerned with the theoretical foundations upon which these methods are based.

The Acoustics of Orchestral Instruments and of the Organ. By E. G. Richardson, B.A., D.Sc., Ph. D. [Pp. 158 and 20 plates.] (London : Edward Arnold & Co., 1929. Price 10*s.* 6*d.* net.)

The development of musical instruments has been to a large extent of an empirical nature and their design has been influenced to a very small extent by theoretical considerations. In this book, which is founded on the 1929 Martin White lectures given at the Northern Polytechnic, London, Dr. Richardson has given an essentially popular treatment of the acoustics of the orchestra and of the organ. Apart from an appendix which deals mathematically with the theory of fingering and cross-fingering on the wood-wind, the book is free from mathematics. It should therefore prove of interest

and help both to musical instrument makers and to players. Separate chapters are devoted to the flute, reed instruments, brass instruments, percussion instruments, and strings. A chapter is devoted to ensemble playing and questions of architectural acoustics. Some space might have been given in this connexion to the acoustic properties of the ear, which play an important part in listening to an orchestra. It may be remarked that, though the organ and church bells are included, the piano is omitted—a somewhat surprising omission.

The book is well illustrated and gives an attractive presentation of the theory underlying the instruments considered. Any one who frequents orchestral performances will find his interest increased by a reading of this book, which will give him a fuller realisation of the many problems involved in design and use of the instruments employed.

Ondes et Corpuscules. By Louis de Broglie. Price 20 fr. *Mécanique Ondulatoire.* By the same author. Price 85 fr. (Paris : Librairie Scientifique, Hermann et Cie, Rue de la Sorbonne.)

Wave Mechanics. Translated by H. T. Flint, D.Sc., Ph.D. Price 12*s.* 6*d.* net. (London : Methuen & Co., 36 Essex Street, W.C. 2.)

In the papers contributed to scientific journals during the last two or three years, the author gives an historical account of the development of the undulatory theory of matter and of the corpuscular theory of light. The photo-electric and Compton effects required for their explanation, the hypothesis that light has a granular structure : in the theory of matter, the same duality appears, the expressions for energy and momentum being equally applicable to radiation and matter. The probability interpretation of the wave theory of matter leads to the result that physical measurements are only capable of finite precision, the quantum uncertainty principle of Heisenberg, a principle which has been claimed to be of equal importance with the principle of relativity.

The German edition, Wellenmechanik, was recently noticed in the pages of this Magazine, and the suggestion made that an English translation would be welcomed. The publishers are to be congratulated on undertaking this task and Dr. Flint for the able translation of de Broglie's standard work. The detailed account of the experimental verification of the wave theory by G. P. Thomson and Rupp was a notable feature of this work ; the author has taken advantage of the appearance of the French edition to include a description of the beautiful experiments of M. Ponte on the diffraction of electrons by

zinc oxide, which show a remarkable agreement between the observed and the theoretical values. Some photographs of diffraction rings, taken from this paper, are here reproduced.

X-rays. By B. L. Worsnop, B.Sc., Ph.D. Price 2*s.* 6*d.* net.
X-ray Crystallography. By R. W. James, M.A., B.Sc. Price 2*s.* 6*d.* net. (London : Methuen & Co. Ltd., 36, Essex Street, W.C. 2.)

A useful introduction to the study of X-rays, their properties and application to crystal structure is provided in these two monographs on physical subjects. Dr. Worsnop traces the development of the researches during the last twenty years, on the scattering, emission, and absorption of X-rays and the measurement of wave-lengths and gives in the concluding chapter a brief summary of the experimental results of Siegbahn on the refraction of X-rays by prisms, and of Compton and Doan on the use of reflexion gratings in the direct determination of wave-lengths and lattice constants.

In X-ray Crystallography, the author sets out the elementary principles of crystallography and of the methods employed in the observation of X-ray spectra by von Laue, Sir Wm. Bragg, and Debye and Scherrer, the measurement of crystal spacing and a number of important results in the analysis of organic and inorganic compounds. In the short bibliographies, references are given to advanced treatises for the more detailed and intensive study of the subject.

Matter and Radiation, with particular reference to the Detection and Uses of the Infra-Red Rays. By John Buckingham, M.A. [Pp. xii + 144, with 15 diagrams and illustrations.] (London : Humphrey Milford. 1930. Price 7*s.* 6*d.* net.)

The subject-matter of this volume falls into two parts which do not bear a very close relationship to one another. The first three chapters are concerned with modern theories of radiation and the electrical structure of matter, and give the main title to the book. These subjects are discussed in a pleasant discursive manner and with an avoidance of technical terms, suitable for the general non-scientific reader. The remaining two chapters deal with the detection and use of infra-red rays, and give the sub-title to the book ; many of the applications which are dealt with are hypothetical to the extent that they have not received serious practical trial, and many difficulties would need to be overcome before they could be considered feasible. Other and more important applications are dismissed in very summary fashion. Thus, the important investigations into planetary atmospheres, carried out at the Lick Observatory, based upon the comparison of photographs

secured by ultra-violet, visual, and infra-red rays, is dealt with in two sentences, one of which is ambiguous, if not misleading :— "Fig. 13 is a photograph of Mars taken half on an ordinary and half on a special plate. The planet, which stands out clearly in one half, cannot be seen at all in the other." These chapters will serve, however, to make clear to the layman that the radiation which is termed infra-red rays possesses practical applications, as well as rays of shorter and longer wave-lengths.

The Mechanism of Nature : Being a simple approach to Modern Views on the Structure of Matter and Radiation. By Professor E. N. da C. Andrade, D.Sc., Ph.D. [Pp. xii + 170.] (London : G. Bell & Sons, Ltd., 1930. Price 6*s.* net.)

Professor Andrade is one of the few men of science who have the gift of expounding modern scientific work and theories in a manner which will appeal to a layman. This volume was written as a holiday-task in response to requests to make plain the achievements of modern physics. The requirements of such a book cannot be better expressed than in the author's own words, from the preface :—" 'It must,' they say, 'be short, for we are men of the age, and cannot long give our attention to one subject : it must be plain, for we have no inclination to struggle with a new jargon, who have to do with jargon enough in our own professions : it must not smell too much of the schoolroom, for we have neither the patience nor the compulsion which render schoolbooks read. Set to.' "

The volume under review fulfils these requirements. It can be read in a couple of hours ; it is written in a literary style such as is possessed by few men of science, with clear and simple phraseology, and is accurate and authoritative. After an introductory chapter dealing with the scope of physics and the purpose of physical theories, succeeding chapters deal with heat and energy, sound and vibrations, light and radiation, electricity and magnetism, the quantum theory, and the atom. Many practical applications of the theories are referred to.

Too frequently the popular exposition of scientific development and achievement has been left, with deplorable results, to the journalistic type of writer, with no scientific qualification. In order that scientific work may receive its due recognition, and that its importance to modern civilization may be appraised at its proper value, the duty devolves upon men of science themselves to supply popular expositions which are accurate and authoritative. Not many have the requisite literary gift. Professor Andrade is to be congratulated upon this volume ; in the interests of science the hope may be expressed that it will be very widely circulated.

[*The Editors do not hold themselves responsible for the views expressed by their correspondents.*]